1-1-2015

A Protective Role Of Autophagy In A Drosophila Model Of Friedreich's Ataxia (frda)

Luan Wang
Wayne State University,

A PROTECTIVE ROLE OF AUTOPHAGY IN A *DROSOPHILA* MODEL OF FRIEDREICH'S ATAXIA (FRDA)

by

LUAN WANG

DISSERTATION

Submitted to the Graduate School

of Wayne State University,

Detroit, Michigan

in partial fulfillment of the requirements

for the degree of

DOCTOR OF PHILOSOPHY

2015

MAJOR: MOLECULAR AND CELLULAR TOXICOLOGY

Approved By:

_____

Advisor Date

_____

_____

_____

_____

DEDICATION

I dedicate my dissertation work to my family, friends, and all the people who helped me. The special thanks to my wife Jiaqi Fu, my son Ethan and my daughter Emma, my parents Duan Song and Chuxiong Wang for their unconditional support and encouragement.

I also dedicate this dissertation to my friends Enbo Zhan and Ruizhuo Ning for their warm consideration and great suggestions. Finally, I have great appreciation for Quanwen Li as my best friend and as a consultant for my experiments.

ACKNOWLEDGEMENTS

I want to thank my committee members for their generous help and expertise. Special thanks for Dr. Douglas Ruden for his continuous support and suggestions. Thanks for Dr. Victoria Meller, Dr. Xiangyi Lu, Dr. Robert Wessells, and Dr. Tom Kocarek for agreeing to serve on my committee. Thanks also go to Dr. Ye Shih Ho and Dr. John Reiners for their help in keeping me on track. Great appreciation goes to Dr. Robert Wessells' lab members, Dr. Nicole Piazza and Alyson Sujkowski, for their help in my training for heart assays and in the preparation of Drosophila strains.

I also wish to thank my lab mates Dr. Parsa Rasouli, Nancy Chia, Jessica Chyz, Laura Denomme, Wen Qu, and Arko Sen. I also thank Dr. Daniel Rappolee, Dr. Zhongliang Jiang, Dr. Quanwen Li and Yu Yang for generous help and for sharing their equipment.

A special thanks for Dr. Karen Occor at Sanford-Burnham Medical Research Institute for the heart assay suggestions. Thanks for Dr. Katja Koehler at ETH Zurich for the gift of Atg8 antibody. Thanks for Dr. Ruth Thomas and Dr. Leo Pallanck for their gift of the Parkin antibody.

TABLE OF CONTENTS

LIST OF TABLES

LIST OF FIGURES

LIST OF ABBREVIATIONS

3-MA	3-methyladenine
8-oxoG	8-dihydro-8 oxo guanine
AAG	2-Methyladenine DNA Glycosylase Type II
AF	Atrial Fibrillation
AMPK	AMP-activated protein kinase
AMPK	AMP-activated protein kinase
ARE	antioxidant responsive elements
Atg	Autophagy-related gene
CAT	catalase
ConA	Concanavalin A
Cox	Cytochrome c oxidase
CQ	chloroquine
DEPTOR	DEP-domain containing mTOR interacting protein
DHE	dihydroethidium
DRAM	Damage regulated autophagy modular
DRAM	damage regulated autophagy modular
DRG	dorsal root ganglion
FADD	FAS-associated death domain
fALS	Familial amyotrophic lateral sclerosis
FaPy	2,6-diamino-4-hydroxy-5-fromamidopyrimidine

Fh	The gene encodes *Frataxin* orthologs in Drosophila melanogaster.
FIP200	FAK-family interacting protein of 200 kDa
FXN	*Frataxin* protein (generic and human gene symbol)
FXN-D	*Frataxin* Deficiency strain with deficiency allele on the X chromosome causing the carrier female *Frataxin* haploinsufficiency and the carrier male lethality.
GAL4	GAL4 yeast transcriptional activator protein. Used to induce ectopic gene expression in transgenic Drosophila
GST	glutathione-S-transferase
hOGG1	Human 8-Oxoguanine glycosylase 1
IDH	Isocitrate dehydrogenase
IGF	Insulin-like Growth Facto
iPSC	Inducible Pluripotent Stem Cell
iPSC	inducible Pluripotent Stem Cell
IRS	Insulin Response Substrate
KD	Knock-down strain. Such as via RNAi
KDM2A	Lysine specific demethylase 2A
LC3	Microtubule-associated protein 1 (MAP1) light chain 3
MCK	muscle creatine kinase
Mitophagy	Mitochondrial autophagy
mLST8/GBL	Mammalian lethal with Sec-13 protein 8/ G protein beta subunit-

	like
MPT	Mitochondrial permeability transition
MQC	Mitochondrial quality control
MQC	Mitochondria quality check
MRI	magnetic resonance imaging
mTOR	Mammalian target of rapamycin
mTORC1	mTOR complex 1
NSE	neuron-specific enolase
OCT	optical coherence tomography
PARP-1	Poly [ADP-ribose] polymerase 1
PAS	phagophore assembly site
PcG	Polycomb Group
PE	Phosphatidylethanolamine
PI3K	Phosphoinositide 3-kinase
PI3K	phosphatidylinoside-3-Kinase
PI3P	phosphatidylinositol 3-phosphate
PKC	protein kinase C
PRAS40	Proline-rich Akt substrate of 40 kDa
RAPTOR	Regulatory Associated Protein of mTOR
rDNA	Ribosomal DNA
rER	rough endoplasmic reticulum

RNAi	RNA interference via double-stranded RNA
SAPK	stress-activated protein kinase
SCP	superior cerebellar peduncle
SOD	superoxide dismutase
*t*BHQ	*tert*-Butylhydroquinone
TET	Ten-eleven Translocation Enzymes.
TGDG	Thymine glycol DNA glycosylase
TIGAR	Tumor protein 53 induced glycolysis and apoptosis regulator
Tin	tinman
TMRM	Tetramethylrhodaminemethylester
TRAP1	TNF receptor-associated protein 1
TrxG	Trithorax Group
UBL	Ubiquitin-like
Ulk1	Unc-51 like autophagy activating kinase 1
UNGase	Uracil-DNA glycosylase
α-KG	α-ketoglutarate

CHAPTER 1: AUTOPHAGY IS UPREGULATED IN A DROSOPHILA FRDA MODEL AND ASSOCIATED WITH APOPTOSIS AND MITOPHAGY

1. Introduction

1.1 Friedreich's ataxia: features and genetics

Friedreich's ataxia (FRDA) is the most prevalent inherited recessive ataxia, affecting about 1 in 40,000-50,000 individual in the United States and Europe (4). It mostly affects Caucasians, as well as North Africans and Middle Easterners, without gender differences (5). The onset of FRDA is usually around puberty, but the range may vary from 2 years old to the late 30s (5). FRDA progressively affects the central nervous system (CNS) and peripheral nervous system (PNS), as well as the heart and skeletal muscles. The symptoms include muscle weakness in the arms and legs, heart disorders, loss of coordination, vision and hearing loss, dysarthria, scoliosis, and diabetes (6). Unfortunately, currently there is no treatment for FRDA. Recent studies show that the addition of the control *Frataxin* gene could rescue the *Frataxin* mutation cells in yeast, mice, and humans (7-9). However, the amount of *Frataxin* expression should be carefully monitored because over-expression up to 8-to-10 fold has deleterious effects in the *Drosophila* model (10). The above research indicates that more detailed information is required for effective treatment of FRDA.

In 1996, Campuzano and colleagues found that FRDA is caused by expansion of GAA triplets at chromosome 9q13-9q21.1 region, which contains candidate gene X25 (11). They further clarified that the disease is caused by a deficiency of an 18kDa mitochondrial membrane protein encoded by X25, which they named *Frataxin* (*FXN*) (12). The human *FXN* gene has 7 exons and extends for 95 kb on the genome (11). *Frataxin* protein is associated with the

mitochondrial inner membrane and crests. It is highly conserved from bacteria to plants and mammals (13, 14). The nuclear-encoded *FXN* gene is transcribed through the first five exons to produce a 210 AA (23 kDa) precursor protein isoform with N-terminal mitochondria targeting sequence. The precursor is then transported into the mitochondria and enzymatically cleaved between Gly41 and Leu42 to form a 169 AA intermediate m42-FXN (intermediate-FXN, corresponding to residues 42-210) by mitochondrial processing peptidases (MPPs) (15). The 19 kDa intermediate then undergoes further cleavage by MPPs to produce the mature form of *Frataxin* protein (16). There are three mature different *Frataxin* protein isoforms reported, m56-FXN, m78-FXN, and m81-FXN. Cavadini and colleagues first described a 155 AA, 17 kDa m56-FXN as a matured and functional form of *Frataxin* in humans in 2000 (16). In 2007, Condo and Testi published their finding of a 130AA, 14.2 kDa m81-FXN as the major form of *Frataxin* protein in human cells, such as human heart and peripheral blood lymphocytes and dermal fibroblasts (17). Another isoform was discovered by Yoon *et al*. in 2007, which is cleaved at site 78 to form a 133AA, 14.5 kDa m78-FXN (18). Currently, it is still not clear about the major form of matured *Frataxin in vivo.* Some explanations were proposed that different isoforms may be the result of different physiological conditions. For example, Gakh and colleagues found that both m42 and m81-FXN were present in normal cells under steady-state conditions, but m42-FXN seems to be degraded faster than m81-FXN in FRDA patients. Besides that, the m42 and m81-FXN also differ in the ability of oligomerization and iron/iron-sulfur cluster delivery which will be discussed later (19).

It is now established that the large expansion of trinucleotide repeats GAATTC within the first intron of the *Frataxin* gene occurs in most clinical cases of FRDA. Around 98% of FRDA

patients are homozygous for the GAA expansions, while the rest carry one expansion allele and one point mutation in the other allele (11). The length of the GAA repeat expansion in the smaller allele is positively correlated to disease progression and negatively correlated with the age of onset (20, 21). The repeats expansion ranges from 43 to more than 1700, compared to the 8-42 in unaffected people. Long repeats significantly reduce the level of *Frataxin* mRNA up to 70% (11, 21).

Multiple hypotheses have been proposed to explain how the increment of GAA repeats reduces the level of *Frataxin* mRNA. One of the major hypotheses suggests that when transcribed, the GAA repeats produced a corresponding mRNA segment that could bind to the DNA template forming DNA triplexes or DNA: RNA hybrid structures (22, 23). According to Grabczyk's work, which was done in vitro with T7 RNA polymerase, the DNA: RNA hybrid structure forms during the transcription of the long repeats and arrests the RNA polymerase at the GAA.TTC region, thus reducing the level of *Frataxin* mRNA (22). The DNA triplex, through interactions with two neighboring long repeated regions, forms a GAA.GAA.TTC structure (termed sticky DNA). This "sticky DNA" not only reduces the transcriptional efficiency but also affects the genetic stability of the DNA locus containing the trinucleotide repeat (23).

On the other hand, some researchers have shown that increasing the number of GAA repeats within the first intron of *Frataxin* does not affect pre-mRNA process, but rather the splicing efficiency of the first intron during the maturation (24). One new hypothesis comes from Saveliev's work, which proposes that long repetitive repeats tend to trigger the heterochromatin-like effect on the genome, thus repressing gene transcription (25). But until

today, the connection between the length of the triplet repeat and *Frataxin* mRNA and protein reduction is still under debate.

The *Frataxin* was expressed in all tissues, but it is enriched in heart, brown fat, kidney, liver, and certain neurons, most of which are highly metabolic and mitochondria-enriched tissues (14, 26). Therefore, as expected, the deficiency of *Frataxin* in FRDA patients usually causes more significant damage to those mitochondria-enriched tissues than in the other organs. The importance of *Frataxin* for survival varies among species. Simple unicellular organisms such as yeast can survive without *Frataxin*, but the complete absence of *Frataxin* is lethal for all studied multi-cellular organisms such as mammals (27). Multiple reviews have been published on the pathology of nervous system dysfunction in FRDA in humans and animal models (5, 28-30). The neuronal system is usually the first to be affected. The early onset FRDA patients commonly show declining motor skills as the first symptoms of the disease (30). Most of the FRDA patients ultimately suffer from cerebellar and brain stem atrophy, as well as lesions of cerebral white matter (31). The FRDA patients show a reduction in spinal cord diameter up to 30% compared to control cases, especially in the thoracic region, indicating fiber loss, such as gracile and cuneate fasciculi (32). The magnetic resonance imaging (MRI) results also revealed more than 60% loss in superior cerebellar peduncle (SCP) volume in FRDA cases (33). Dentate nuclei (DN) atrophy, accompanied by the degeneration of gray matter, occurs in most cases and becomes a biomarker for the diagnosis of FRDA (28, 34).

Currently, the most accepted hypothesis is that *Frataxin* is involved in iron metabolism in the mitochondria (27). The deficiency of *Frataxin* usually results in the abnormal accumulation of iron deposits in the mitochondria, and this apparently causes multiple enzyme deficits,

mitochondrial dysfunction, and oxidative damage. Eventually, this leads to neuron degeneration and a shortened lifespan (35). The deposit of iron in myocardial cells of three FRDA cases were first confirmed by Lamarche *et al*. in 1980 (36). Based on structural analyzes, *Frataxin* is possibly required for the assembly of iron-sulfur clusters (ISC). The negatively charged amino acids on the *Frataxin* surface could bind ferrous iron and promote the mitochondrial synthesis of ISC by controlling the ability of iron to participate in redox reactions (37). The detailed role of *Frataxin* in the ISCs is also being extensively studied. The ISC are involved in a series of important processes such as electron transport, energy metabolism, DNA repair and iron handling (38). The cluster consists of a group of proteins, including two molecules of IscS (Nfs1 in mammals) and two molecules of IscU to form the scaffolds of the complex (37). It is still debatable if the *Frataxin* protein directly binds to the IscU proteins.

1.2.1 ROS and Autophagy in FRDA

Reactive Oxidative Species (ROS) refers to a group of highly reactive, oxygen-containing chemicals such as hydroxyl radical (•OH), hydrogen peroxide (H_2O_2), and superoxide radical (O_2•-). Under physiological conditions, ROS molecules such as O2•− were produced in the mitochondrial matrix by Complex I and III and quickly removed by matrix manganese superoxide dismutase (MnSOD) (39). Because the O2•− produced in the matrix cannot cross the membrane unless it is protonated, the O2•− accumulates in the mitochondrial matrix. ROS, especially •OH that is produced by Fe(II) and H_2O_2 through the Fenton reaction, attack and oxidize the lipid, DNA and protein molecules inside the cell, causing cellular structural changes that are often associated with diseases.

The connection between *Frataxin* deficiency and ROS damage was first discovered in yeast. The *Frataxin* deficiency yeast strains *ΔYFH1* and YDL120 were hypersensitive to oxidative stress (40, 41). This was confirmed by Wong *et al.* in 1999 in mouse models when they observed that mouse FRDA fibroblasts show hypersensitivity to iron stress and hydrogen peroxide, suggesting the significant impact of ROS to disease progression (42). Amoros and colleagues reported that in SH-SY5Y human neuroblastoma cells with reduced *Frataxin* level have an increase in oxidative stress markers such as superoxide radical anion production and protein carbonylation, suggesting that there is an upsurge in oxidative stress upon *Frataxin* deficiency (43). Another piece of direct evidence for increased ROS production in *Frataxin* deficiency was attributed by measuring the level of O_2•− in FRDA-mutant mouse lymphoblasts using the dihydroethidium (DHE) method, which is a dye that localizes to mitochondria with a normal electron density gradient. It showed that there is an increase in ROS in FRDA-deficient cells about 80% compared to control cells(44).

There are several theories being developed on the effect of ROS in FRDA model organisms (45-47). One of the major hypothesis is that the increased ROS cause damages by interfering with the essential Fe-S cluster synthesis associated with *Frataxin*. The integrity of Fe-S clusters in the mitochondrial respiratory complex enzymes must be well maintained to prevent the failure of electron transfer. It allowed the electron leakage to be kept at the minimal level to avoid the production of ROS (48). The $O_2^{\bullet-}$ in FRDA-mutant *E. coli* inactivated prosthetic Fe-S cluster-containing enzymes through an oxidative attack (39). The research by Anderson *et al*. showed that ectopic expression of H_2O_2 scavenging enzymes, such as catalase (CAT) and SOD1, could partially rescue the short lifespan phenotype in *Frataxin*-deficient *Drosophila (49).*

The sensitivity of FRDA-deficient yeast cells to H_2O_2 was associated with an increase in the activated form of Caspase 3, a possible link to increased apoptosis (50). Second, it was proposed that the ROS-related damage in FRDA-deficient mouse cells includes mitochondrial DNA damage and nuclear DNA loss (51, 52). The work from Karthikeyan *et al.* confirmed that *Frataxin-deficient* yeast showed higher DNA damage reporter signals accompanied by increased ROS levels(53). Under normal conditions, superoxides are produced in the mitochondrial matrix and removed by superoxide dismutase (SODs) (54). The SODs, which belong to the Phase II detoxification pathways, were controlled by Nrf2 (nuclear factor-erythroid 2-related factor 2). Nrf2 is a cytosolic protein sequestered by Keap1 protein, and its activity is repressed at basal levels (3). Once the oxidative stress increases, the Keap1 protein is modified through oxidation, which releases Nrf2 into the nucleus. Nrf2 is phosphorylated by protein kinase C (PKC) at Ala 40 and tethered with a small protein heterodimer MafG binds to antioxidant responsive elements (ARE) DNA sequences. The binding in turn activates the transcription of Phase II antioxidant genes, such as SODs, glutathione, glutathione reductase, and glutathione-S-transferase (GST) to counteract the stress (55-57).

The defects of antioxidant mechanisms, including the reductions of SODs and glutathione, were also reported in FRDA cases. The SOD levels were only moderately up-regulated, and its upstream Nrf2 signaling pathways were defective in FRDA cells. Data showed that in cultured human FRDA fibroblasts, Nrf2 failed to associate with the clustered, phalloidin-reactive filamentous structure, termed actin stress fibers, to translocate into nucleus (58). As a result, the antioxidant enzymes such as catalase, GSTP1, NQO1, and SOD2 all showed significantly reduced induction under oligomycin or *tert*-Butylhydroquinone(*t*BHQ) treatment,

indicating a dysregulation of Nrf2 signaling during oxidative stress (58). In FRDA yeast, the total glutathione level was reduced to 20% compared to control samples, as well as glutathione peroxidase activity (59).

There are studies published about the beneficial effects of antioxidant supplement methods, including ectopic expression of SODs and increasing glutathione levels. For example, some studies of FRDA drug therapies have investigated the use of idebenone, which is a synthetic short-chain benzoquinone similar to the mitochondrial antioxidant coenzyme Q10(60). Idebenone is capable of reducing the membrane damage and protecting mitochondrial function as an electron carrier in FRDA cells. Research has shown that idebenone is beneficial for reducing the neurological dysfunction in the *Drosophila* FRDA model. However, clinical trials of idebenone failed to provide significant therapeutic benefits in FRDA patients (61-64). These results indicate that the oxidative-stress reducing pathways through SODs are partially affected in FRDA patients. However, the anti-oxidative stress mechanisms in FRDA are affected by multiple factors and need further clarification.

Besides antioxidant enzymes, autophagy is another major defensive mechanisms against ROS by removing oxidative-stress damaged cytosolic contents, especially long-lived and aggregated proteins and damaged organelles (65). Briefly, a double-membrane vesicle called the autophagosome extends and encompasses cytosolic components, such as defective mitochondria or large protein aggregates. The autophagosomes then fuse with the lysosomes or endosomes where the contents are degraded and subsequently recycled (65). Autophagy dysfunction has been linked to several diseases, including systemic lupus erythematosus, Danon

Disease, Parkinson's diseases, and cancers (66-70). But the description of autophagy in FRDA is limited.

The autophagy pathway includes initiation, nucleation, elongation, fusion and the final degradation steps, which require over 31 autophagy-related (Atg) genes (71). The protein mTOR, which is short for the mammalian target of rapamycin, is the major sensor of cellular nutrition deprivation and controls the initiation of the autophagy pathway. Autophagy starts with the initiation of a double-membrane structure called the phagophores, which form after stress signals such as starvation, hypoxia, or oxidative stress. The phagophores associate with other proteins such as RAPTOR (Regulatory Associated Protein of mTOR), DEPTOR (DEP-domain containing mTOR interacting protein), MLST8 (mammalian lethal with Sec-13 protein 8**,** also termed GβL (G protein beta subunit-like)), and PRAS40 (proline-rich Akt substrate of 40 kDa) to form mTOR complex 1 (mTORC1), which suppresses the activity of the Atg1 complex. The induction process requires the suppression of mTORC1 and activation of the Atg1 complex. The Atg1 complex in yeast contains Atg1-Atg13-Atg17, and the complex in *Drosophila* possesses Atg1, Atg13, and RB1CC1(72, 73). In mammalian cells, Ulk1 (unc-51 like autophagy activating kinase 1), which is the mammalian Atg1 homolog, Atg13, and RB1CC1 are constitutively bound. But under normal conditions, mTOR inhibit the Atg1/Ulk1 complex by hyper-phosphorylating Atg1/Ulk1 and Atg13 (74, 75).

During starvation or other stress signals, mTOR is inactivated. Ulk1 and Atg13 are dephosphorylated and activated. The dephosphorylation of Ulk1 activates its kinase activity, which phosphorylates FIP200(FAK-family interacting protein of 200 kDa, mammalian Atg17 homologue) to form the Ulk1-Atg13-RB1CC1-FIP200 complex and translocate to the isolation

membrane, termed pre-autophagosome or phagophore (75). It is suggested that the binding of Atg13 increases Atg1 stability (76). Currently, the origin of the double membrane is not entirely understood. It is suggested that the source of raw materials to build the phagophores may be the rough endoplasmic reticulum (rER), Golgi or mitochondria (77). It is found that Atg9 may contribute to induction by collecting and chaperoning the membrane components from an unknown cytosolic pool to the phagophore assembly site (PAS) (78). The structure characteristic of autophagy, the double membrane phagophore, accumulates in the PAS and enters the next step of expansion.

Current studies reveal that the expansion of the phagophore is controlled by phosphatidylethanolamine (PE) conjugated Atg8b, which is catalyzed by two ubiquitin-like (UBL) systems. The first UBL system is the direct binding of Atg8a to the pre-autophagosome membrane (79). Shortly after the synthesis of Atg8a protein or its mammalian ortholog LC3-I (microtubule-associated protein 1 (MAP1) light chain 3 form I), Atg8a/LC3-I is cleaved by Atg4 to reveal a C-terminal glycine residue and Atg8a/LC3-I then resides in the cytosol (79). Atg8a/LC3-I next conjugates to the PE to produce Atg8b/LC3-II. Atg8b/LC3-II incorporates into the autophagosome membrane and remains attached until the autophagosome is degraded by the lysosome when the two organelles fuse at the end of the autophagosome cycle.

Atg8b/LC3-II is a widely used marker for autophagy quantification (80). The second UBL system is the formation of Atg12-Atg5-Atg16 complex, which is independent of Atg8a/b (81). After the activation by Atg 7, Atg12 is then covalently bound to Atg5 through a series of ubiquitin-like conjugation reactions. Atg16 is also necessary for the membrane biogenesis (82). The Atg12- Atg5 conjugate interacts with Atg16 to form the Atg12- Atg5- Atg16 complex which

possesses enhanced affinity for negatively charged lipid and help tethering the phagophores membrane (81, 83). The membranes gradually extend and engulf the cytosolic contents and fuse with endo-lysosome in the form of autophagosomes for degradation. The contents and the inner membrane of the autophagosomes are degraded by the lysozymes, and the remnant are released back into the cytoplasm for recycling (84). The induction of autophagy is relatively slow. For example, in *Drosophila* adults and larvae, the autophagosomes are typically induced in the fat body 60 minutes after starvation is initiated (85).

The major function of autophagy is to maintain cellular homeostasis and to repair damage caused by stress such as ROS, through the constitutive or induced autophagy. Constitutive autophagy occurs at basal levels and is used as a general mechanism for cellular protein and organelle quality control under normal situation. The process is especially important in cells that do not readily replicate, such as neurons, cardiac cells, and hepatocytes. In a study by Sou *et al.*, neural-cell specific Atg5-/- mice were created to inhibit autophagy (86). The mice exhibited ubiquitinated protein aggregates and symptoms of neurological pathology, suggesting that basal autophagy is critical to maintaining neural health. Induced autophagy occurs in response to nutrient deprivation, cell stress, and numerous pharmacological reagents.

In cells undergoing nutrient deprivation, autophagy is used to break down cellular contents into amino acids and other components, and the cells can utilize the amino acids as an energy source (87). The importance of maintaining energy homeostasis during nutrient deprivation was stated in the study performed by Kuma *et al.* (88). Here, Atg5 $^{-/-}$ mice failed to survive the period of neonatal starvation that occurs following the birth and the sudden termination of transplacental nutrient supply. During this period, a massive increase in

autophagy was reported in the heart muscle, diaphragm and alveolar cells of WT transgenic mice labeled with a GFP-LC3 marker (88).

Autophagy could act as a pro-survival mechanism by antagonizing ROS and removing damaged organelles such as mitochondria. As stated above, ROS surging-induced Nrf2 could bind to ARE to increase the transcription of antioxidant-related genes, as well as autophagy-related genes, such as P62 (89). Another major connection between ROS and autophagy is tumor suppressor gene P53, which is also a central hub for stress signaling pathways. Under normal circumstances, cytosolic P53 suppresses autophagy by directly interacting with FIP200 (human ortholog of yeast Atg17) and inhibits Ulk1 complex. Increased ROS levels stimulate the redistribution of P53 from cytosol to nucleus, and directly regulates the transcription of several downstream genes related to autophagy, including subunits of AMPK (AMP-activated protein kinase), which activates autophagy triggered by starvation and hypoxia, and DRAM (damage regulated autophagy modulator), which promotes autophagy (90-93).

The reduction of cytosolic P53 also releases the suppression of Ulk1 complex and induces the initiation of autophagy (91). At the same time, cytosolic P53 also translocates to the mitochondrial matrix and interrupts the proton electrochemical gradients across the mitochondrial membrane, thus reducing the mitochondrial membrane potential ($\Delta\Psi m$). The reduction of $\Delta\Psi m$ may cause the selective autophagic removal of dysfunctional mitochondria (94). Evidence of direct interactions between ROS and autophagy proteins has also been found. Among the autophagy-related proteins, Atg3, Atg7 and Atg10 are the most sensitive to ROS because they are involved in the ubiquitin-like reactions to catalyze the conjugation of PE to LC3-I, which depends on the thiol group of the cysteine residue (95). The Cys^{81} of Atg4 is modified by

starvation-induced ROS production, specifically H_2O_2, thus inducing autophagy, which is visualized by LC3-II incorporation into the autophagosome membrane (92). Conversely, the inhibition of autophagy may increase the formation of reactive oxidative species, as well as increased ubiquitinated proteins and dysfunctional mitochondria (96). In summary, the above evidence suggests that autophagy could be affected by the increase of ROS level in FRDA.

In addition to its pro-survival roles, autophagy also shows a pro-apoptosis function as a mediator of cell death in many occasions. Autophagic cell death is accepted as a unique form of cell death and has received the title of Type II programmed cell death (97). The cells undergoing autophagic death exhibit an accumulation of autophagosomes in the cytoplasm. Yet the presence of autophagosomes in the cytoplasm is not sufficient evidence to conclude that a cell is undergoing autophagic death. Cell death can occur solely through autophagy as seen in MCF-7 cells treated with the drug tamoxifen (98). There is also evidence that autophagic cell death can accompany apoptotic cell death, and the two pathways are not necessarily mutually exclusive. For example, in the removal of *Drosophila* salivary glands in the pupae, apoptotic features such as caspase activation and DNA fragmentation are observed alongside the accumulation of autophagosomes (99).

Besides the above observations, it is also reported that autophagy can participate in the activation of traditional apoptosis. For example, treatment of cells with the pan-sphingosine kinase inhibitor SKI-I could induce apoptosis by activating caspase-8. But the absence of *Atg3* or *Atg5* reduces the caspase-8 activation. Young and colleagues found that Atg5 could facilitate apoptosis by forming a complex with caspase 8, FAS-associated death domain (FADD) and activating caspase-8 activity (100). Recently, it was reported that intrinsic apoptosis pathways

are activated in β-cells and neurons from FRDA rat, mediated by Bcl-2 family proteins Bad, DP5, and Bim (101). Mincheva-Tasheva et al. found induced apoptosis in the primary cultured neurons from FRDA rat dorsal root ganglion (DRG). They also found that the apoptosis could be reverted by the addition of BH4 domains from Bcl-xL protein, which inhibits autophagy through inhibitory interaction with Beclin-1/Atg6 (102). It is intriguing to explore if autophagy is involved in the loss of neurons, cardiomyocytes or other cell types in FRDA patients by promoting apoptosis under a certain level of stress. The above data suggest that the autophagy could function in anti-apoptosis and/or pro-apoptosis ways in FRDA.

Currently, there are several autophagy modification chemicals available, including inducers and inhibitors, and some of them have been tested in clinical trials or therapies. The canonical autophagy inducer is rapamycin (sirolimus), a fungicide with immunosuppressive property (103). Rapamycin affects autophagy by forming complex with cytosolic FKBP12 proteins and destabilizing mTOR complex, thus activating Ulk1 complex for autophagy initiation (104). Another chemical, methylthioninium chloride, also named methylene blue (MB), was also discovered to be a strong inducer of autophagy. The report suggested that MB stimulates autophagy through the activation of AMPK, possibly by inhibiting mTOR and activating the Ulk1 complex to initiate autophagy (105). At the same time, MB also reduces the phosphorylation level of Insulin Response Substrate (IRS), which in turn activates Insulin-like Growth Factor (IGF) receptor and the Phosphoinositide 3-kinase (PI3K). PI3k next phosphorylates Akt, which inhibitorily phosphorylates GSK-3 to lower its activity, thus facilitates the interaction of Bif-1 and BECN-1, leading to the formation of an SH3GLB1-BECN1 complex that activates PI3K to increase autophagy (106).

On the other hand, common autophagy inhibitors include chloroquine (CQ), bafilomycin A1, and 3-methyladenine (3-MA). CQ inhibits autophagy by altering the pH of the lysosome to interfere with lysosomal acidification, resulting in interrupted degradation of autophagosomes/autolysosomes (107). Similarly, bafilomycin A1 suppresses autophagy by blocking the vacuolar type H^+-ATPase on the lysosomal membrane to disrupt the lysosome acidification and autophagosome/lysosome fusion (108). The function of 3-MA comes from its interaction with class III phosphatidylinoside-3-Kinase (PI3K) which inhibits the production of phosphatidylinositol 3-phosphate (PI3P), thus suppressing the recruitment of Atg proteins to the phagophore during the initiation stage (109). These modifiers provide us with powerful tools to study autophagy in FRDA.

1.2.2 Mitochondria Homeostasis and Mitophagy in Neurodegenerative Diseases and FRDA

Beside the quantification of autophagy in FRDA, we are also interested in the detailed mechanism of autophagy in FRDA progression. Currently, it is not clear the downstream events of the increased ROS and Fe-S cluster dysregulation in FRDA. The details of how autophagy affects neurons and cardiac cells in those neurodegenerative diseases are still unclear and sometimes controversial. As mentioned before, autophagy participates in the regulation of protein and organelle degradation, especially in the long-lived postmitotic cells like cardiomyocytes and neurons. Autophagy has been proven to be one of the major mechanisms in degrading aggregation of misfolded proteins in Alzheimer's disease, Parkinson's disease, and amyotrophic lateral sclerosis (110). We hypothesize that the autophagy could play a role in FRDA by affecting mitochondrial homeostasis, inducing apoptosis, or initiating mitophagy. In other

words, autophagy could be the link between mitochondrial dysfunction and the neurodegeneration and neuron loss in FRDA.

As the powerhouse of the cells, mitochondria are subject to the ROS damages results from oxidative stress in diseases, including FRDA (111). When mitochondrial functions are interrupted, they become the major source of ROS production such as H_2O_2 and O2•- (112, 113). The damaged mitochondria usually show up-regulated ROS production (114). Considering that *Frataxin* is localized in the matrix, the mitochondria are the direct target of the cellular stress and hence raise the possibility that the mitochondrial could be an important factor in FRDA pathogenesis.

Defective mitochondria have been recognized as a key feature of Friedreich's ataxia. The deletion of yeast *Frataxin* homolog YDL120 reduced the mitochondrial respiration ability up to 40% compared to WT [26]. B. Amoros and colleagues reported that reduced *Frataxin* in SH-SY5Y human neuroblastoma cells caused dysfunctional mitochondria (43). The lower ATP production (50% or less), reduced Cytochrome C oxidase 1 and 2 (Cox I/ II) protein level and increased depolarization of mitochondrial membrane potential (reduced $\Delta\Psi_m$) were observed in SH-SY5Y cells (43). The lowered mitochondrial membrane potential was confirmed by Mincheva-Tasheva *et al.*, who showed that in cultured DRG neurons, 5 days after the *Frataxin* KD, there is a significant reduction of mitochondrial membrane potential (102).

It was reported that by measuring the ratio of citrate synthase and aconitase activities, the mitochondrial respiratory chain activity shows 84% decrease in FRDA patients' heart samples (43). In the meantime, the abnormal iron contents inside the mitochondria were 8-12 times higher than the WT cells. The same pattern was observed in human FRDA patients. Iron

accumulation is also seen in heart samples from FRDA mouse (115). There were changes in mitochondrial morphology and reductions in mitochondria numbers, as well as an increase in mitochondrial fusion (43). But until today, the research of mitochondrial homeostasis in FRDA is relatively limited and often controversial.

Several hypotheses were developed in the connection between dysfunctional mitochondria and FRDA, including the involvement of mitochondria induced apoptosis and the defects in mitochondrial quality control (MQC) pathways, such as fission/fusion and, to our most interest, mitophagy (101, 116-118). As stated above, autophagy could participate in type I or type II cell death, and the induced apoptosis of neuron cells has long been associated with neurodegenerative diseases. For example, Magrane *et al*. showed that morphologically altered mitochondria accumulate in familial amyotrophic lateral sclerosis (fALS) transgenic rat motor neurons right before the neuron death (119).

It is still unclear about the connection between dysfunctional mitochondria and FRDA pathological symptoms such as neuron degeneration and myocardial cell loss. Multiple studies explored the possibility of apoptosis mediated by *Frataxin* deficiency in those cell types, but the results were controversial. Increased apoptosis was reported in rat DRGs neurons and was observed in *Frataxin*-deficient clonal rat INS-1E β-cells, and inducible Pluripotent Stem Cell (iPSC)-derived neurons originated from FRDA patients (102) (101). Bolinches-Amoros et.al observed limited proliferation rate and shorter survival time in *Frataxin* KD SH-SY5Y cell lines. The *Frataxin* KD cells showed a higher level of senescence related β-galactosidase (SA-β-gal) activities but no changes in apoptosis-related cytosolic cytochrome C contents and the overall active form of caspase-3 in *Frataxin*-KD cells. The conclusion was that *Frataxin* depletion

accelerates cell senescence but does not induce apoptosis. However, this finding is partially shadowed by the fact that the finding was observed in the SH-SY5Y neuroblastoma cell line, of which the anti-apoptotic property may produce bias while performing apoptosis assay (43). The debate on the mitochondrial homeostasis and possible mitochondrial induced apoptosis in FRDA will require more research in the future.

Given the importance of providing essential energy for maintaining cellular activities, mitochondria are strictly monitored by multiple levels of MQC mechanisms. Different strategies of MQC are used against various types of stress. MQC can remove damaged mitochondria through mitochondrial fission/fusion to reduce the stress in the anti-apoptotic direction. While mitochondrial fission and division lead to apoptosis, mitochondrial fusion usually protects the cell against apoptosis (120, 121). Under other circumstances, MQC would promote mitochondrial fragmentation and mitochondrial autophagy (mitophagy) for energy and material recycling, as well as the aforementioned induced apoptosis. The presence of dysfunctional mitochondria in FRDA shows a possible absence or dysregulation of MQC, which may be caused by iron deposits and defective MQC components, or limited MQC capacity compared with increased abnormal mitochondria (122). We are especially interested in the function of mitophagy in FRDA.

It has been confirmed that increased mitophagy occurs in Alzheimer ’s disease, which indicates that abnormal autophagy activities are associated with neurodegenerative diseases [44]. Evidence showed that the mitochondria, either healthy or dysfunctional, could be found in autophagosomes in rat hepatic cells (123). Studies conducted in *S. cerevisiae* verified that the strains with Atg mutations, including Atg1, Atg6, Atg8, and Atg12, show defects in mitochondrial

degradation (124). Lower mitochondrial electron transport chain activities and higher levels of ROS are detected in those strains, which were similar to FRDA symptoms, showing the importance of mitophagy in maintaining mitochondrial functions (125).

Mitophagy, the removal of mitochondria through autophagy is considered selective. The specificity of mitophagy is confirmed by targeting the mitochondria through photo damaging agents. Chan *et al.* observed that in mouse lung cells with increased oxidative stress, GFP-LC3 highly co-localized with RFP-labelled citrate synthase, a mitochondrial protein, indicating the removal of the damaged mitochondria through mitophagy (126, 127). Starvation followed by glucagon supplementation activates the engulfment of mitochondria with several fold increase of autophagosomes, indicating the selective removal of depolarized mitochondria through mitophagy (128). Starvation also increases the amount of autophagosomes and autolysosomes that co-localize with mitochondria remnants (129).

It has been shown that it takes about 6 minutes for the mitochondria to be engulfed by phagophores or pre-autophagosomes (130). The sequestered mitochondria depolarize within 10 minutes by losing their fluorescent signal after Tetra-methyl-rhodamine-methy-lester (TMRM) treatment, a dye fluoresces when mitochondria are depolarized (130). The real-time analysis reveals that it takes an average of 7 minutes to digest the mitochondria after their sequestration into the autophagosomes (129).

Two major proteins involved in mitophagy are E3 ubiquitin ligase Parkin, which is encoded by *Park*2, and PTEN-induced putative kinase Pink1. When the depolarized $\Delta\Psi m$ is detected, Parkin re-distributes from the cytosol to the mitochondria, and is accompanied by the loss of mitochondrial markers such as Tom20, Cytochrome C, and TNF receptor-associated

protein 1 (TRAP1) (131). Pink1 is rapidly degraded by presenilin-associated rhomboid-like protein, a rhomboid protease in healthy mitochondria. But in dysfunctional mitochondria with diminished membrane potential, Pink1 is stabilized on the outer mitochondrial membrane while forming complexes and recruiting Parkin (132, 133). Research suggests that Pink1 recruits Parkin through its cytoplasmic kinase domain by phosphorylating Parkin at its Thr175 and Thr217 sites (134). The recruited Parkin then induces ubiquitination of mitochondrial membrane proteins such as VDAC and Mitofusin1/2, which promotes the degradation of the mitochondrial membrane and the following mitophagy (135-137).

Research also indicates that Parkin could induce mitochondrial fragmentation to facilitate mitophagy, by degrading mitochondrial protein Mitofusin 1 and 2 by proteasomes (138). The mitophagy regulation signaling pathways are extensively studied, and multiple genes are linked to the events. The Dynamin-related protein 1 (Drp1), which is recruited to the outer mitochondrial membrane, was reported to initiate mitophagy by binding to the mitochondrial outer membrane protein Fission 1 (Fis1). The deficiency of *Drp*1 causes diminished mitochondrial function in respiratory function and ATP production, as well as lost mtDNA. Most importantly, mitophagy in *Drp*1–KD cells is suppressed (139). On the other hand, *Drp*1 over-expression promotes mitochondria elimination by promoting mitophagy (140). It is possible that Drp1-dependent mitochondrial fragmentation primes mitophagy (141).

An interesting discovery is that the mitochondria, after a cycle of fusion/fission, can be divided into two categories: those that undergo refusion and those that do not (142). Currently, it is not clear what sorting mechanism is behind these two subpopulations (143). Generally, fission produced two subpopulations of mitochondria. Ones with lowered membrane potential

(ΔΨm) tend to incorporate with autophagosomes for degradation The other ones with higher potential remain in the cytosol for possible fusion(142). Mitochondria that never undergo re-fusion show a lower ΔΨm and tend to co-localize with LC3-GFP labeled autophagosomes, implying the possibility that mitophagy is the destination of unsalvageable mitochondria (144).

The depolarized mitochondria are observed to be sequestered in the autophagosomes by the lysosomal inhibitor Pepstatin A and E64D (144). Optic atrophy 1 (OPA1) is also considered to regulate mitophagy since the over-expression of *OPA*1 can effectively reduce the mitochondrial fraction in autophagosomes (145). Recent findings also suggest that mutated *NIX*, which encodes a BH3 family protein, reduces the presence of mitochondria in autophagosomes. The $NIX^{-/-}$ reticulocytes containing mitochondria are more sensitive towards stress from anemia, implying that the inability of removing malfunctioning mitochondria may be detrimental to the cell (146). Currently, NIX, ULK1, and Parkin are identified as signals that could specifically activate mitophagy in mammalian cells (147). In addition, some Atg genes may also participate in the regulation of mitochondria degradation. For example, knockdown of Atg7 reduces mitochondria removal in K562 cells. It is interesting to note that the KD of the essential Atg5 gene does not impede mitophagy in reticulocytes from neonatal animals (147).

In summary, the function of mitophagy has been associated with other neurodegenerative diseases such as Parkinson's disease, but not in FRDA yet. We are interested in testing the status and possible role of mitophagy in FRDA *Drosophila* models.

1.2.3 Drosophila models of cardiovascular disease and FRDA

Drosophila melanogaster is used extensively as a model system for genetics and developmental studies. It has the great advantages of low cost and a short generation time (2

weeks). More importantly, the homologs of 75% of known human disease genes can be found in *Drosophila,* which implies that the knowledge obtained from the *Drosophila* model is transferable to humans (148). The genome projects of high-density P-element and PiggyBac element insertions throughout the *Drosophila* genome make it an even more powerful model organism (149, 150). The understanding of numerous diseases has benefited from the *Drosophila* model, including Parkinson's disease, diabetes, cancer and, especially, heart disease (151).

The *Drosophila* heart (dorsal vessel) is morphologically different from the vertebrate heart but is evolutionarily conserved (152). In the *Drosophila* open circulatory system, the heart is defined as the section of the dorsal vessel between abdominal segments A5-A8 (153). The section anterior to the heart is a narrow tube called the aorta, which expands from thoracic segment T3 to abdominal segment A5 (153). In *Drosophila* pupae, the heart tube consists of two layers of cells. The inner cell layer contains two rows of myocardial cells, which form the tightly-jointed inner surface for contractile functions and with ostia cells in between which permit the entrance or exit of hemolymph (*Drosophila* blood) (153, 154). The relatively loosely organized outer layer has two rows of pericardial cells with possible excretion functions. The myocardial cells can be distinguished by their expression patterns of *tinman* (Tin). The homeobox gene *tinman* is expressed in each segment of the dorsal vessel and in four of the six pairs of cardial cells. Its expression patterns provide a powerful tool for researchers to investigate the cardiac function and development in the *Drosophila* model.

In *Drosophila,* different forms of cardiac dysfunction were observed such as cardiac arrhythmias, including atrial fibrillation and cardiac arrest (152). In addition, there are plenty of

well-established *Drosophila* techniques available, including edge-measurement microscopy and electrical pacing methods (155, 156). The recent development of optical coherence tomography (OCT) provides nondestructive and noninvasive ways to detect the *in vivo* cardiac morphological changes, which is difficult to achieve in mammalian models (151). By optically tracking the movement of both edges of the heart, OCT examines the heart rate and contractile function by measuring differences in diastole and systole diameter at the same point in time. OCT can be used to calculate the contractile velocity by determining the heart tube diameter changes in a certain time frame, using video recording and picture analysis software. In addition, external stress sources, such as square-wave electric pacing and chemical treatments can be applied to the *Drosophila* heart before and during the optical analysis.

The frequency of stress-induced permanent or temporary arrests and the uncoordinated contraction of heart tubes, which is similar to atrial fibrillation in vertebrates, can be calculated as a measure of cardiac function (157). The effectiveness of cardiac assays in *Drosophila* has been proven in many publications. Occor *et al.* found that a KD mutation in the *KCNQ* potassium channel in myocardial cells increased the sensitivity to pacing-induced heart failure, which mimics the effects of aging (158). Wessells *et al.* investigated the role of insulin-IGF receptor signaling pathways for the reduction of cardiac function during the aging process. While the heart rate decreased and pacing-induced heart failure rate increased with aging, the cardiac function could be restored by overexpressing the phosphatase dPTEN or the transcription factor dFOXO (159).

Friedreich's ataxia affects not only the central nervous system but also other organs, especially the heart. Because of its high energy demand and extensive mitochondria enrichment,

the heart is one of the most affected organs in FRDA cases. Iron overload cardiomyopathy is the one of the leading causes of cardiovascular mortality in FRDA patient (160). Heart diseases in FRDA patients may be severe, which contributes to the disability and premature death, particularly in early-onset cases (161). A study conducted by Harding *et al*. found that among 115 FRDA patients, more than 2/3 acquire the signs of cardiomyopathy. Other frequent symptoms included shortness of breath (in 40% of patients) and palpitations (in 11% of patients) (30).

In one of the most sensitive investigations for FRDA-associated cardiomyopathy, electrocardiography shows inverted T-waves in virtually all patients and ventricular hypertrophy in most patients (162). Around 5-10% of the patients are affected by atrial fibrillation (AF), which is one of the most common cardiac arrhythmias and usually leads to increased risk of cardiovascular mortality and stroke (163, 164). Studies show that various hypertrophic cardiomyopathies are present in almost all FRDA patients (165). Over 50% of the FRDA patients will eventually die from the complications associated with heart disease, which makes cardiac malfunction a leading cause of FRDA patients' death (125, 166). In a survey of FRDA patients lethality, Tsou and colleagues reported 59% of the deaths in their FRDA samples were caused by cardiac dysfunction, which causes earlier death than in non-cardiac FRDA patients (median death age 29 vs. 17). Among deceased FRDA patients, the cardiomyopathy of FRDA includes congestive heart failure (29.5%), arrhythmias-related (16%), ischemic heart diseases (4.9%), and atrial fibrillation related stroke (6.6%) (167).

Genetically, the deterioration of hypertrophic cardiomyopathy is associated with the size of repeat expansion in the smaller allele of *Frataxin* (21). Some observations of postmortem FRDA patients' heart tissue made by Michael and colleagues showed that, besides the muscle

fiber necrosis and increased tissue scars, there were also perinuclear iron deposit granules accumulating between myofibrils. However, the total cellular iron in the left ventricular wall in FRDA patients is similar to control cells (168). Together with the findings of increased electron density of mitochondrial deposits, it pointed to the possibility that the mitochondrial damage is induced by iron deposits. It speculated that iron deposits lead to muscle fiber necrosis and myocarditis (168). Mottram *et al.* showed reduced left ventricular volume and increased thickness of the left ventricular wall in FRDA patients, as well as impaired peak systolic and atrial velocities. The peak systolic and early diastolic level were both reduced in FRDA cases (169).

Research in animal models confirmed the findings that peak systolic and early diastolic level were both reduced in FRDA cases. For example, Puccio *et al* constructed two conditional *Frataxin*-deficient mouse lines, in which the mutant *Frataxin* allele is driven by tissue-specific Cre transgene controlled by either muscle creatine kinase (MCK) or neuron-specific enolase (NSE) promoters. The achieved muscle specific deficient FRDA mouse line, which has a heterozygous mutant allele of *Frataxin* in cardiac muscles, showed reduced left ventricular contractile function, both systolic and diastolic. The heart rate and the blood flow velocity in the ascending aorta were also reduced in the FRDA mouse model compared to control mouse (170, 171). Vyas and colleagues showed ultrastructure cardiac results of *Frataxin* KD mouse with disrupted arrays of sarcomeres and abnormally shaped mitochondria while the normal mouse heart shows orderly arranged myofibrils with uniformly shaped mitochondria (170).

From the views of biochemistry and molecular pathology, the data from the *Frataxin* knockout fibroblast and mouse model constructed by Vyas *et al.* showed that the aconitase protein level and activity in whole heart were reduced (170). Aconitase is a mitochondrial

enzyme that is especially sensitive to inactivation by oxidative stress. The numbers of mitochondria in FRDA cardiomyocytes are widely increased with decreased number of myofibrils. There is nearly a 10-fold increase in activated caspase-3 positive cell staining, which suggestsa a possible increase in mouse cardiomyocytes apoptosis (170). All of the above data suggest that the *Frataxin* deficiency causes severe damage to the heart in FRDA. We are interested in finding if the heart damage also occurs in *Drosophila* and if it is related to the autophagy.

In addition to the *Frataxin* deficiency, the condition of *Frataxin* overexpression is also interesting. In mammalian cells such as 3T3-L1 preadipose cells and mouse models, the overexpression has shown no adverse effects (172, 173). However, aforementioned overexpression of either human or *Drosophila Frataxin* impairs the nervous system and brain function, as well as locomotive ability (174). This indicates the *Frataxin* may be involved in different cellular response pathways under different concentrations. It is not clear how the *Frataxin* over-expression models relate to the symptoms present in FRDA patients since over-expression has never been observed in patients. But since the overexpression situation is a potential danger in gene therapy, the study of *Frataxin* overexpression status will be helpful for future research.

1.3 AMPK and SAPK stress response pathway are involved in inducing autophagy in FXN-KD *Drosophila*

Increased autophagy could reduce the stress level by removing damaged organelles, thus enhance the tolerance towards stress. On the other hand, increased autophagy could promote autophagic death/apoptosis in the cells and cause malfunction of certain tissues. So we assume

that the stress response pathway may participate in autophagy regulation. It is known that autophagy activation from oxidative stress is controlled primarily at two critical hubs: mammalian target of rapamycin (mTOR) and AMP-activated protein kinase (AMPK). Under conditions of low intracellular energy, activated AMPK induces autophagy both by phosphorylating Ulk1 for activation and by inhibiting mTOR complex 1 (mTORC1) via direct phosphorylation of mTOR binding partner raptor (175).

The other important stress response pathway involves stress-activated protein kinase (SAPK/JNK) signaling pathways. In Alzheimer's diseases, the interaction of abnormal mitochondria and oxidative stress response elements induces the production of oxygen species in dysfunctional neurons, which in turn activates SAPK as a long-term stress-responsive mechanism (176). Research in the intestinal epithelium showed that oxidative stress can induce autophagy requiring JNK signaling (177). The activation of JNK in the intestinal cells can increase autophagy and induce the expression of several Atg genes (178). Further details about the involvement of AMPK/SAPK in FRDA requires more research.

Until now, a lot of work has been done on the effect of ROS in FRDA patients, but very few studies have investigated the fate of the malfunctioning mitochondria. My goal of the project is to determine whether the mitophagy process is altered in FRDA KD *Drosophila*. Considering that autophagy is also deemed as the major mechanism against oxidative stress as stated above, we propose that autophagy plays a significant role in the pathogenesis of FRDA in two possible ways: promoting apoptosis in certain cell types or removing damaged mitochondria through mitophagy, separately or combined. Our work will be the first to examine the possible role of turnover of damaged mitochondria through mitophagy in FRDA. If it is confirmed that the

mitophagy is affected in FRDA *Drosophila*, the manipulation of autophagy or mitophagy might be a possible direction for FRDA therapy.

2. Statement of Problem

Currently, a lot of work has been done on the mechanisms of how *Frataxin* deficiency affects FRDA patients. The role of *Frataxin* in iron sulfur cluster synthesis and in maintaining normal mitochondrial function has been well explored. However few details are available about the downstream activities of dysfunctional mitochondria due to the *Frataxin* reduction, such as the fate of the malfunctioning mitochondria, and status of mitochondria quality control mechanisms. As one of the major anti-stress response pathways and the damaged organelle removal mechanisms, the dynamic of autophagy under *Frataxin* deficiency is intriguing. Our work will be the first to examine the turnover of damaged mitochondria through mitophagy in FRDA. If it is confirmed that the mitophagy is affected in FRDA *Drosophila*, the manipulation of autophagy or mitophagy might be a possible direction for FRDA Therapy.

3. Materials and Methods

Drosophila **culture:** *Drosophila* strains: UAS-fh.IR (w[1]; P (w[+mC]=UAS-fh.IR)2), UAS-fh.wt (w[1]; P(w[+mC]=UAS-fh.A),1), UAS-Atg1.IR (y^1 v^1; P{TRiP.JF02273}attP2), w[*]; P(w[+mW.hs]=GAL4-da.G32)UH1, UAS-GFP.IR, and FXN-D (Bl3694, Df(1)9a4-5, y[1] cv[1] v[1] f[1] car[1]/FM7C) were obtained from Bloomington Stocking Center. The GMH5-Gal4 stock was a gift from Dr. Robert Wessells. All *Drosophila* strains were maintained in 23 ml plastic vials on Bloomington recipe for Drosophila Medium. The vials were kept in the incubator of 18°C or 25°C and 50% relative humidity. Each vial were transferred to a new vial every 3-4 days. UAS-fh.IR or W1118 was used as a control strain.

Starvation and chemical treatment: Starvation was initiated by transferring *Drosophila* into an empty vial with a cotton ball containing 4 ml H_2O at the bottom to avoid dehydration. Numbers of surviving *Drosophila* were counted every 24 hours and recorded. Chemical treatments were using chemical incorporated medium in which the chemicals were dissolved in distilled water according to the different final concentrations of 1 liter medium. The dissolved solutions were added to food medium at 55°C during preparation. The medium was stirred for even distribution before poured into vials. For small quantity chemical treatments or reagents that were fragile to heat, such as rapamycin, the chemicals were dissolved in ethanol and add to 6% sucrose solution. *Drosophila* were transferred to vials containing cotton balls with 3ml of sucrose solution. *Drosophila* were transferred to new vials with the same treatment every four days.

Locomotive Assay: For each experiment, 10 adult *Drosophila* 24 hours after eclosion were placed in one 30 cm graduated cylinder that were evenly marked for three parts: bottom, middle, and top sections. The *Drosophila* were placed in the cylinder for 5 minutes before the test. Next the *Drosophila* were gently knocked down to the bottom of the cylinder and the numbers of *Drosophila* climbing up to each section in 10 seconds was recorded. The experiment for each group was repeated three times.

Real-Time PCR: Certain amount of *Drosophila* were homogenized in Trizol reagent from Invitrogen (Carlsbad, CA). RNA was extracted using the RNeasy mini kit from Qiagen (Hombrechtikon, Switzerland). The acquired RNA contents were quantified using Nanodrop (Wilmington, DE). The cDNA was synthesized using 20ng mRNA by oligo (dT) primers and Superscript III reverse transcriptase from Invitrogen (Carlsbad, CA). The Taqman primer sequences were adopted from previous publications and purchased from Applied Biosystems

(Foster City, CA). The PCR reaction was performed using Taqman PCR Master Mix and the ABI 7500 PCR machine. The thermal cycling conditions were 95°C for 10minutes, 45 cycles at 95°C for 15 seconds/60°C for 60 seconds. The results were normalized by using internal controls such as GAPDH and 18s rRNA. The Ct (Cycle of threshold) value was detected automatically, and the relevant RNA abundance was calculated by ABI software.

Immunostaining: Each 2 ml Eppendorf tube contained 20 larvae or 15 pupae, or 15 adults that were quickly frozen at -20°C after collection. The samples were homogenized in liquid nitrogen for 1 minute. Then 200 ul of Pierce RIPA lysis buffer (Thermo) with protease and phosphatase inhibitors (1:100, Thermo) was added to each vial and homogenizes for another 60 seconds. The samples were sonicated for 10-15 seconds and centrifuged for 15 minutes at 4°C and 15000 rpms. The supernatants were collected for acetone precipitation to remove extra lipids, salts, polysaccharides, etc. Briefly, 4X sample volume of -20°C acetone was added to the supernatant. The tubes were vortexed for 10 seconds and incubated for 10 minutes at -70°C. The vials were then centrifuged 10 minutes at 13000 g and 4°C. The supernatants were carefully removed, and the vials were air dried for 5 min. The pellets were dissolved in 200 ul RIPA buffer with protease and phosphatase inhibitor and quantified using the Bradford method. The proteins were separated by SDS-PAGE 4-20% precast gradient polyacrylamide gels (Bio-Rad) and then transferred to nitrocellulose membranes using a semi-dry transfer machine (Bio-Rad). The membranes were hybridized using primary antibody and HRP second antibody stained by luminol solution (GE). The results were imaged and analyzed by ImageJ software.

Measurement of heart rates and diastole/systole diameter: Methods was adopted from Wessells et.al (179). For each group, 50 gender and age-matched *Drosophila* from both mutant and

control strain were tested. The *Drosophila* were anesthetized by FlyNap (Carolina Biological Supply, Inc.) for 4 minutes and placed on the soft gel on top of the slice with the abdomen toward the light source. Each slice contained 8 *Drosophila* and the slice was placed under the microscope. The beating of each individual heart was recorded. For the purpose of precision, the measurement is performed on the first cardiac ventricle of the heart tube. For each *Drosophila*, a 10-second movie was recorded. The video was reviewed later, and the results were presented as beats per minute. The end-diastolic and end-systolic dimensions were measured on the still images from the movie clips. The position is chosen at the midpoint between two of the major transversal tracheal tubes passing through the first cardiac ventricle.

Electrical pacing: For each treatment group, the data of 50 male and 50 female *Drosophila* were collected. For the pacing, 50 *Drosophila* were anesthetized by FlyNap (Carolina Biological Supply, Inc.) anesthetizer for 4 minutes. Then the *Drosophila* were placed between two electrodes touching conductive gel spread over the electrodes. The hearts were shocked with a square wave stimulator (Phipps & Bird, Inc.) producing a current for 40 V and 6 Hz for 30 seconds. Heart failure rate is defined as the percentage of *Drosophila* that enter either cardiac arrest or fibrillation during or immediately after the pacing. The recovery rate is defined as the number of *Drosophila* return to normal after pacing-induced arrest or fibrillation within 2 minutes of pacing cessation. Total recovery indicates the proportion of *Drosophila* with normal heartbeat 2 min after cessation of pacing. During each pacing, 8 *Drosophila* were treated and recorded using Nikon NIS-Elements Advanced Research System. For each genotype, the data of 50 *Drosophila* were collected within 50 minutes to avoid the variation of anesthesia status. Each strain was repeated three times.

Statistical analysis: Experiments will be conducted in triplicates to reduce variation, except where noted. The data will be analyzed as Mean ± SEM in those experiments that had triplicates. In the experiments where duplicates were done, the spread was shown but p-value significance was not determined because it cannot be done with n = 2. A one-way analysis of variance (ANOVA) was performed to compare between groups, when indicated.

4. Results

4.1 Construction of *Frataxin-deficient* and overexpression *Drosophila*

To test the autophagy activity in *Frataxin-deficient* and overexpression *Drosophila*, we obtained *Drosophila* stocks of *Frataxin* partially knock-down, *Frataxin* deficiency, and *Frataxin* overexpression. We used two types of *Frataxin-deficient Drosophila*. The *Frataxin*-deficient stock (BL3694, Df(1)9a4-5, y[1] cv[1] v[1] f[1] car[1]/FM7C) ,termed **FXN-D** line, was obtained from Bloomington Drosophila Stock Center. It contained segment deletion on X chromosome, from 8C7 to 8E2. The deleted *Frataxin* gene was located at 8C14. The absence of the segment was balanced by balancer chromosome FM7C. The homozygous deficient progeny did not survive. Female heterozygous-deficient progeny are viable and fertile with a reduced *Frataxin* expression level.

The *Frataxin* partial knock-down line da^{G32}-fh.IR termed **FXN-KD,** was achieved using the UAS-Gal4 system (180). The *Drosophila* UAS-Gal4 system had been established for many years because of its versatility and convenience to manipulate gene expression. The ubiquitous or tissue specific expression of Gal4 proteins bind to the UAS promoter region to start the transcription of the inverted repeat product, a hairpin RNA which will be processed later by Dicer complex through siRNA pathways and will target and degrade endogenous *Frataxin* mRNA at

certain tissues. The UAS stocks that carried an inverted repeat sequence of *Frataxin* was UAS-fh.IR (w[1]; P{w[+mC]=UAS-fh.IR}2) and was constructed by Anderson in 2005 (181). The other available *Frataxin* knock-down strain produced by Anderson is w^1; P{UAS-fh.IR}**1,** which contains the insertion on the third chromosome. Because this stock is weak, and the survival rate is extremely low even at 18 degrees, we used the stocks with 2^{nd} chromosome insertion for the following work. The inverted repeat sequences were located on the 2^{nd} chromosome of UAS-fh.IR strains. For the driver *Drosophila* stocks, we used da^{G32}-Gal4 lines for whole body expression, which contains a *daughterless* (*da*) gene promoter that ubiquitously expresses the target gene in all tissues at a very high level. We also obtained *Frataxin* overexpressing *Drosophila* by crossing UAS-fh.wt (w[1]; P{w[+mC]=UAS-fh.A}1) stocks that carry wild-type *Frataxin* sequences to a da^{G32}-Gal4 promoter stocks. For comparison, *Atg*1 deficient line, UAS-*Atg*1.IR (y^1 v^1; P {TRiP.JF02273} attP2) was also obtained by crossing with promoter strains to provide negative controls for the investigation. Previous studies show that the GAL4 activity was properly initiated at 16°C, and 29°C provides the maximal effects without jeopardizing the viability and fertility of the fruit *Drosophila*. In our study, the original stocks were stored, collected, and crossed at 25 ^{0}C. The crossed strains which are larvae/pupal lethal stocks were crossed and raised at 18 ^{0}C until they developed into adults. The tests were performed at 25 ^{0}C in the adults.

4.2 Characterization of FXN-KD stock

By crossing the da^{G32}-Gal4 driver stock with *Frataxin* knock down stock (UAS-fh.IR), we obtained *Frataxin* partial knockdown *Drosophila*, da^{G32}-fh.IR. The parental stocks, da^{G32}-Gal4 and UAS-fh.IR, are viable, fertile, and with normal life span at 18 ^{o}C and 25 ^{o}C, which indicates the daughterless gene, and the insertion of inverted repeat sequences did not affect the *Drosophila*

Ubiquitous	18 ºC	25 ºC	29 ºC
da^{G32}–fh.IR	√	×	×
da^{G32}– Atg1.IR	√	×	×
da^{G32}– fh.wt	√	√	×
da^{G32}– GFP.IR	√	√	√

Table 1: Viability of da^{G32}-Gal4 driven *Drosophila* strains under different temperatures. The ubiquitously expressed Gal4 strain da^{G32}-Gal4 was crossed with different target strains in one of the three temperatures for diverse efficiency. The survival phenotype is indicated as "√" symbol while the lethal phenotype is indicated as "X" symbol. *Frataxin* inverted repeat containing strain, UAS-fh.IR (w[1]; P[w[+mC]=UAS-fh.IR]2) was crossed with da^{G32}-Gal4 to obtain *Frataxin* KD da^{G32}-fh.IR strain. The progeny survived at 18**°C**, but not 25**°C** and 29**°C**. Similar results were observed in Atg1 KD da^{G32}-Atg1.IR strains

viability and fertility. The progeny da^{G32}-fh.IR *Drosophila* are viable and fertile at 18^{o}C. At 25^{o}C the da^{G32}-fh.IR *Drosophila* are viable through larval stage with a high lethality rate before pupal stage**,** while 100% of the pupal development terminated in late pupal stage (**Table 1**). The size of the larvae are larger compared to the control strain before the development stops. The result is

in accordance with the description from Anderson et al that the *Frataxin* deficiency causes shorter life span, high rates of early termination, and late pupal lethality (181).

The partially KD adults are viable and could be collected at 18^{o}C, but the survival rate is very low. The collected adults have lifespans of about 7-14 days at 18^{o}C. When they were transferred to 25^{o}C immediately after collection, they had a much shorter longevity about 24-72 hours, with few escapers that can survive up to 5 days (**Figure 1**). The difference in the longevity is possibly due to the siRNA efficacy of the UAS-Gal4 system, which was more efficient at 25^{o}C than at 18^{o}C. The *Frataxin* mRNA level was reduced to a lower level at 25^{o}C compared to that of 18^{o}C, which produce more deleterious effects such as lower survival rate and shorter longevity.

The results showed that the da^{G32}-fh.IR *Drosophila* have the phenotypes of *Frataxin* deficiency matching the previous reported *Frataxin* knock-down studies. To avoid the possibility of unspecific effects of Gal4 protein or the inverted repeat structure in the siRNA, we also tested the da^{G32}-Gal4 and da^{G32}-GFP.IR lines, which ubiquitously silence the GFP gene as negative controls. Both lines were viable, fertile, and within the normal range of lifespan in both 18 and 25^{o}C. It excluded the non-specific influence of Gal4 protein and inverted repeat insertion.

To exclude the possibility of *Frataxin* siRNA off-target effects, we crossed the UAS-fh.wt stocks, which carried an allele of wild type *Frataxin*, with the UAS-fh.IR siRNA stock, and the lethal phenotypes were partially rescued. But one of the constructs, UAS-FF2-h, which contains a recombinant chromosome carries both wild-type *Frataxin* allele (UAS-fh) and the short hairpin *frataxin* allele stock (UAS-fh.IR). When crossed to da^{G32}–Gal4, its progeny, da^{G32}-FF2-h, showed 10-fold overexpressed *Frataxin* mRNA levels, but nevertheless displayed similar phenotypes to the FXN-KD *Drosophila*. The overexpression is possibly caused by the insertion of multiple copies of wild type *Frataxin* allele during construction. A similar strategy was applied by Anderson et. al and their cross rescued the knock-down phenotypes. We concluded that the da^{G32}-fh.IR fit into the description of the original knock-down strain and the *Frataxin* knock down is effective.

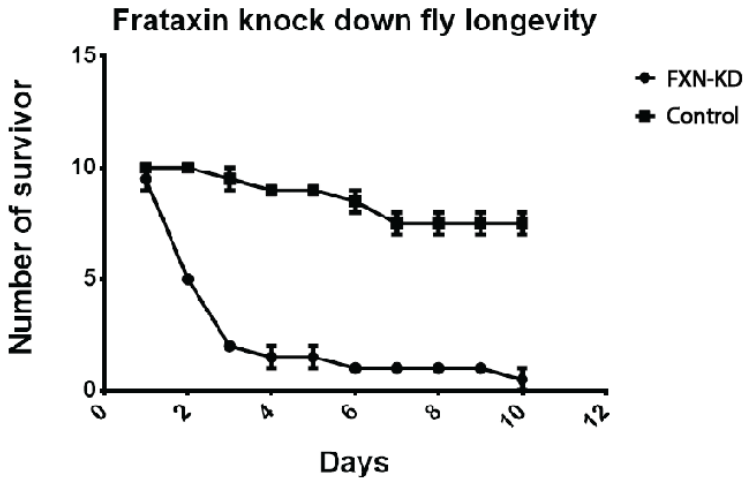

Figure 1: *Frataxin* reduction significantly reduce the life span of *Drosophila* The longevity and survival assay for control (UAS-fh.IR) and FXN-KD (da^{G32}-fh.IR) *Drosophila* at 25℃ showed that FXN-KD *Drosophila* have a lower survival rate. Control and FXN-KD adult *Drosophila* from 18 ^{o}C were immediately transferred and maintained in 25^{o}C for 10 days.

Next, we performed a series of assays to measure the impact of *Frataxin* reduction on da^{G32}-fh.IR *Drosophila*. First, we tested the longevity of partially *Frataxin* knock-down *Drosophila*. The adult da^{G32}-fh.IR *Drosophila* were collected from eclosion within 24 hours at 18^{o}C and transferred immediately into incubation at 25^{o}C. The *Drosophila* were transiently transferred to new vials every 72 hours at room temperature and immediately returned to 25^{o}C. The da^{G32}–fh.IR *Drosophila* show significant shorter life span compared to UAS-fh.IR adult *Drosophila* at 25^{o}C (**Figure 1**). It confirmed the essential role of *Frataxin* in maintaining normal survival and development of the *Drosophila*.

Because one of the defects of *Frataxin* deficiency is progressive mobility deterioration, we measured the locomotive ability of control and da^{G32}-fh.IR *Drosophila* through mobility assay. Briefly, 10 1-day old *Drosophila* were placed in a 19 cm gradient cyclinder at room temperature. The cylinder was evenly marked into 3 sections: top, middle, and bottom. The *Drosophila* were tapped down to the bottom of the tube and were given 10 seconds to climb to the top base on their anti-gravity instinct. After 10 seconds, the numbers of the *Drosophila* stayed at each section were recorded. The high percentage of flies to stay on the top section indicated stronger locomotive ability. The adult *Drosophila* of FXN-KD at 1 day of age showed lower percentage to be able to stay on the top section of the cyclinder during climbing assays, which indicate reduced mobility in *Frataxin* reduced *Drosophila* **(Figure 2)**. The shorter longevity and lower mobility resembled the features of human FRDA patients.

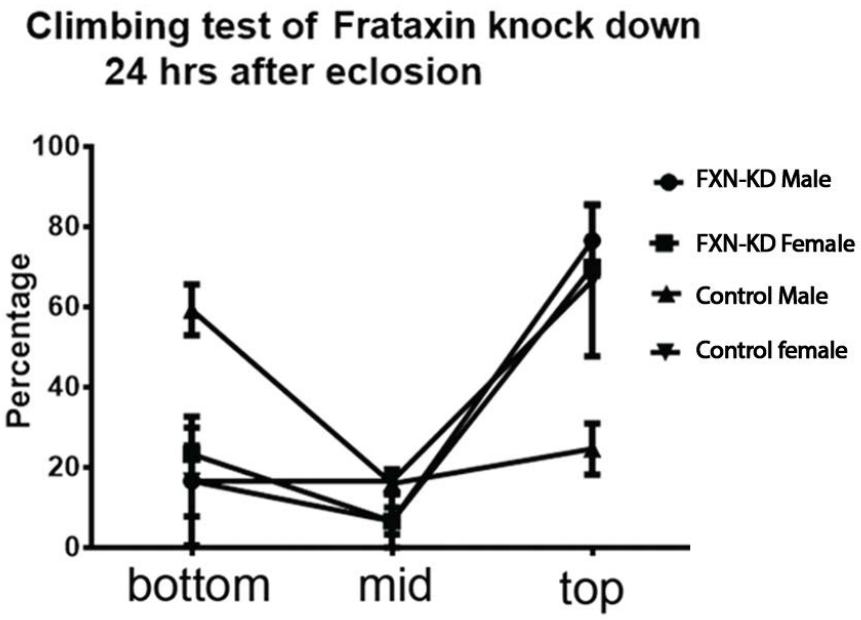

Figure 2: Climbing assay confirms the declined locomotor ability in FRDA *Drosophila*. The assay was performed using a 2.4cm diameter and 19cm high glass measuring cylinder. The column is demarcated evenly into three sections: Bottom, Mid, and Top. At 24 hours after eclosion, two groups of 10 *Drosophila* from each phenotype were tested for three times individually. The *Drosophila* were allowed for 10 seconds movement, and the numbers of the *Drosophila* that stay in each section will be counted and calculated to show their mobility. Both male and female FXN-KD showed lower locomotive activity comparing to Control (UAS-fh.IR) *Drosophila*

Next, we used quantitative real time-PCR (qRT-PCR) to measure the *Frataxin* knock down level in da^{G32}-fh.IR *Drosophila*. The test was carried out on adult *Drosophila* collected from 18°C and immediately transferred to 25°C for 24 hours. The *Frataxin* mRNA level was reduced 50% in female *Drosophila* and 30% in male *Drosophila* at the age of 24 hours (Figure 3). Because the further reduction of *Frataxin* would be lethal for da^{G32}-fh.IR *Drosophila*, we consider this moderately knock-down *Frataxin Drosophila* to be a proper FRDA model. The western blot showed that the *Frataxin* protein levels in female da^{G32}-fh.IR *Drosophila* are also reduced

compared to the control *Drosophila*, which indicates the successful knock down of *Frataxin* through RNAi (Figure 4).

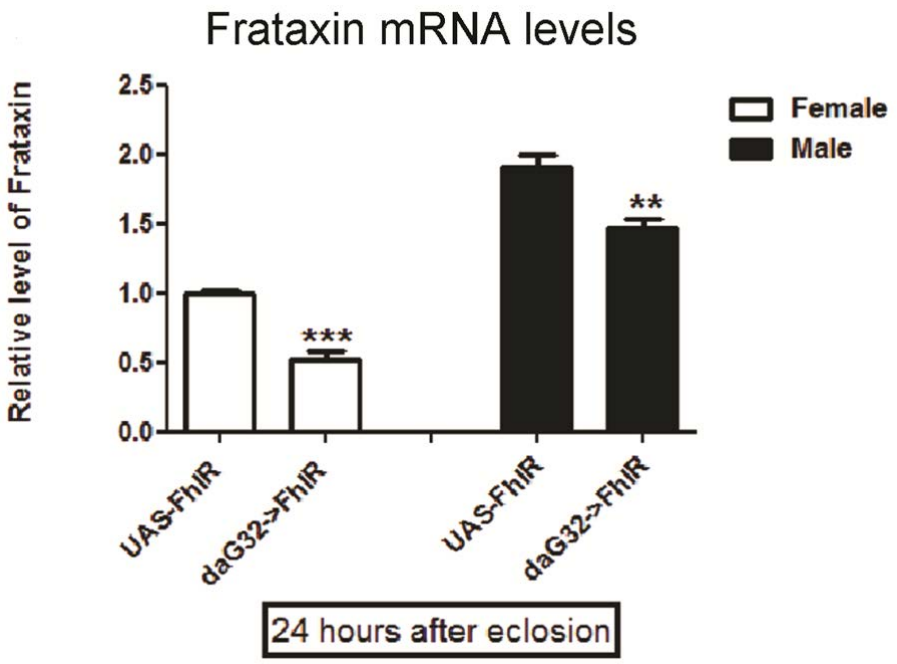

Figure 3: TaqMan Real-Time PCR (qRT-PCR) showed the *Frataxin* mRNA levels were reduced in FXN-KD *Drosophila* 24 hours after eclosion at 25 degrees. The *Drosophila* eclosed at 18°C and were immediately transferred to 25°C and maintained for 24 hrs. Each sample were pooled using 20 files and were homogenized and extracted for mRNA. For PCR, each sample with three technical repeats was tested and plotted for comparison. The FXN-KD females showed more than 50% reduction of *Frataxin* mRNA compared to controls ($p < 0.001$). The FXN-KD males showed about 25% reduction in mRNA compared to control males ($p < 0.01$).

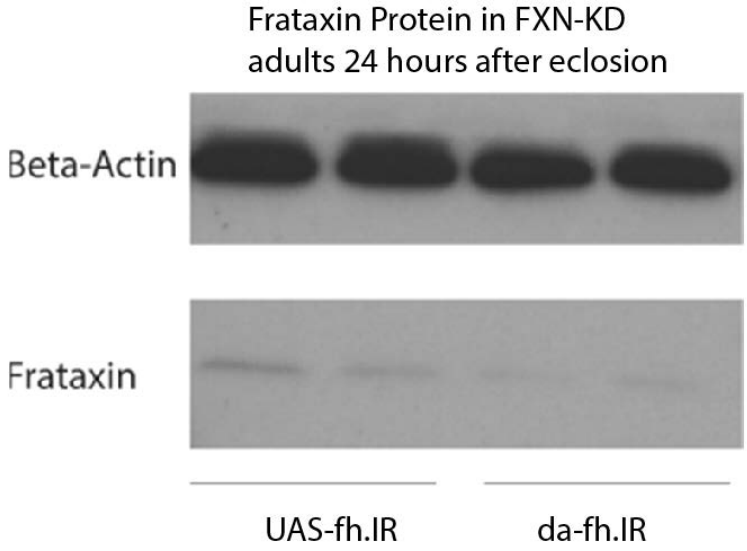

Figure 4: *Frataxin* protein expression is decreased in FXN-KD female *Drosophila* at 25 ºC. The *Drosophila* eclosed at 18 ºC were immediately transferred to 25 ºC and maintained for 24 hrs before tests. Ten *Drosophila* were pooled for each sample. The da^{G32}-fh.IR female showed less *Frataxin* protein compared to UAS-fh.IR control females.

4.3 Autophagy is upregulated in *Frataxin* partial knock down da^{G32}-fh.IR *Drosophila*

Next, we characterized the autophagy activity in da^{G32}-fh.IR *Drosophila*. First we measured FXN-KD *Drosophila's* mRNA level of *Atg*1 and *Atg*5. Atg1 is a protein kinase which plays a key role in the initiating autophagy. The *Atg*1 knock down stock, da^{G32}-*Atg*1.IR, was used as a positive control. The RT-PCR results of da^{G32}-fh.IR adult *Drosophila* 24 hours after eclosion showed that *Atg1* mRNA level in was up-regulated 100% in female *Drosophila*, and over 30% in male *Drosophila*, indicating the increased initiation of autophagy when *Frataxin* is reduced (**Figure 5 A**). As positive control, the realtime-PCR results showed that *Atg1* mRNA level in da^{G32}-*Atg*1.IR *Drosophila* was decreased to less than 50%.

The mRNA level of *Atg5,* which is another marker for autophagy activity, was also examined. We do not observe dramatic change of *Atg5* mRNA levels compared to the controls in the female and male da^{G32}-fh.IR *Drosophila* (**Figure 5:B**). The explanation could be that the *Atg*5

transcription level does not change in *Frataxin* deficiency. Another explanation for the relatively stable transcription level is that the *Atg5* is downstream of *Atg1* in the expanding stage of the autophagy pathway, parallel to the L*C3/*Atg*8* branch. The results indicate that the *Frataxin* deficiency does induce autophagy increase in the transcriptional stage in da^{G32}-fh.IR *Drosophila*, and may be associated with *Atg5* independent autophagy mechanisms.

The most convincing marker for the autophagy activation is the level of Atg8 protein,

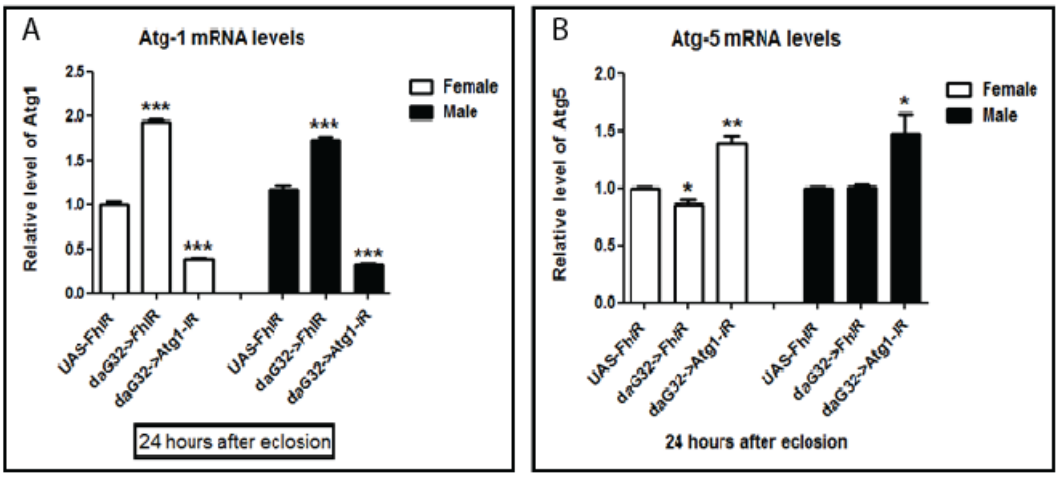

Figure 5: The measurement of *Atg1 and Atg5* mRNA levels in FXN-KD adult *Drosophila* 24 hours after eclosion. The Atg1 KD strain, da^{G32}-*Atg1*.IR was used as positive control. The *Drosophila* eclosed in 18 ^{o}C were immediately transferred to 25 ^{o}C and maintaining for 24 hrs. Each sample containing 10 adult *Drosophila* were homogenized in lysis buffer. The mRNA were extracted and quantified by Nanodrop. **(A)** The FXN-KD female showed 90% increase of *Atg1* mRNA compared to UAS-fh.IR controls($p < 0.001$), while The FXN-KD male *Drosophila* showed 30% increase in *Atg1* mRNA compared to control ($p<0.001$). The Atg1 KD female and male *Drosophila* both showed 70% reduction in *Atg1* mRNA ($p < 0.001$). **(B)** The female FXN-KD *Drosophila* showed relatively decreased *Atg5* mRNA compared to control in female *Drosophila*. The male FXN-KD *Drosophila* showed unchanged *Atg5* mRNA compared to control males. Both male and female *Atg1* KD *Drosophila* showed increased *Atg5* mRNA level ($p<0.01$) and ($p<0.05$).

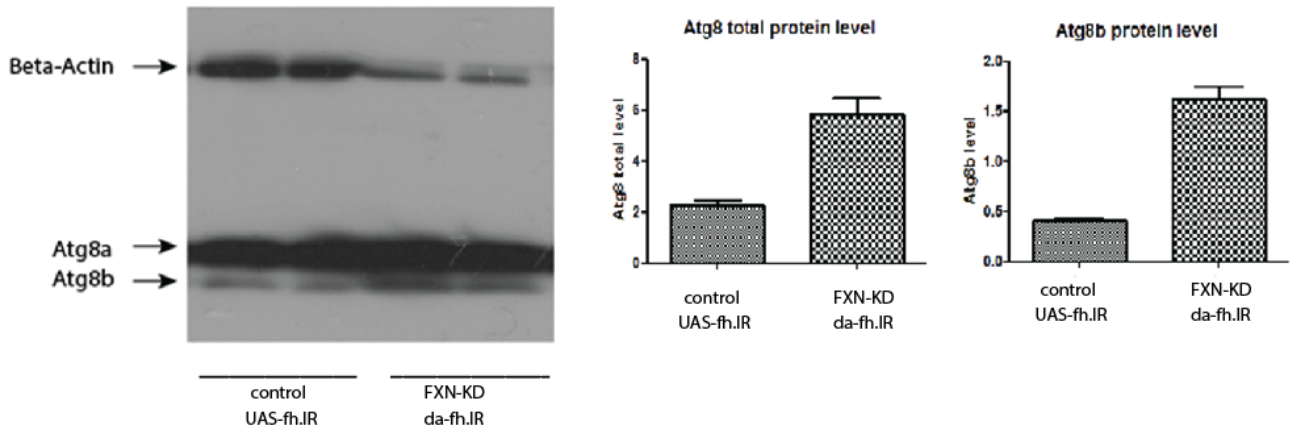

Figure 6: Atg8 a/b protein levels increase in FXN-KD larvae. Third stage larvae were collected at 25 °C. Each sample contained 20 larvae and was homogenized in lysis buffer. Proteins were extracted, purified and quantified by the Bradford Method(3). The ratio of Atg8/Actin was used to determine the relative Atg8 protein level. The *da*^{G32}-fh.IR females showed a 2-fold increase in Atg8 total protein and over three-fold increase in Atg8-II protein, which indicates the quantity of autophagosomes, compared to control larvae.

which indicates the quantity of 1autophagosome formation (182). Atg8a indicates the unlipidated form of Atg8, which is free, cytosolic form dissociated from autophagosomes. Atg8b is the lipidated and autophagosome-membrane-bound form. We performed western blot on Atg8 to compare its levels between *Frataxin* deficiency stocks *vs* control *Drosophila* in different development stages, including larvae, pupae, and adults 24 hours after eclosion. In the larval stage, we found that da^{G32}-fh.IR showed higher level of both Atg8a and Atg8b protein. The quantification of Atg8 showed that the da^{G32}-fh.IR had three-fold more Atg8 protein compared to control *Drosophila* while Atg8b also had more than three-fold up-regulation in the larval stage (**Figure 6**). The increase of Atg8 proteins in larval stages of FXN-KD implicated the autophagosome accumulation and upregulated autophagy activity in the *Frataxin* deficiency *Drosophila*.

Next, we tested the Atg8 protein level in da^{G32}-fh.IR pupae. Because the observed pupae development termination in da^{G32}-fh.IR, we collected pupae at 48 hours after the pupation, right before the termination at the dark pupal stage. The western blot showed that the Atg8a is moderately increased in da^{G32}-fh.IR pupae while the Atg8b exhibits 2.5 fold increases compared to control *Drosophila* (Figure 7). The increase in Atg8b indicated the upregulation of autophagy in the *Frataxin* deficiency in the pupal stage.

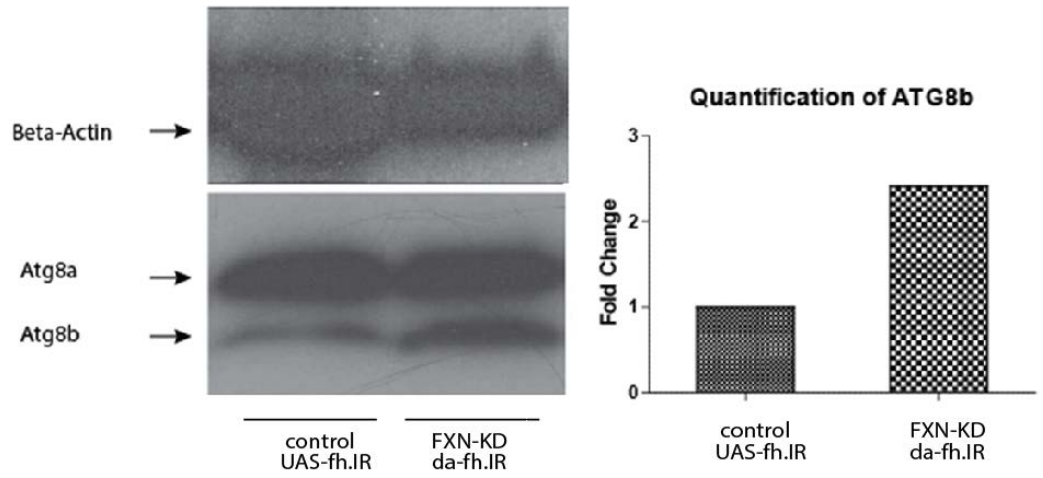

Figure 7: Atg8 protein level increases in FXN-KD pupae. White pupae were collected at 25 ^{o}C. Each sample contained 20 pupae and was homogenized in lysis buffer. Proteins were extracted and quantified. The ratio of Atg8/Actin was used to determine the relative Atg8 protein level. The FXN-KD showed a 150% increase in Atg8-II protein compared to UAS-fh.IRcontrol pupae.

The adult stage FXN-KD *Drosophila* were tested too. The da^{G32}-fh.IR female *Drosophila* and control *Drosophila*. The western blot results showed that FXN-KD female *Drosophila* showed higher Atg8 level than UAS-fh.IR *Drosophila* (Figure 8), confirmed that *Frataxin* deficiency induces autophagy in all developmental stages.

Along with Atg8 levels, we also found that another Atg family member, Autophagy related 16-like 1 (Atg16 L1) protein level was up-regulated in FXN-KD compared to UAS-fh.IR *Drosophila*, which provide further support for the autophagy activation in *Frataxin* partial knockdown *Drosophila* (Figure 9).

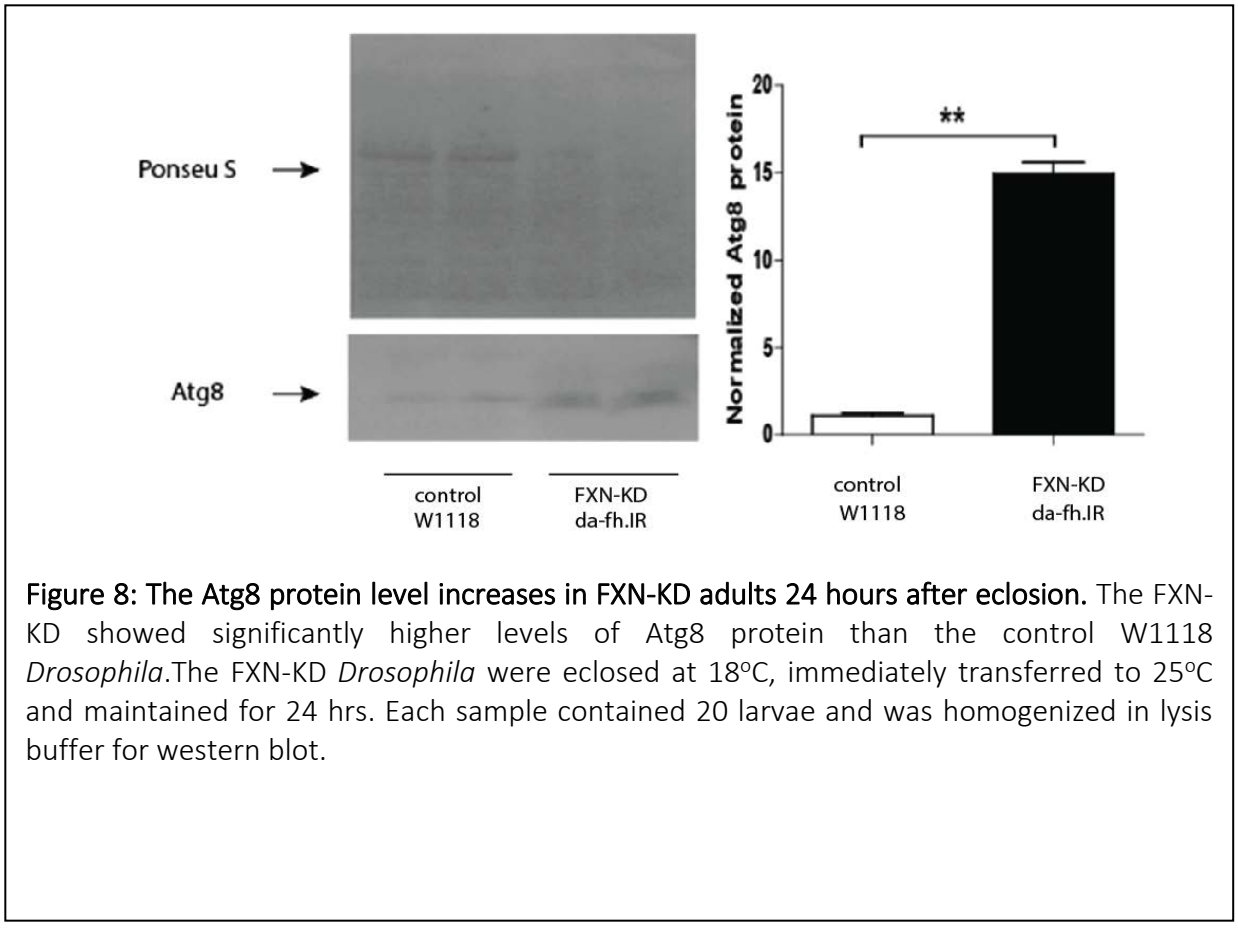

Figure 8: The Atg8 protein level increases in FXN-KD adults 24 hours after eclosion. The FXN-KD showed significantly higher levels of Atg8 protein than the control W1118 *Drosophila*.The FXN-KD *Drosophila* were eclosed at 18^{o}C, immediately transferred to 25^{o}C and maintained for 24 hrs. Each sample contained 20 larvae and was homogenized in lysis buffer for western blot.

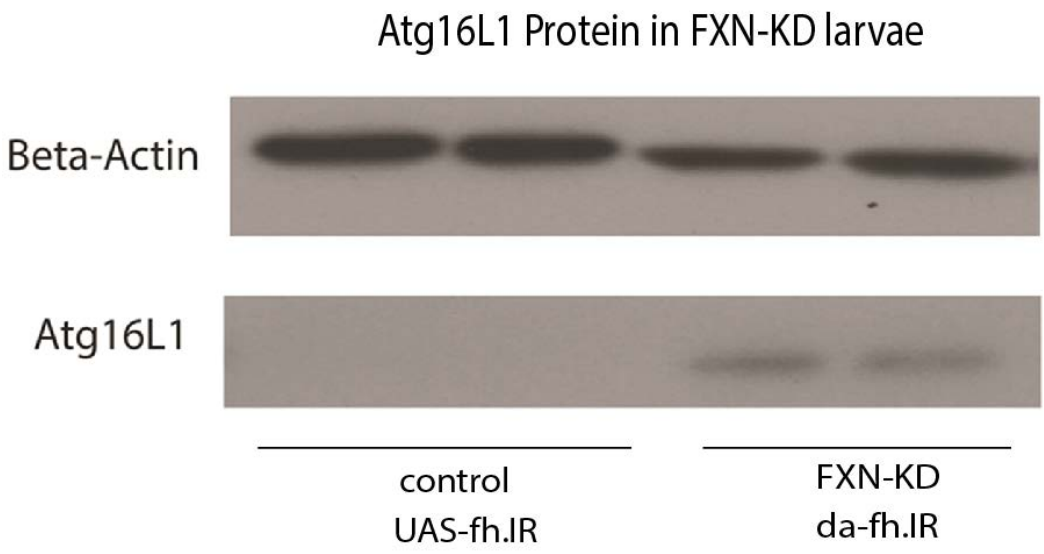

Figure 9: The protein level of Atg16 increases in da^{G32}-fh.IR larvae. The da^{G32}-fh.IR and UAS-fh.IR strains were maintained and tested at 25^{o}C. Each sample contained 20 3rd instar larvae and was homogenized in 200 ul lysis buffer. Proteins were extracted, purified and quantified by the Bradford Method. The da^{G32}-fh.IR showed increased Atg16L1 protein level compared to controls. It indicated up-regulation of autophagy activities in da^{G32}-fh.IR *Drosophila*.

To further test the status of autophagy in *Frataxin* deficiency, another *Frataxin* X-chromosome deficiency strain FXN-D (Df(1)9a4-5, y[1] cv[1] v[1] f[1] car[1]/FM7C) was also tested. Since only the FXN-D adult females are hemizygous for *Frataxin* deficiency, we compared the Atg8 protein level between FXN-D and w1118 female adults. The western blot results showed that FXN-D female *Drosophila* showed higher Atg8 protein level than W1118 *Drosophila*, confirming that *Frataxin* deficiency induces autophagy **(Figure 10)**. The similar results from two different *Frataxin* reduction stocks supported the upregulation of autophagy induction in the *Frataxin* deficiency *Drosophila*.

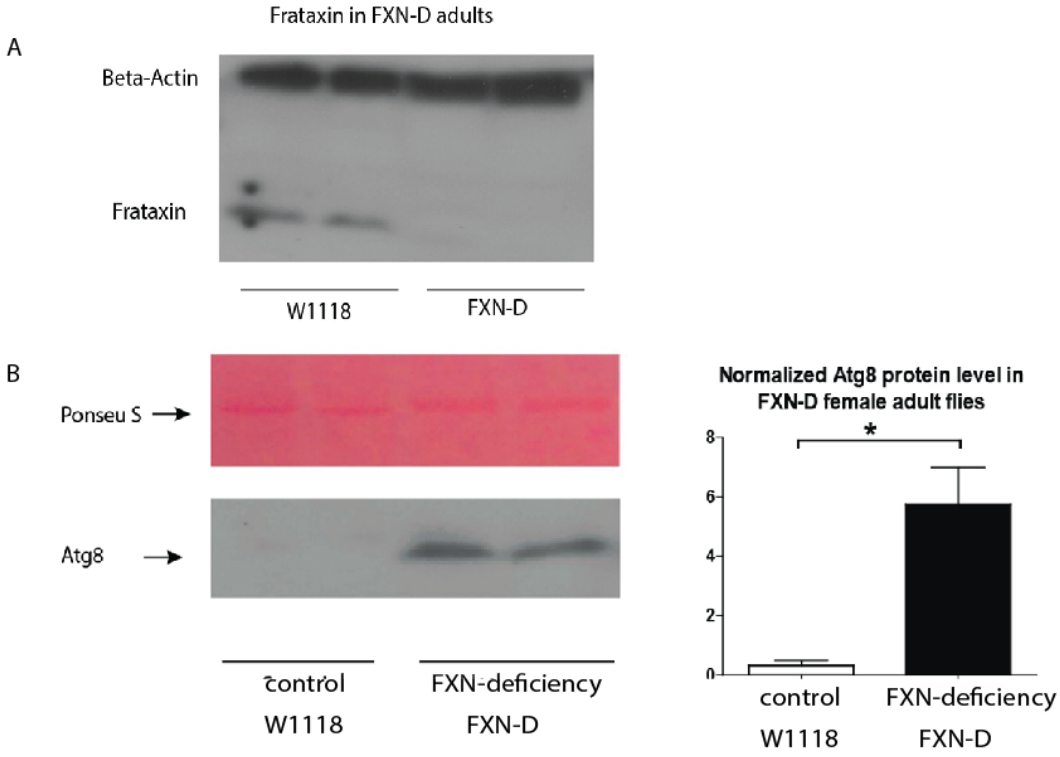

Figure 10: **The Atg8 protein level increases in *Frataxin* deficiency (FXN-D) adult females.** **(A)** The FXN-D female showed less *Frataxin* protein compared to W1118 control females. **(B)**The *FXN*-D females showed significantly increased Atg8 protein level compared to control ($p < 0.05$), indicating a higher level of autophagy. The total protein was shown to be approximately equivalent by Ponceau S staining. The *FXN-D* and control strains were maintained at 25 ^{o}C. Each sample contained 10 files and was homogenized in lysis buffer. Proteins were extracted, purified and quantified by the Bradford Method.

Then we asked the question: what is the function of autophagy in *Frataxin* deficiency *Drosophila*? Based on previous research, there are two possible theories. First, the autophagy could have a anti-oxidative and pro-survival role in *Frataxin* deficiency *Drosophila*. Treatment of autophagy inducer should increase the longevity of FXN-KD *Drosophila* while an autophagy inhibitor should show negative effect on the FXN-KD *Drosophila*. We treated the da^{G32}-fh.IR with media that contains autophagy inducer methylene blue (MB), concentrations of 0.1 µM, 0.5 µM, 1.0 µM, 5.0 µM, and 10 µM. The treatment of UAS-fh.IR control *Drosophila* in MB does not

shown difference up to 7 days after eclosion from 0.1 uM to 0.5 uM (**Figure 11**). The higher dose of MB from 1.0 to 5.0 uM showed certain level of toxicity by reducing the larvae survivor number and pupae formation. Together it showed that the autophagy induced by MB does not affect wild type *Drosophila*, especially in lower doses.

But when we crossed UAS-fh.IR and *da*^{G32}-fh.IR in media containing 0.1 µM, 0.5 µM, 1.0 µM, and up to 5.0 µM MB at 25 ^{o}C, the outcomes were different according to the concentration. In lower doses of MB from 0.1 µM to 0.5 µM, we observed significant less death rates of 2nd and 3rd stage larvae compared to that of control media. The number of 3rd stage larvae was directly associated with the concentration of MB between 0.1 µM and 0.5 µM. More pupae were formed in 0.1-0.5 uM range, which indicates the beneficial effect of induced autophagy. But none of the lower doses of MB treatments were able to rescue the papae lethal phenotype.

When the concentration of MB increased to 1.0 µM and 5.0 µM, we found that almost 100% da^{G32}-fh.IR larvae die before they reach 3rd stage. Very few 2nd stage larvae and no pupae were formed **(Figure 1B)**. The beneficial effect of low concentration and the deleterious effect of high concentration of MB may indicate that mild induction of autophagy could partially rescue the phenotype of FXN-KD larvae while the over-induction of autophagy will produce contrary effect. Although the induction of autophagy cannot rescue the pupal lethal phenotype in da^{G32}-fhIR *Drosophila*, this piece of evidence supported that induction of autophagy within certain ranges could act as protective role in *Frataxin* deficiency *Drosophila*.

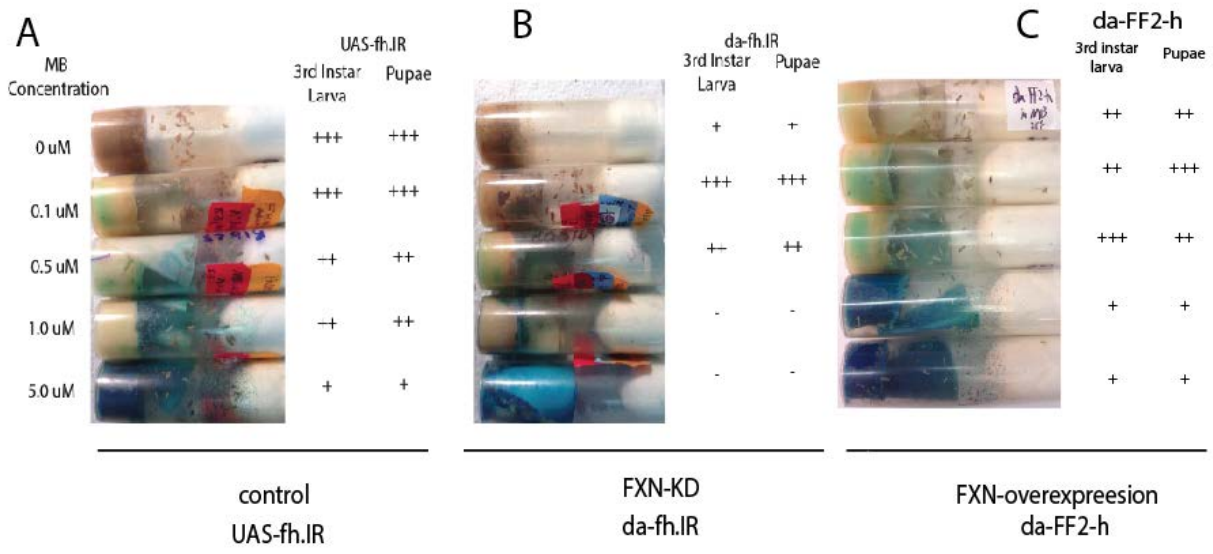

Figure 11: Autophagy inducer Methylene Blue treatment partially rescues the larval lethal rates of da^{G32}-fhIR larvae. (A) 0.1-0.5uM methylene blue does not affect larvae viability and pupae formation rate in UAS-fh.IR *Drosophila*. The treatment of 0.1-0.5uM MB does not affect the larvae viability and pupae formation rate, while 1.0 uM and 5.0 uM concentration showed increased toxicity by reducing the number of larvae and pupae. The methylene blue was dissolved in ethanol and added to the media to the final concentration of 0.1uM, 0.5uM, 1.0uM and 5.0uM. For each concentration, 3 vials were tested, including control vials with normal media. 10 female and 10 male of UAS-fh.IR *Drosophila* were maintained in each vial for 48 hours and then removed. The vials containing eggs were cultured in 25^{o}C. The number of newly emerged larvae and pupae were recorded daily **(B)** The 0.1-0.5uM methylene blue restored larvae viability and pupae formation rate in FXN-KD *Drosophila*. The 1.0 uM and 5.0 uM MB showed reduced number of larvae and pupae. The media preparation is stated above. For each concentration, 3 vials were tested, including control vials with normal media. In each vial, 10 virgin female UAS-fh.IR and 10 male da-Gal4 were maintained for 48 hours and then removed. The vials containing eggs were cultured in 25^{o}C. **(C)** The *Frataxin* overexpression da^{G32}-FF2-h did not affected by MB treatment at 0.1 and 0.5 uM, but the larvae survival rate and pupae formation were reduced at higher MB concentration at 1.0 and 5.0uM. For each vial, 10 virgin female of UAS-FF2-h and 10 male da-Gal4 *Drosophila* were maintained in each vial for 48 hours and then removed. The vials containing eggs were cultured in 25^{o}C.

4.4 Apoptosis is induced in FXN-KD larvae

Because FRDA features accelerated loss of the sensory neurons in DSG, it is reasonable to question if an abnormal apoptosis process is involved in the progression of FRDA (183). However, current findings about apoptosis in FRDA are limited and controversial. It is found that the apoptotic cell death is observed in rats' primary DSG cells in a rat FRDA model (102). Mariana et.al reported that the *Frataxin* knock-down human iPSC derived neurons, and rat β-cells show signs of intrinsic apoptotic pathway activation (101). Our findings of early development termination in both larval and pupal stage in da^{G32}-fh.IR *Drosophila* also implicated the possible role of apoptosis in FRDA *Drosophila*. It is interesting that although *Frataxin* is generally considered a protective role in cells by anti-oxidative stress and DNA damages, recent evidence also revealed its role as tumor-suppressor by promoting apoptosis (184).

Based on the above evidence, we asked whether the *Frataxin* deficiency could trigger the increased apoptosis in the FRDA *Drosophila*, and whether it is through the induction of autophagic cell death (Type II apopotosis). So we hypothesized that *Frataxin* deficiency induces apoptosis and causes the increment of caspase-3 and possibly cytochrome C, which is a mitochondrial protein related intrinsic apoptosis pathway, in FXN-KD *Drosophila*. First we tested the apoptosis marker caspase-3 levels in FXN-KD *Drosophila* vs. control *Drosophila*. The western blot results showed that da^{G32}-fh.IR larvae showed a significant increase of cleaved caspase-3, indicating up-regulation of apoptosis pathways in *Frataxin-deficient* larvae **(Figure 12).**

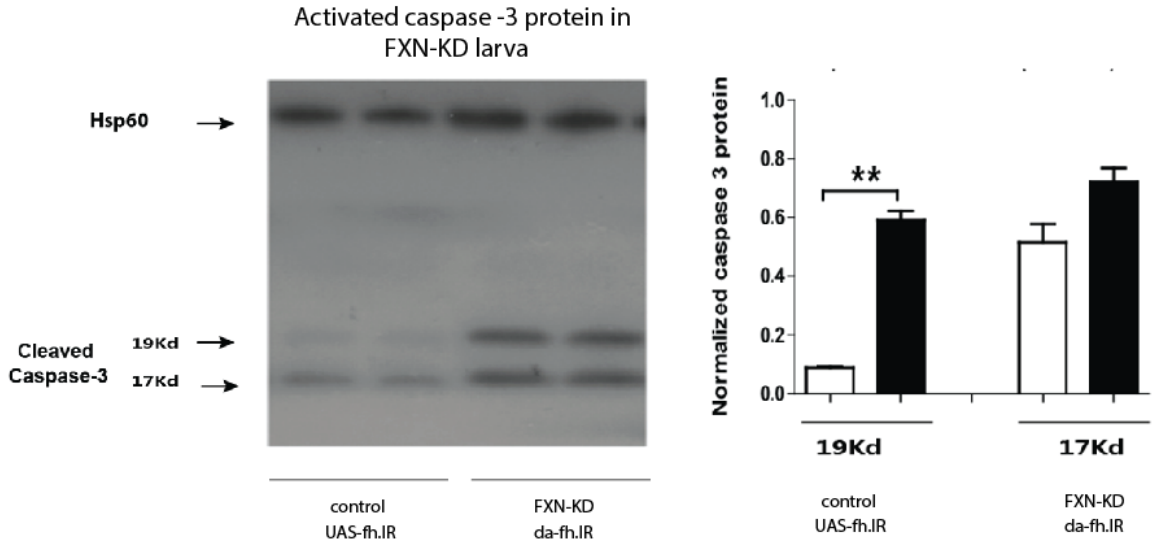

Figure 12: The protein level of apoptosis-related activated caspase-3 increases in da-fh.IR FXN-KD) larvae. The protein level of apoptosis-related activated caspase-3 increases in da^{G32}-fh.IR (FXN-KD) larvae. It showed that adult female *Drosophila* contain a higher level of cleaved caspase-3, indicating a higher level of apoptosis. Two different repeats are shown with HSP60 as the loading control. The FXN-KD and control strains were maintained in 25^{o}C. Each sample containing 10 *Drosophila* was homogenized in lysis buffer. Proteins were extracted, purified and quantified by the Bradford method.

Because *Frataxin* deficiency is closely associated with mitochondrial homeostasis and apoptosis, we decided to test if the apoptosis is activated through intrinsic pathway. A previous study showed when the apoptosis pathways were triggered, mitochondrial cytochrome C were released into cytosol and bound with Apaf-1 and caspase-9 to cleave and activate caspase-3 protein for apoptosis (185). The western blot results showed that in the da^{G32}-fh.IR larvae and pupae, total cytochrome C was significantly higher than the control *Drosophila* in both stages (Figure 12 and Figure 13), indicating an increase of cytochrome C level in the *Frataxin* deficiency *Drosophila* early developmental stages. It implied the increase of apoptosis in FRDA *Drosophila* is through intrinsic pathway. In summary, the deficiency of the *Frataxin* deficiency induced apoptosis in FRDA *Drosophila*, possibly through intrinsic pathways.

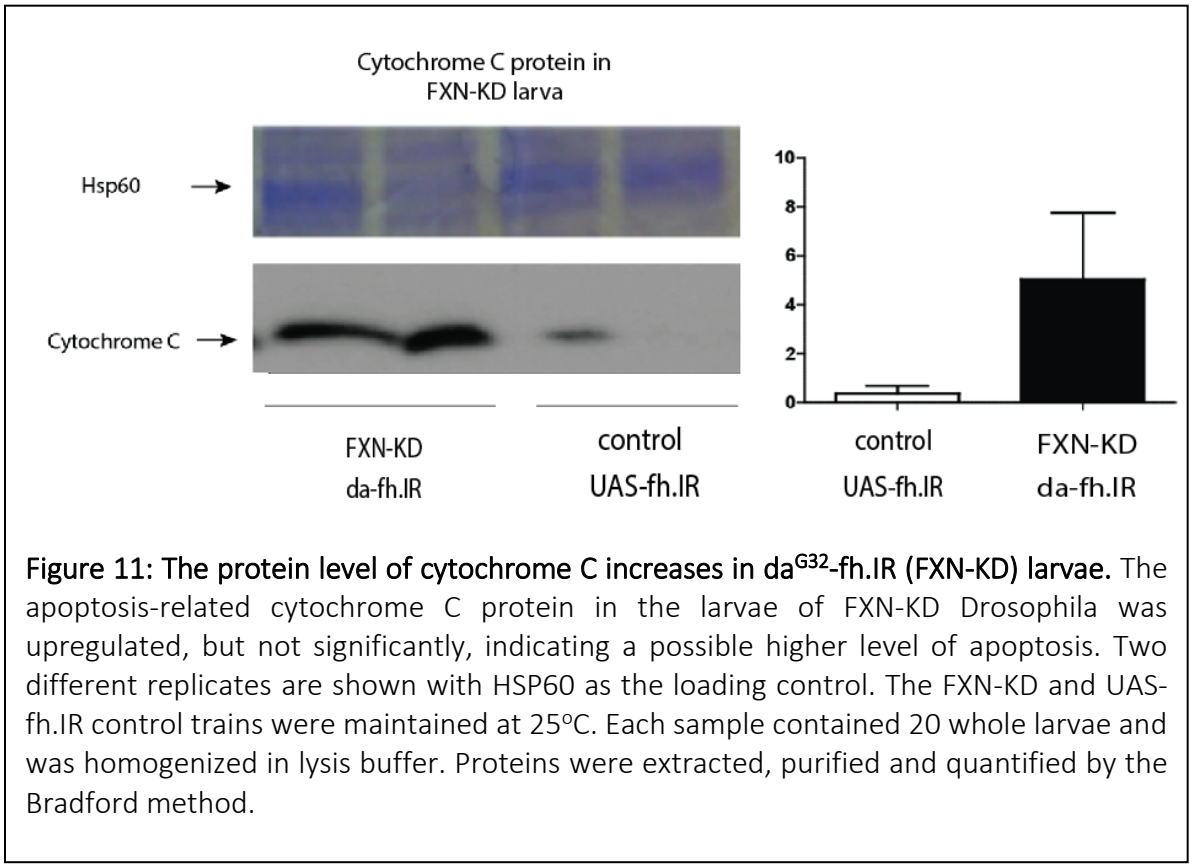

Figure 11: The protein level of cytochrome C increases in da^{G32}-fh.IR (FXN-KD) larvae. The apoptosis-related cytochrome C protein in the larvae of FXN-KD Drosophila was upregulated, but not significantly, indicating a possible higher level of apoptosis. Two different replicates are shown with HSP60 as the loading control. The FXN-KD and UAS-fh.IR control trains were maintained at 25°C. Each sample contained 20 whole larvae and was homogenized in lysis buffer. Proteins were extracted, purified and quantified by the Bradford method.

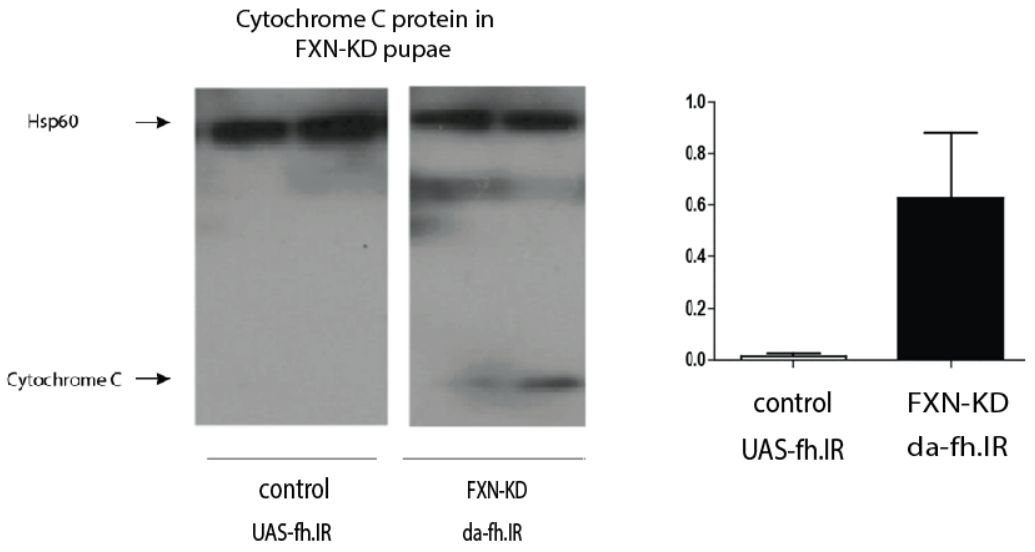

Figure 12: The protein level of cytochrome C increases in pupae of da^{G32}-fh.IR (FXN-KD). The apoptosis-related cytochrome C in the pupae of FXN-KD *Drosophila* was upregulated, although not significant, indicating a possible higher level of apoptosis. Two different replicates are shown with HSP60 as the loading control. The FXN-KD and control UAS-fh.IR strains were maintained at 25°C. Each sample contained 20 pupae and was homogenized in lysis buffer. Proteins were extracted, purified and quantified by the Bradford method.

4.5 Autophagy is induced in *Frataxin*-overexpression da^{G32}-FF2-h *Drosophila*

Our previous study showed detrimental phenotype in FRDA *Drosophila*, so we decided to test if overexpressing wildtype *Frataxin* in *Frataxin* deficiency background could rescue the phenotypes such as larval and pupae lethal. We crossed the UAS-FF2-h stock with da^{G32}-Gal4 to obtain the *Frataxin* overexpressing da^{G32}-FF2-h progeny. The progeny was pupal lethal at 25°C and had normal fertility and viability at 18°C. Real-time PCR showed that da^{G32}-FF2-h *Drosophila* have over 10 folds *Frataxin* mRNA level compared to control *Drosophila*, in both genders (**Figure 14**). Considering the abnormal fertility and viability of da^{G32}-FF2-h *Drosophila* in 25°C, the significant *Frataxin* overexpression negatively affected *Drosophila* viability and fertility, similar to the *Frataxin* deficiency *Drosophila*. In summary, both *Frataxin* deficiency and overexpression in a

large scale both negatively impact the survival rate and longevity of *Drosophila*.

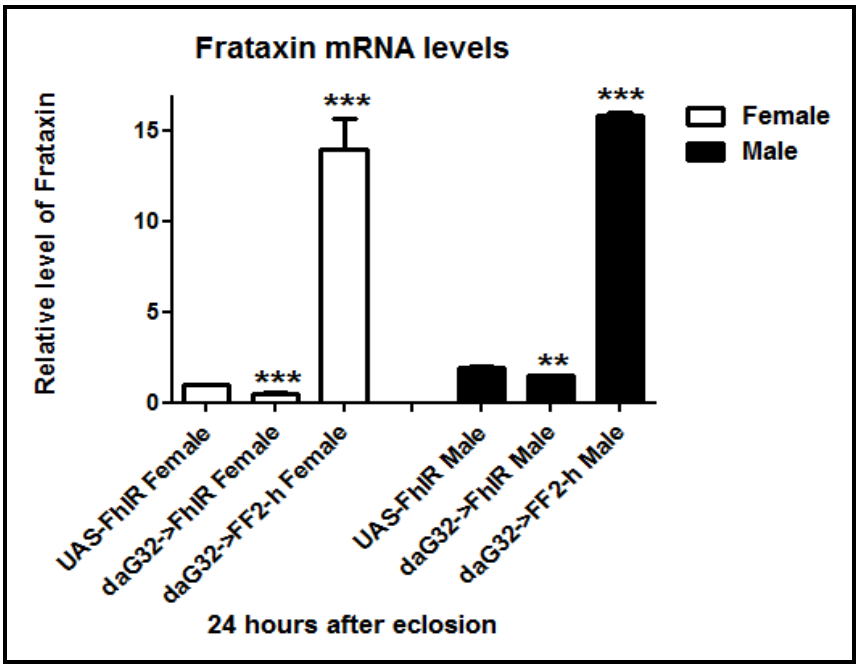

Figure 13: The *Frataxin* mRNA level increase in *Frataxin* overexpressing (da^{G32}-FF2-h) Drosophila 24 hours after eclosion. The *Frataxin* mRNA level increase in *Frataxin* overexpressing (**da^{G32}-**FF2-h) Drosophila 24 hours after eclosion. The *Frataxin* overexpressing female showed 12 fold increase of *Frataxin* mRNA compared to control ($p < 0.001$) while *Frataxin* overexpression male showed a 15-fold increase over control males ($p < 0.001$). The Drosophila eclosed at 18 ^{o}C and were immediately transferred to 25 ^{o}C and maintained for 24 hrs. Each sample contained 10 Drosophila and was homogenized in lysis buffer. The mRNA was extracted, purified and quantified by Nanodrop. The experiments were done in triplicate. *, p-value<0.05; **, p-value < 0.01; ***, p-value < 0.001. The significance symbols are the same for all of the gene expression figures that follow.

To assess if *Frataxin* overexpression is associated with autophagy alterations, we compared *Atg1* and *Atg5* mRNA levels in da^{G32}-FF2-h *Frataxin*-overexpression *Drosophila* and control UAS-FF2-h *Drosophila*. The real-time PCR results showed that *Atg1* mRNA level increased about 2.5-fold and 3-fold compared to female and male control *Drosophila*. The *Atg1* level in *Frataxin* overexpression *Drosophila* was 25% and 80% higher than that of *Frataxin*-deficient *Drosophila* (Figure 15A). When comparing *Atg5* mRNA levels, we found that similar to *Frataxin*-

deficient *Drosophila*, *Frataxin overexpression Drosophila* do not show a significant increase in *Atg5* transcription levels. On the contrary, the *Atg5* mRNA was reduced in both male and female da^{G32}-FF2-h *Drosophila* (**Figure 15B**). Based on the above results, we concluded that the overexpression of *Frataxin* in *Drosophila* increases *Atg1* mRNA but does not change Atg5 mRNA.

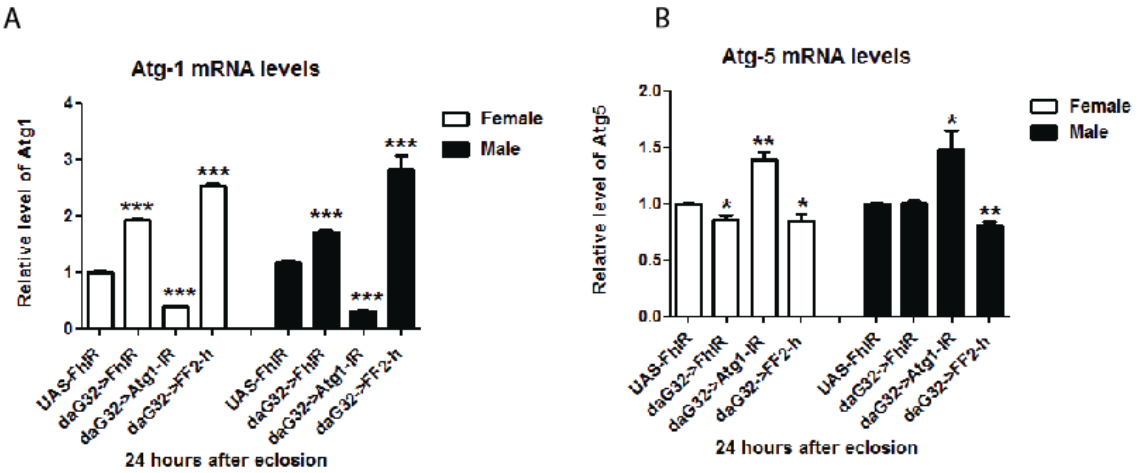

Figure 14: The mRNA level of *Atg1* and *Atg5* genes in FXN-KD and overexpression *Drosophila*. **(a)** *Atg1* mRNA levels in *Frataxin-deficient* (da^{G32}-fh.IR), overexpressing (da^{G32}–FF2-h), and UAS-fh.IR control adult *Drosophila* 24 hours after eclosion are different. The *Atg1* KD strain, da^{G32} -*Atg1*.IR was used as positive control. The *Frataxin* overexpressing female showed 150% increase in *Atg1* mRNA while FXN-KD *Drosophila* showed 100% increase in Atg1 mRNA compared to control adults ($p < 0.001$). The FXN-KD male *Drosophila* showed 30% increase in Atg1 mRNA compared to WT ($p<0.001$) while *Frataxin* overexpressing *Drosophila* showed a 200% increase in *Atg1* mRNA compared to control male *Drosophila*. **(b)** *Atg5* mRNA level in FXN-KD, da^{G32}–FF2-h, and control adult *Drosophila* 24 hours after eclosion. The female *Frataxin* overexpressing *Drosophila* showed about 15% reduction in *Atg5* mRNA ($p<0.05$) compared to control females, similar to FXN-KD females. The male *Frataxin* overexpressing *Drosophila* showed 25% reduction in Atg5 mRNA compared to control males ($p<0.01$). The *Drosophila* eclosed at 18^{o}C and were immediately transferred to 25^{o}C and maintaining for 24 hours Each sample contained 20 larvae and was homogenized in lysis buffer for PCR.

We also treated the da^{G32}-FF2-h *Drosophila* with autophagy inducer MB. The *Frataxin* overexpression da^{G32}-FF2-h were not distintly affected by MB treatment at 0.1 and 0.5 uM, but the larvae survival rate and pupae formation were greatly reduced at higher MB concentration at

1.0 and 5.0uM, showing further increase of autophagy would be detrimental (Figure 11C).

4.6 Pathways of mitochondrial quality control and mitophagy in FRDA *Drosophila*

As mentioned before, damage of mitochondria was intensively studied in FRDA. It is still not clear about the possible events downstream of dysfunctional mitochondria. Based on our our results, we asked the question that if the changes of autophagy are associated with mitochondrial function or the mitochondrial autophagy (mitophagy), a major mechanism to remove damaged mitochondria. First, we examined the status of mitochondria in FXN-KD. The levels of two mitochondrial proteins were tested. The mitochondrial matrix protein *Hsp60* was measured as mitochondrial quantity while the pyruvate dehydrogenase is measured as an indicator of mitochondrial function. The western blot results showed that the Hsp60 protein level remains stable in FXN-KD larvae compared to controls, in both 18 ^{o}C and 25 ^{o}C, suggesting that the quantity of mitochondria does not change (Figure 16). The pyruvate dehydrogenase protein level, however, was reduced in da^{G32}-fh.IR at 25^{o}C, suggesting a possible dysfunction of the mitochondria (Figure 16) and matches the description from previous research of mitochondria in FRDA models.

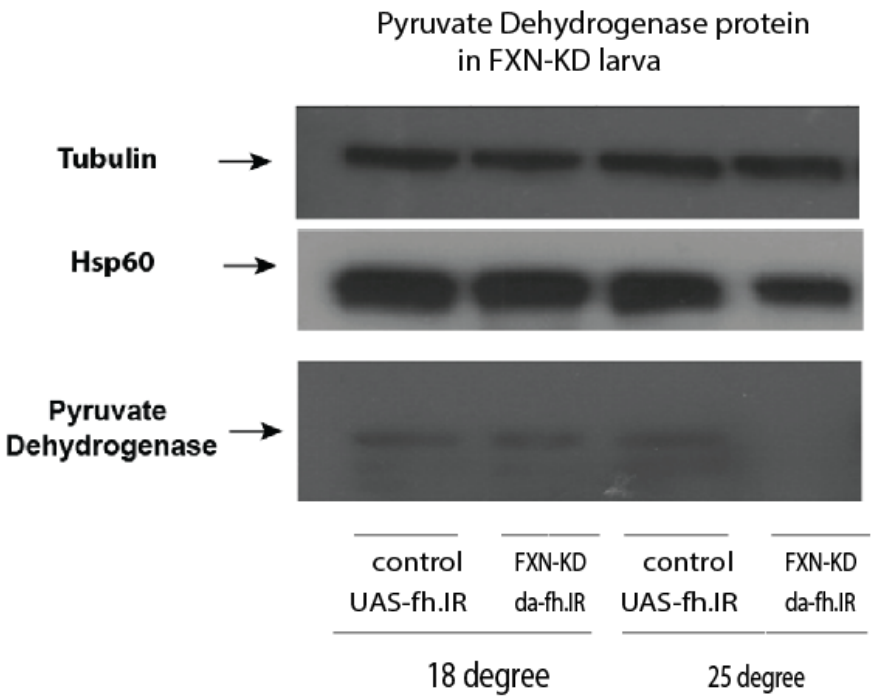

Figure 15: The protein level of Hsp60 and pyruvate dehydrogenase in da^{G32}-fh.IR (FXN-KD) larvae. The results showed that the mitochondrial marker Hsp60 does not change, but the amount of pyruvate dehydrogenase is reduced in FXN-KD *Drosophila*, indicating possible functional loss in the mitochondrial respiratory chain, but the mitochondrial quality is not altered.

Next, we tested the level of mitophagy by mitophagy marker protein Parkin, whose level usually increases upon environmental stress factors, in 24 hours old FXN-KD *Drosophila*. The results showed that the level of *Parkin* is slightly but not significantly increased in da^{G32}-fh.IR adult *Drosophila* (Figure 17). It is also possible that the *Parkin* does not change dramatically in translational level during the induction of mitophagy, but changes the distribution between cytosolic and mitochondrial.

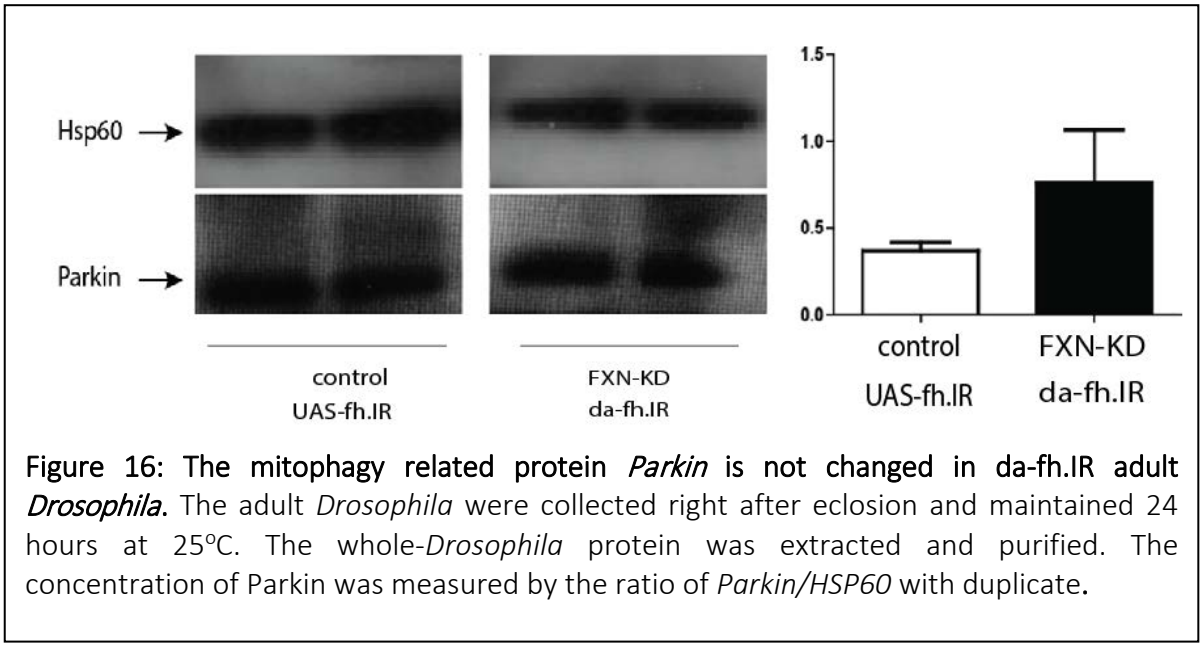

Figure 16: The mitophagy related protein *Parkin* is not changed in da-fh.IR adult *Drosophila*. The adult *Drosophila* were collected right after eclosion and maintained 24 hours at 25°C. The whole-*Drosophila* protein was extracted and purified. The concentration of Parkin was measured by the ratio of *Parkin/HSP60* with duplicate.

4.7 Heart functions are not changed in *Frataxin*-deficient *Drosophila*

One of the most distinct features of FRDA patients is high rates of cardiomyopathy incidences (30). So we attempted to test if the *Drosophila* heart function in *Frataxin* deficiency *Drosophila* is also affected using heart pacing assay (156). We chose to perform the heart assay

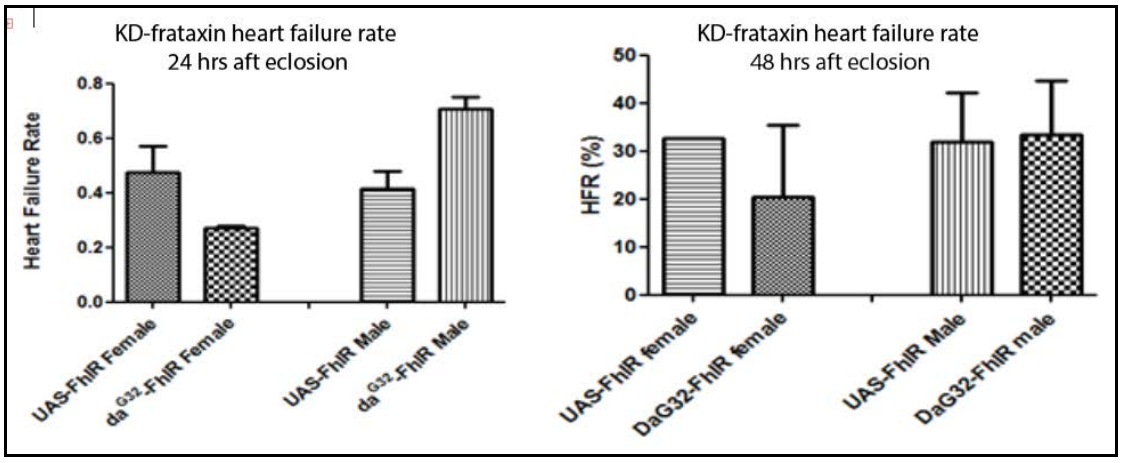

Figure 17: The Heart Pacing Assay in da-fh.IR *Drosophila* at 24 hours and 48 hours after eclosion. The KD-FXN female *Drosophila* showed reduced heart failure rate at 24 hours of age compared to control female *Drosophila*, but the differences is not significant at 48 hours. The male KD-FXN *Drosophila* showed higher heart failure rate at 24 hours of age compared to control males but not at 48 hours of age. The adult *Drosophila* were collected right after eclosion and maintained 24 hours at 25°C. In each group, 50 *Drosophila* were anesthetized with flynap and electrically pacing for 10 seconds at 20 Volts under microscope.

on two different *Frataxin* deficiency stocks, the ubiquitous *Frataxin* knock-down strain FXN-KD da^{G32}-fh.IR and the heart-specific *Frataxin* knock down strain GMH5-fh.IR. To obtain the GMH5-fh.IR, we crossed the UAS-fh.IR Drosophila with heart-specific GMH5-Gal4 Drosophila (Gift from Dr. Wessells) to get the GMH5-fh.IR Drosophila, which were normal in viability and fertility at 25^{o}C. In summary, we did not observe a significant difference in stress-induced heart failure rate between da^{G32}-fh.IR and control Drosophila at 24 hours and 48 hours after eclosion (**Figure 18**). The same result was observed on the GMH5-fh.IR Drosophila with a very high variation range. Our explanation is that the strength of the heart pacing assay may be too intense to distinguish the chronical cardiac changes between *Frataxin* deficiency Drosophila and control Drosophila.

4.8 AMPK, but not pSAPK was upregulated in *Frataxin* Deficiency Drosophila

The above data of our study showed increased autophagy in *Frataxin* deficiency Drosophila and its possible relationship with apoptosis and mitophagy. We are also interested in the upstream events that may be inducing autophagy. As one of the central controller of the oxidative stress response, AMPK is associated with autophagy induction by phosphorylating and activating *Atg1*, under stress or starvation condition (186). First, we examined the level of phosphorylated AMPK in FXN-D Drosophila 24 hours after eclosion because AMPK is activated through phosphorylation. We measured the phosphorylated AMPK (pAMPK) level in hemizygous *Frataxin* deficiency FXN-D female Drosophila vs. FXN-D male Drosophila as a control. The test was performed in both whole-body and heads (neurons) from adults 24 hours after eclosion. The results showed that the pAMPK level is increased in FXN-D females, in both whole body and neurons (**Figure 19**). It indicated the increased phosphorylation level of AMPK in the whole body and neurons in *Frataxin* deficiency Drosophila. The similar expression pattern of pAMPK and Atg8

suggests a possible role of AMPK in regulating autophagy in FXN-D Drosophila.

Besides AMPK, the other stress regulating pathway, the SAPK pathway, also attract our attention. It is proposed that neurons in Alzheimer disease are exposed to low, but chronic, levels of oxidative stress that lead neurons to elicit adaptive responses such as the activation of stress-activated protein kinase pathways (SAPK) (187). We tested the level of phosphorylated SAPK (pSAPK) in FXN-KD Drosophila at 24 hours after eclosion. The result shows the level of pSAPK in FXN-KD is not changed (Figure 20). This may indicate the change of *Frataxin* level in FXN-KD *Drosophila* does not alter the phosphorylation status of SAPK. In summary, the experiments

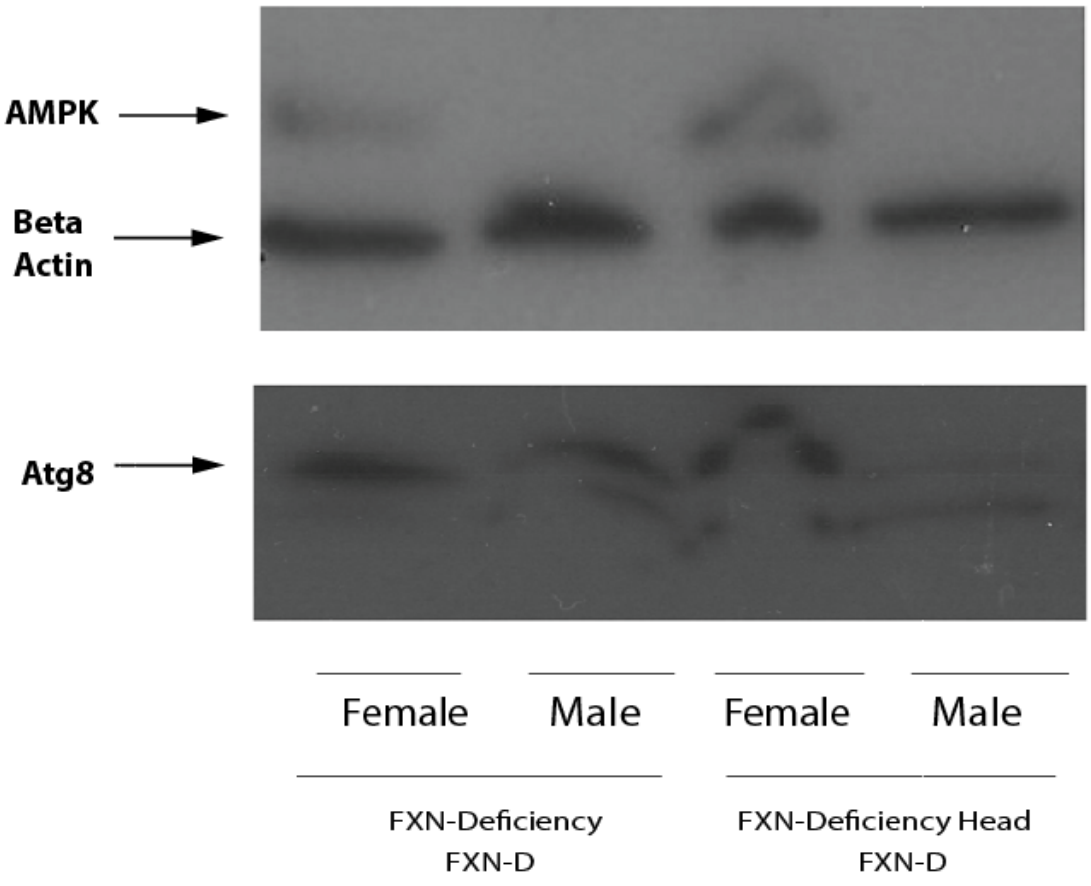

Figure 18: pAMPK level increases in FXN-D adult Drosophila. FXN-D male and female *Drosophila* at the age of 1 day were collected. The protein was extracted and detected using beta-Actin and Phospho-AMPK-α (Thr 172) antibody (1:500). The ratio of pAMPK/Beta-Actin was recorded.

showed that the increase of pAMPK was observed in *Frataxin* deficiency *Drosophila*, but not the pSAPK level.

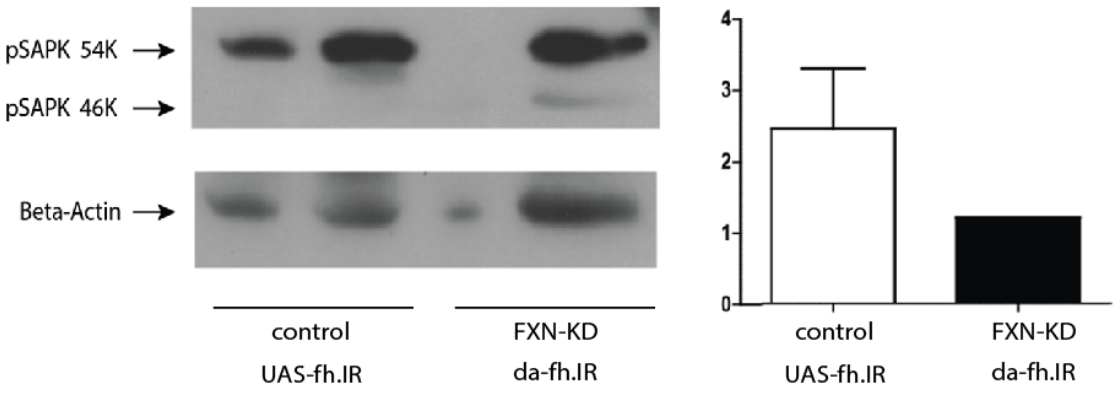

Figure 19: pSAPK protein level is not changed in da^{G32}-fh.IR *Drosophila*. FXN-KD male and female *Drosophila* at the age of 1 day were collected. The protein were extracted and detected using beta-Actin and Phospho-SAPK/JNK (Thr183/Tyr185) antibody (1:500). The ratio of pSAPK/Beta-Actin were recorded.

5. Discussion

As an evolutionarily conserved process, autophagy plays an important role in many biological activities. To investigate its involvement in *Drosophila* FRDA model, we first obtained two *Frataxin* deficiency stocks, da^{G32}-fh.IR, which expresses an inverted repeat hairpin RNA of *Frataxin* gene under control of Gal4, which we term FXN-KD, and FXN-D, which is a deficiency stock. The FXN-KD efficiently reduced the *Frataxin* mRNA and protein levels to 50-70% and 40%, respectively, from real-time PCR and Western blot results. The percentage of reduction in the *Drosophila* model resembles the *Frataxin* protein levels in FRDA patients, which is around 40-70% percent reduction (11). A review of recent studies of *Frataxin* KD experiments from other laboratories shows that the viable KD strains maintain an average of 25%-50% protein levels compared with wild-type levels. The KD efficiency in existing FXN-KD mouse models and cell lines

vary from 20%-80% (171, 188). The further reduction of *Frataxin* in *Drosophila* by up-regulating the expression of the UAS-Gal4 system from 18C to 25 ^{o}C renders premature death of da^{G32}-fh.IR pupae. So the 60% reduction in *Frataxin* protein level in our model could be deemed an effective KD.

The reduced longevity and diminished mobility in FXN-KD *Drosophila* may be due to the increasing accumulation of oxidative stress damage from the *Frataxin* reduction. This is in accordance with the results obtained by Anderson et.al in 2005 (181). This result proved the constructed da^{G32}-fh.IR line resembles the phenotype in human FRDA patients. Since the UAS-GAL4 system depends on the siRNA pathway, we constructed control strains to avoid the effects from hairpin RNA. The da^{G32}-GFP.IR showed normal longevity and fertility in 25^{o}C, proving the *daughterless* gene from da^{G32}-Gal4 strains and inverted repeat hairpin RNA structure do not interfere with control *Drosophila*. For further confirmation of the *Frataxin* knock down deficiency, we also tested the FXN-D deficiency strains with hemizygous *Frataxin* allele deficiency. Although the FXN-D strain has better fertility, the similar phenotypes in longevity and locomotive ability proves that the defects are associated with the *Frataxin* deficiency, which proves the da^{G32}-fh.IR and FXN-D *Drosophila* qualify for FRDA model animals for the following works.

The autophagy has been closely associated with ROS metabolism and mitochondrial homeostasis in FRDA patients and other model systems. We are the first lab to characterize and quantify the autophagy in FXN-KD *Drosophila* models. We detected an increase of Atg1 in transcription level in FXN-KD da^{G32}-fh.IR adult *Drosophila* that were 24 hours old. It has been reported that the *BmAtg1* (the *Atg1* homologue in silkworm, *Bombyx* mori) mRNA increased 50% to 400% in different stages in the fat body of silkworms under starvation compared to control

samples (189). The Ulk1 mRNA level doubles when the drug Baicalein induces autophagy in HT29, HCT116, MCF7 and U373-MG cell lines (190). So the observed increase of *Atg1* mRNA strongly supports that autophagy activity is induced in FXN-KD *Drosophila*.

On the other hand, the mRNA level of Atg5, another essential gene for autophagy, did not change in FXN-KD *Drosophila*. It is possible that Atg5 mRNA level does not change significantly Previous studies showed that Atg5 mRNA and protein levels increase when the oxidative stress level increases in rats (191). One possible explanation is that the induction of autophagy in FRDA may be through the Atg5-independent pathway which is regulated by Ulk1 and beclin-1. This Atg5/Atg7 independent autophagy pathway in mouse MEFs was described at 2009 and 2014 by Nishida and colleagues (157, 192). In the lens of the mouse's eye, *Atg5* knockout did not affect the organelle degradation, which also indicates the existence of *Atg5* independent autophagy pathway (193). Although currently it is no evidence that such pathway exists in *Drosophila,* the further study will be helpful to examine if the relatively unchanged Atg5 mRNA levels in the FXN-KD *Drosophila* model is a result of the Atg5/Atg7 independent autophagy induction pathways.

The western blot results showed an increase of autophagy marker Atg8a/b protein levels in FXN-KD. The increased levels of both Atg8a and Atg8b proteins in all stages (larvae, pupae, and adult) indicated the accumulation of autophagosomes, which indicating up-regulation of autophagy in FXN-KD and FXN-D *Drosophila*. We also tested the level of Atg16, and it showed signs of increase. Although the increase is not significant, the increase served as another line of proof for the upregulation of autophagy.

After the confirmation of autophagy increase, we further looked into the possible functions of autophagy in *Frataxin* deficiency *Drosophila* model. We decided to observe the

effect of autophagy inhibitors and inducers on the *Frataxin* deficiency *Drosophila*. Our results indicate that inhibitor chloroquine reduced the longevity of FXN-KD *Drosophila* while autophagy inducer methylene blue increased the longevity of FXN-KD and FXN-D, showing a protective role of autophagy in *Frataxin* deficiency. But increased concentration of MB could not be able to increase the survival rate of pupal lethal in FXN-KD at 25^{O}C. Additionally, when the lower concentration of MB (0.1 to 0.5 uM) reduced the lethal rates and increased number of 3^{rd} instar FXN-KD *in* larvae, higher concentration of MB (1.0-5.0 uM) showed limited number of survival larvae and no sign of 3^{rd} instar lavae and pupae. This indicates that the protective mechanism of autophagy induced by *Frataxin* deficiency may be affected by multiple factors, and further research is required.

In the MB treatment experiments, we observed that when the concentration of MB increases to more than 5 μM, the beneficial effect on FXN-KD *Drosophila* diminished. The FXN-KD *Drosophila* in a higher concentration of MB showed high levels of early larval lethal rates and resembled the high lethal rate in non-treatment FXN-KD larvae at 25^{o}C. So we hypothesize that the *Frataxin*-deficiency may induce apoptosis in certain stages, possibly through autophagy. Our test confirmed that apoptosis marker, cleaved caspase-3 protein levels are significantly increased in the third larval stage of FXN-KD with 97-99% lethal rate. The following test showed the increase of cytochrome C indicating the increased apoptosis could be due to the cytochrome C mediated apoptosis. This type of apoptosis is originated from the damage of mitochondrial, which is in accordance with the previous observations in FRDA samples. Further works to test the outcome of apoptosis inhibitor and autophagy inhibitor in FXN-KD *Drosophila* could help one understand the mechanisms in more detail.

We also found that the *Frataxin* overexpression *Drosophila*, da^{G32}-FF2-h, which have 6-10 fold higher levels of *Frataxin* mRNA than control, also showed an increased *Atg1* mRNA level, as well as defects in longevity. To our knowledge, this is the first time that *Frataxin* overexpression is associated with autophagy upregulation. The previous studies recorded various results from *Frataxin* overexpression animal models. Some research shows that the overexpression of wild-type FRDA in FRDA-mutant cells could rescue the mutant phenotype. For example, Tan et.al showed *Frataxin* overexpression by transfecting *Frataxin* cDNA into FRDA lymphoblast, with 147% and 85% mRNA level compared to controls, reverts the symptoms such as decreased mitochondrial membrane potential and increased filterable mitochondrial iron (8). The *Frataxin* overexpression up to 4 fold in *Drosophila* showed resistance to oxidative stress insults, increased antioxidant production and extended longevity (194). Overexpression of *Frataxin* at 4 fold in hearts and at 10 fold in the pancreas showed similar phenotypes as their controls and did not show a significant difference in antagonizing DOX (doxorubicin) induced cardiotoxicity (195).

Similar to our results, there is also a study that showed that the overexpression of *Frataxin* in *Drosophila* at high levels disrupts development (10). When the *Frataxin* level was brought to 9-fold, the *Drosophila* had a shorter life span and reduced locomotor phenotypes. *Frataxin* overexpression is also induced cell degeneration and lipid droplet accumulation in glial cells. The sensitivity to oxidative stress damage was also increased in *Frataxin* over-expressing cells, with a reduction in both aconitase activity and NDUFS3 protein level (10). Collectively, our results showed that *Frataxin* high dose overexpression (10 fold) in *Drosophila* exhibits similar symptoms as *Frataxin-deficient Drosophila*, which is in agreement with the findings of Navarro *et al.* (10). As we found with FXN-KD *Drosophila*, we also found that *Atg1* mRNA is increased in

Frataxin overexpression *Drosophila*. The similarity of responses of the Atg genes at the transcriptional level from our study indicates that both deficiency and high dose overexpression of *Frataxin* in *Drosophila* introduces detrimental effects on longevity and locomotive activity through autophagy activation. This piece of information will be helpful for the clinical applications for FRDA patients.

Because previous research does not reveal the detailed outcomes of the damaged mitochondria in FRDA, we started to look at the status of mitochondrial quality control mechanisms in the *Frataxin* deficiency *Drosophila*, especially the mitophagy process. Since previous reports did not find a significant reduction in mitochondrial contents despite the extensive evidence of damage, we hypothesize that there is a potential failure in mitophagy, the major mitochondria removal pathway. We showed the relatively stable level of HSP60 in FXN-KD larvae, indicating the mitochondrial contents do not change significantly. Our further test of mitochondrial protein pyruvate dehydrogenase showed decreased protein level in da^{G32}-fh.IR larvae at 25^{o}C, implicating the reduction of mitochondrial function. To measure the status of mitophagy, we tested the protein level of PARKIN in the da^{G32}-fh.IR larvae. The level of PARKIN in whole-cell lysate from da^{G32}-fh.IR larvae remains the same level. This indicates the PARKIN does not change in translation level. The test of mitochondrial membrane-bound PARKIN will be more accurate to determine the status of mitophagy in da^{G32}-fh.IR.

We also extended our research into the possible cardiac defects in FXN-KD *Drosophila*, and whether those defects could be detected using electric heart pacing arrays. However, the heart pacing results were inconclusive. When being paced at 20 volts, da^{G32}-fh.IR *Drosophila* did not show significant differences in the rate of heart failure and fibrillation compared to control

Drosophila. Our explanation is that the sensitivity of the heart pacing assay may not be enough to detect the chronical progression of heart function loss caused by *Frataxin* deficiency. Another possibility is that in da^{G32}-fh.IR *Drosophila*, the reduction of *Frataxin* in the heart may not as much as cardiac cell specific knockout. Another work recently published by Tricoire and colleagues, used a heart-specific Hand-GS Gal4 promoter to construct HandGS/ (fhRNAi) FRDA *Drosophila*. The knockdown effect was induced by RU486 treatment in the media. Their *video* imaging to measure the heart tube M-Mode patterns showed that the *Frataxin* reduced heart has impaired dilatation and systolic function (196). Our work, together with their findings, showed the value of FXN-KD *Drosophila* as an *in vivo* system for the neurodegenerative and cardiac diseases such as FRDA.

In summary, our work shows that autophagy increases in both *Frataxin* deficiency and overexpression *Drosophila*. The mitochondria function changes in FRDA *Drosophila* but the mitophagy level does not change significantly. Our work proves the further value of the *Drosophila* FRDA model in better understanding the mechanisms of this devastating disease in humans.

CHAPTER 2: THE DROSOPHILA TET ORTHOLOG, dTET, IS REQUIRED FOR HYDROXYMETHYLATION OF NUCLEAR AND MITOCHONDRIAL DNA AND ENHANCES THE POLYCOMB-MUTANT PHENOTYPE IN ADULTS

1. Introduction

1.1 DNA methylation and mitochondrial DNA.

The regulation of gene transcription by epigenetic modification during essential developmental stages, such as cell differentiation and genomic imprinting, has drawn an increasing amount of attention in recent years. Interest has grown dramatically after the discovery of the importance of epigenetic reprogramming during the generation of induced pluripotent stem cells (iPSCs). The epigenetic modification process includes DNA and histone modification, among which DNA methylation is one of the most understood mechanisms. The major form of DNA methylation is 5-methylation of cytosine (5-^{m}C), which involves the addition of a methyl group (CH_3-) to the number 5 carbon of the cytosine base. 5-^{m}C is enriched in CpG dinucleotides, and it has been shown to be involved in transcriptional silencing, X chromosome inactivation, normal development, and carcinogenesis (197). Recent research has revealed that the relatively stable 5-^{m}C pattern in stem cells is the result of a dynamic balance between DNA methylation by DNA methyltransferase and demethylation by Dnmt1. The DNA methylation process consists of *de novo* DNA methylation by DNA methyltransferase (Dnmt3a and 3b in mammals) and maintenance of DNA methylation after DNA replication by DNA methyltransferase 1 (Dnmt1). Dnmt3a/3b enzymes bind to unmethylated DNA sequences for *de novo* methylation while Dnmt1 preferentially binds to hemi-methylated DNA strands and methylates the 5-^{m}C sites on the daughter strand after DNA replication (198, 199). In comparison, however, the demethylation process, which happens largely during zygotes and the

primordial germ cell (PGC) stage, has remained largely unknown until the recent discovery of 5-hydroxymethylcytosine (5-^{hm}C) and Ten-Eleven-Translocation (TET) family proteins which convert 5-^{m}C to 5-^{hm}C (200, 201). Previous studies have shown that there are two possible ways for demethylation - passive dilution through cell replication and active removal of methylcytosine through enzymatic reactions converting 5-^{m}C to 5- ^{hm}c and further oxidative products, 5 carboxyl-cytosine (5-caC) and 5-formly-cytosine (5-fC), which is the focus of our current research(201, 202).

1.2 DNA demethylation and hydroxymethylation

Similar to 5-^{m}C, 5-^{hm}C is another epigenetic DNA marker, which was found several decades ago in T4 bacteriophage (203). In 2009, researchers discovered that 5-^{hm}C is enriched in mouse embryonic stem (ES) cells and Purkinje neurons (204, 205), although the role of 5hmc is still to be elucidated. Some studies have suggested that 5-^{hm}C is a stable epigenetic mark that is enriched in active transcriptional promoters. Recent findings also suggested that 5-^{hm}C may act as an intermediate in the process of DNA active demethylation. The TET family proteins were found to convert 5-^{m}C to 5-^{hm}C through α-ketoglutarate- and Fe (II) dependent dioxygenase reactions (206).

Currently, there are three members found in the mammalian TET family: Tet1, Tet2, and Tet3 (206). Mouse TET1 and TET2 proteins are mainly expressed in embryonic stem cells (ESCs) while TET3s are highly expressed in germline cells (207). The conversion of 5-^{m}C into 5-^{hm}C requires cofactors such as a-ketoglutarate (α-KG) and Fe (II), and vitamin C (201). Because α-KG was produced in the mitochondrial TCA cycle by isocitrate dehydrogenase (IDH) family proteins, we speculate that the IDH expression level is closely related to the hydroxymethylation process.

It is reported that mutant IDH was found in several types of cancers, which could reduce the hydroxymethylation level by irreversibly converting the TET co-factor α-kG into R-2-hydroxyglutarate (R-2HG) (208). 5-^{hm}C could be further oxidized by TET into 5-Formylcytosine (5-^{f}C) and 5-Carboxylcytosine (5-^{ca}C)(209). The following removal of 5-^{f}C or 5-^{ca}C through thymine-DNA glycosylase (TDG) and the base excision repair (BER) pathway could replace the original 5-^{m}C with unmodified cytosine, finishing the demethylation process (210), The changed 5-^{hm}C level and mutation of TET and IDH had been reported in multiple diseases. Genome-wide mapping of 5-^{hm}C showed its level was reduced in melanoma but not in benign tumors. It was accompanied by the down-regulation of IDH2 and TET proteins, and could be rescued by reintroducing active *TET2* and *IDH2* (211). The same trends were reported in breast, liver, gastric, and colorectal cancers (212-215). At the same time, reduced 5-^{hm}C level was correlated to the up-regulation of TDG proteins, indicating the active demethylation process (216). But the exact detail of this demethylation pathway is still unclear.

In addition to the role of TET protein's essential role in demethylation pathways, recent research has found that TET may be engaged in epigenetic modification of histones through its partnership with *O*-linked β-*N*-acetylglucosamine (O-GlcNAc) transferase (OGT). OGT catalyses *O*-GlcNAcylation through the addition of *O*-GlcNAc onto the hydroxyl moiety of serine/ threonine residues through post-translational modification (217). In *Drosophila*, OGT is encoded by a Polycomb Group (PcG) gene, super sex comb (sxc), located on chromosome 2R (218, 219). It has been confirmed that both TET2 and TET3 directly interact with OGT *in vivo* in mammalian cells. Yu, etc. found that in mouse ES cells.

TET2 interacted with OGT through its carboxyl terminal catalytic double-strand β-helix (DSBH) domain and OGT's N-terminal tetratricopeptide repeats (TPR) 5 and 6 (220). Currently there is no evidence that the interaction of TET and OGT altered DNA property beyond the conversion of 5-^{m}C to 5-^{hm}C because no new base modifications were detected after the incubation of TET2 and OGT together with 5-^{m}C *in vitro (220)*. It was observed that when TET2 level is reduced using short hairpin RNA (shRNA) in ES cells, the interaction between OGT and chromatin was abolished, as well as the H2B Ser112 GlcNAcylation. The conclusion was made that TET2 might be essential for OGT's function and its targeting on chromatin (220). Conversely, however, when the OGT was KD with shRNA, it did not affect its function and the association with TET2. Furthermore, the enzymatic null TET2 mutant could still interact with OGT and maintained the GlcNAcylation, which suggests the OGT's physical interaction with TET2, instead of enzymatic activity, is more important for OGT function.

With the great potential of TET in both DNA and histone modifications, more work is needed to understand better the role of TET in regulating epigenetic states. Here we characterized the phenotype of a loss of function dTET KD *Drosophila* by using a powerful and robust *Drosophila* model. We found that the dTET KD *Drosophila* had reduced 5-^{hm}C content, similar to the observation in mammalian models. We also showed that dTET is a Polycomb Group protein member because it has genetic interactions with the *Polycomb*^{4} (*Pc*^{4}) mutation. Furthermore, we showed that the mitochondrial genes and genes near the chromosome 3L telomere region have been greatly reduced in mRNA and hydroxymethylation levels in dTET KD *Drosophila*.

The jumonji C domain-containing histone lysine demethylase KDM2A was reported to bind to unmethylated CpG in ribosomal DNA (rDNA) promoter region through its CXXC zinc finger motif, which also presents in dTET protein, and inhibit the rDNA transcription(221). Further investigation revealed that another KDM family member, KDM4D, requires PARP-1 and RNA-binding to associate to DNA damage sites. Its accumulation may be related to double strands break repair in mammal cells (222). This finding associates the change in chromatin protein property with the activity of DNA transcription, showing that some enzymes could regulate epigenetic changes by regulating histone and DNA at the same time.

The human mitochondrial genome is a double-stranded, circular structure of 16,569 bases. It contains two ribosomal RNAs (rRNA), 22 tRNAs, cytochrome c oxidase subunits I-III, cytochrome b, ATPase subunit 6 and several predicted proteins coding sequences (223). The non-coding region of the mitochondrial DNA sequences were termed D-Loop, which provides the interaction and transcription sites for nuclear-encoded mitochondrial proteins (224). In 2008, Zhang lab identified there are 940 mitochondrial proteins in murine cardiac cells, of which 99% were encoded in the nucleus (225). Recently, the Lee lab reported that the mitochondrial DNA (mtDNA) copy numbers are regulated by the methylation level of the mtDNA-specific polymerase gamma A (POLGA) exon 2. The cancer cells and pluripotent cells were highly methylated at the exon 2 of POLGA while possessing low mtDNA copy numbers. After the demethylation agent treatment of 5-azacytidine for 28 days, the glioblastoma cells showed increased mtDNA copies accompanied by decreased POLGA exon2 methylation (226). This is another possible mechanism to regulate the expression of mitochondrial genes.

2. Statement of Problem

The research on 5-^{hm}C and TET protein were dramatically expanded after the discovery of their possible roles in active demethylation process. But the details of the involvement of TET protein in the hydroxymethylation process is far from clear. Although TET knock-down/knock-out animals were produced, few works were carried out in the *Drosophila* model. In this project, we are characterizing the outcome of dTET (*Drosophila* TET) knock down in dTET deficiency *Drosophila*. The epigenomic landscape of the dTET deficiency *Drosophila* was analysed, especially global hydroxymethylation. Genetic crossing were performed to further explore the property of dTET. Because the DNA repair proteins participated in the DNA active demethylation process, so the global distribution pattern of typical DNA repair related proteins were also tested. The outcome of this project could reveal more details of TET protein and its analogue in *Drosophila,* one of the most important epigenetic models. Our findings will accelerate the understanding of DNA active demethylation and provide insights for the future therapy for diseases such as cancers and neurodegenerative diseases.

3. Materials and Methods

Drosphila Stocks: All of the stocks are from the Drosophila Stock Center in Bloomington, IN. :" *Oga*^{P} (*y*^{1} *w*^{67c23}; *ry*^{506} P[SUPor-P]Oga^{KG04950}); *dTET*^{EP} (*w*^{1118}; P[w+mC]=EP]EP995[EP995]/TM6B,*Tb*^{1}); *Pcl*^{11} (In(2R)*Pcl*^{11}/SM5); *Scm*^{D1} (*st*^{1} *in*^{1} *kni*$^{ri-1}$ *Scm*^{D1}/TM3,*Sb*^{1}); *sxc*^{6} (*OGT*) (*sxc*^{6} *bw*^{1} *sp*^{1}/SM1); *Scr*^{17} (*Scr*^{17}/TM6B, Tb^{1}), Df(3L)TL (dTet-Left Deficiency) (*w*^{1118}; Df(3L)Exel6091, P[w+mC]=XP-U]Exel6091/TM6B,*Tb*^{1}), Df(3L)TR (dTet-Right Deficiency) (*w*^{1118}; Df(3L)Exel6092, P[w+mC]=XP-U]Exel6092/TM6B,*Tb*^{1}); Df(3L)BigT (Df(3L)BSC23, *rho*$^{ve-1}$ *e*^{1}/TM2, *p*^{p}); *w*^{1118}; *Kr*$^{ff-1*}$ (made in our lab); T(2;Y)*kis*^{L124} and *Pc*^{4} *p*^{p}/TM3,*Sb*^{1} (gift from J. Kennison); *mt2*^{hw} (gift from K. Maggert). In this study, we generated the stocks: 1) T(2;Y) *kis*^{L124} ; *Pc*^{4} *p*^{p}/TM3,*Sb*^{1} that was used to test for

enhancement or suppression of the extra-sex-combs phenotype; 2) w^{1118}; $dTET^{EP}$ Oga^{P}/TM6,Tb^{1} which has dTET and Oga on the same chromosome; and 3) w^{1118}; $dTET^{Rev1}$ /TM6,Tb^{1} was made by excision of the P-element in $dTET^{EP}$ by crossing it to *Drosophila* with the genotype w^{1118}; Sb^{1} □(2-3)/TM2 (which expresses the P-element transposase), isolating F1 males with the genotype w^{1118}; $dTET^{EP}$/Sb^{1} □(2-3), crossing the males in individual vials to w^{1118} ; TM2/TM3, Sb^{1} virgin females, and selecting 50 F2 *Drosophila* with white eyes. Three precise-excision lines, $dTET^{Rev1}$, $dTET^{Rev2}$ and $dTET^{Rev3}$, were saved and validated to be precise excisions of the P-element by PCR. The w^{1118}; $Kr^{lf\text{-}1}$ (without ELBOs) and the w^{1118}; $Kr^{lf\text{-}1*}$ (with ELBOs) stocks were made as described previously (227).

Statistical analysis of RNA-Seq data: *.Fastq files for RNA Seq was aligned to the dm3 build reference genome using TopHat2. The *.sam files were converted to *.bam files and sorted according to genomic position using samtools. The *rmdup* function from samtools was used to remove potential PCR duplicates. The processed *.bam files were further analyzed using R package DESeq2(228). A FDR corrected p-value cut-off of 0.1 was used to call differentially expressed genes. Correlation and overlaps were performed in R (R> 3.0.0).

DNA digestion with PvuRst1L and DNA sequencing: PvuRts1I (Pvu) restriction enzyme can directly cleave hydroxymethylated DNA 12-14 bps away from the 5hmC site(229). We developed a new technique that we call Pvu-seq which allows direct detection of 5hmC without chemical modification of 5hmC or bisulfite conversion. A paper describing this technique was published in *BMC Genomics (230)*. Briefly, the whole genomic DNA extracted from dTet KD, Mt2 KD and w1118 pupae, was digested with PvuRts1I and sequenced using 50 bps paired end sequencing reads in Illumina™ HiSeq 2500.

Statistical analysis for Pvu-Seq data: Pvu-Seq was used to confirm the presence of 5hmC in the predicted Pb-dependent high density 5hmC clusters (230). *.Fastq files for Pvu-Seq was aligned to the dm3 (UCSC) reference genome build using bowtie2. The *.sam files were converted to *.bam files and sorted according to genomic position using samtools. *rmdup* function from samtools was used to remove potential PCR duplicates. The data was further filtered using a mappability score cut-off of 10 and only reads with mapped mate pairs was used for downstream analysis. The differential coverage between w1118 and dTet was calculated using R package MEDIPS within 200bps genomic windows (R> 3.0.0). Genome wide differential coverage between two groups of samples where modelled as a negative binomial distribution. For this, MEDIPS applies edgeR(231) and its functions for normalization, estimation of over dispersion, and statistical testing. The log2 fold change is coverage was estimated as log2 (Experiment/w1118, control). DhMs were called for all peaks with FDR corrected p-value ≤ 0.1. Adjacent windows were merged together to form larger windows to reduce the number of regions. Reads per kilo base per million reads (rpkm) values were processed *.bam files and outputted as *.wig files for visualization in Integrative genome viewer. Distance of the peaks from the nearest 5' end of genes, and the distance from the gene were calculated using *annotatePeak* function from R package ChIPSeeker, using TxDb.Dmelanogaster.UCSC.dm3.ensGene as the reference database. Correlation and overlaps were performed in R (R> 3.0.0).

Motif Discovery: For discovery of the consensus sequences for dTET enzymatic activity, we selected all unmerged significant DhMs and did a de-novo motif discovery using motifRG package in R (R> 3.0.0) (232). We used the dm3 genome build tile into 200 bps regions as the background sequence to estimate the seed motif, and search for the enrichment of seed motif in DhMs. The

top 5 motifs are reported in the paper. For determination of known transcription factor binding motifs in DhMs located in the Promoter regions of the differentially expressed genes we used PWMEnrich package in R (R> 3.0.0) and search for significant enrichment against a database of known transcription factor binding motifs, which can found in Bioconductor database PWMEnrich.Dmelanogaster.background in R (R> 3.0.0).

4. Results

4.1 Sequence comparison of TET homologs

While mammals possess three types of TET protein, TET1, TET2 and TET3, *Drosophila* has only one TET homolog, CG2083 (CG43444), which we renamed dTET. The dTET gene is located on chromosome 3L, is 92kb long and has 12 exons (233). The translated product of dTET (isoform F) contains 2921 amino acids. To determine the possible function of the dTET, we first compared

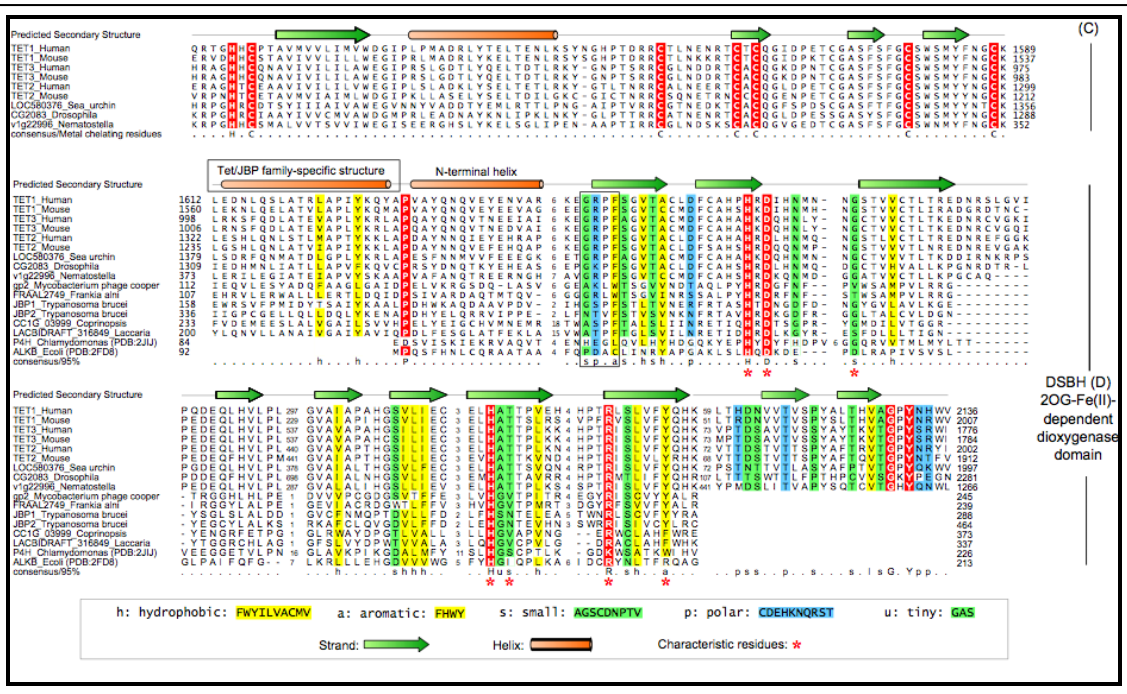

Figure 20: Comparison of the similarity of predicted protein secondary structure of dTET and its homologs from different species using ScanPosite analysis. The comparison sequences include TET1_human, TET1_Mouse, TET2_Human, TET3_Mouse, TET2_Human, TET2_Mouse, LOC580376_Sea Urchin, CG2083_*Drosophila*, V1g22996_nematostella, gp2_mycobacterium phage cooper, FRAAL2749_Frankia alni, JBP1_Trypanosoma Brucei, JBP2_Trypanosoma Brucei, CC1G_03999_Coprinopsis, LACBIDRAFT_316849_Laccaria, P4H_Chlamydomonas (PDB:2JIJ), ALKB_Ecoli (PDB:2FD8).

the predicted amino acid sequence of dTET with its homologs in different species (Figure 21). ScanPosite analysis showed that dTET contained a Zinc Finger CXXC structure from AA647 to AA687. There were two Tet/JBP family signature domains, between sequences AA1857 -AA2091 and AA2527-AA2727, which consisted of a double-stranded beta helix (DSBH) fold domain belonging to the 2-oxogluatarate (2OG)-Fe (II)-dependent dioxygenase (2OGFeDO) superfamily. All three mammalian TET members possess the DSBH domain, and this is essential for the binding of metal ions that catalyze the oxygenase function (234).

The CXXC domain is only possessed by TET1/3 and is required for the binding to chromatin. However, the mammalian TET2 lacks the CXXC domain and needs the assistance of another protein, IDAX, (possible *Drosophila* homolog: CG9973) for binding (235). The analysis of multiple sequence alignment through Blast protein indicated that dTET shared a similar Zinc Finger CXXC domain, Tet/JBP family-specific structure, and the amphipathic helix pattern with TET1 and TET3 in human and mouse, as well as orthologs in Sea urchin and *Nematostella*. The similarity extended into the DSBH-2OG-Fe (II)-dependent dioxygenase domains, shared by the characteristic residues and beta strand.

It is clear that the dTET possessed all structural elements and catalytic residues characteristic of the TET/JBP superfamily: Histidine and Aspartic acid, a small amino acid in the strand after the N-terminal Helix and the Histidine, the small amino acid, Arginine and the aromatic amino acid in the stands close to the C-terminal. But it is worth noticing that dTET shares more similarity with TET1 and TET3 than mammalian TET2 because TET2 lacks the Zinc Finger CXXC domain. As mentioned above, since dTET possesses the catalytic domain of DSBH and the chromatin binding domain of CXXC Zinc Finger, it is possible dTET can directly interact

with chromatin.

4.2 dTET is Required for Optimal Transcription and Hydroxymethylation of the Nuclear and Mitochondrial Genome

Our investigation on the role of dTET has been carried on a loss-of–function dTET mutation strain, the pupal-lethal dTET$^{EP/EP}$, which has a homozygous PiggyBack insertion between exon 6 and 7. The allele information was shown in Table 2. Next, we compared the dTET mRNA level in control *Drosophila* (w^{1118}) and dTET mutants using an RNA sequencing technique. The data showed that the dTET mRNA level in *dTET*$^{EP/EP}$ was significantly reduced compared to w1118 *Drosophila* (**Figure 22, a and b**), which indicates successful dTET KD in dTET$^{EP/EP}$ strains at the transcription level. Next we explored how the reduction of dTET protein would affect the genome hydroxymethylation level in *Drosophila*.

We used Pvu-sequencing to identify hydroxymethylation sites in both w1118 and dTET$^{EP/EP}$ pupae. Pvu-sequencing is a new technique developed in the Ruden laboratory by digesting the purified genomic DNA sample with PvuRts1I, which is a Type 2 restriction endonuclease that recognizes single 5-^{hm}C sites within CGAT/CG sequences and generates fragments with 3'-cohesive termini, followed by next-generation DNA sequencing (236). Since the distances between the cleavage sites and 5-^{hm}C sites are often 11-13 nucleotides in the top strand and 9-10 nucleotides in the bottom strand(237), Pvu-seq could be an ideal method to detect the density and distribution of 5-^{hm}C in the genome and also the relative genomic 5-^{hm}C levels in particular regions. As expected, we observed about a 50% reduction of 5-^{hm}C levels in *dTET*$^{EP/EP}$ mutant *Drosophila* while the distribution pattern of 5-^{hm}C was similar between mutant and control *Drosophila* (**Figure 22, c and d**). We also noticed that long intron in which EP995

resides is poorly spliced in the KD pupae. It shows the insertion mutation of the EP995 transposon between exons 6 and 7 in the dTET gene (**Figure 22, e)**. The results confirmed that dTET was KD at the transcription level and was directly associated with generation 5-^{hm}C in *Drosophila*.

In addition to the nuclear 5-^{hm}C level reduction, we also observed that the global hydroxymethylation level in dTET$^{EP/EP}$ *Drosophila* was significantly reduced compared to control *Drosophila* (**Figure 235,** dTET gene as example). This shows the importance of dTET in the process of maintaining DNA hydroxymethylation level in *Drosophila*. We also observed substantially

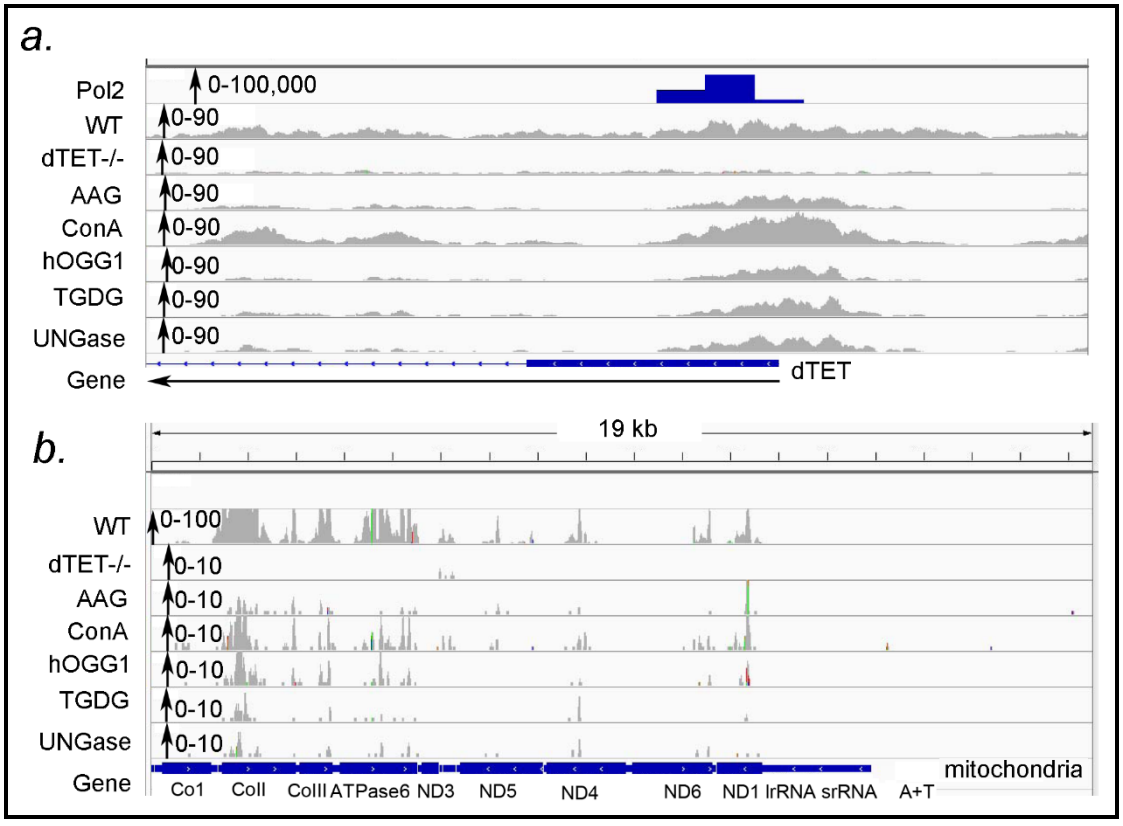

Figure 21: The global hydroxymethylation level in dTETEP/EP *Drosophila* was significantly reduced compared to WT *Drosophila*. (a) 5-^{hm}C and oxidative modification marker results of WT and *dTET*$^{EP/EP}$ at the dTET site. (b) 5-^{hm}C and oxidative modification marker results of WT and *dTET*$^{EP/EP}$ at mitochondrial DNA. Both results showed a reduction of 5-^{hm}C in *dTET*$^{EP/EP}$ strains and the sites are similar to the distribution of oxidative modification markers.

Genotype	Phenotype
dTET^{Rev-1} / T-L	Precise Excision of EP; adults survive
Oga^{P} / *Oga*^{P}	Adults survive; partial male sterile
dTET^{EP} / T-R	Adults survive; weak climber
dTET^{EP} *Oga*^{P} / T-R	Adults survive; weak climber
T-L / T-R	Some adults survive; weaker climber
dTET^{EP} / T-L	Black pupal lethal
dTET^{EP} *Oga*^{P} / dTET^{EP} *Oga*^{P}	Black pupal lethal
dTET^{EP} *Oga*^{P} / T-L	Black pupal lethal
dTET^{EP} / dTET^{EP}	White pupal lethal

Table 2. Allelic Series of dTET and Oga single and double mutant phenotypes. The weakest phenotype is on the top, and the most severe phenotype is on the bottom.

4.3 dTET is Required to Oxidatively Modify the Mitochondrial Genome

Recent discoveries revealed that TET proteins may have participated in the oxidation of 5-^{m}C into 5-^{hm}c, 5-^{f}C, and 5-^{ca}C followed by the BER DNA repair pathway. It is possible that oxidative damage could have occurred at a higher rate near hydroxymethylation sites. After confirming the role of dTET in global hydroxymethylation, we conducted a series of assays to measure different types of DNA oxidative damage in control and dTET$^{EP/EP}$ *Drosophila*. The experiment was performed by treating control and dTET$^{EP/EP}$ *Drosophila* DNA with five different DNA oxidation damage specific glycosylases followed by next-generation DNA sequencing to reveal the distribution of oxidative damage (**Figure 23** and **Table 5**). The glycosylases we tested includes 2-

Methyladenine DNA Glycosylase Type II (AAG), which initiated base excision repair (BER) when certain substrate bases were recognized such as 3-methyladenine, 3-methylguanine, and 7-methylguanine, etc., after DNA damage; Concanavalin *A* (ConA) is a lectin (carbohydrate-binding protein) which specifically interacts with glycoprotein and glycolipids; Human 8-Oxoguanine glycosylase 1(hOGG1) recognizes and remove the DNA damage product 7,8-dihydro-8 oxo guanine (8-oxoG) and 2,6-diamino-4-hydroxy-5-fromamidopyrimidine (FaPy); Thymine glycol DNA *glycosylase* (TGDG) removes DNA bases damaged by UV light and produces a single nucleotide gap, Uracil-DNA glycosylase (UNGase) eliminates uracil produced from cytosine deamination through BER pathways.

According to the results, we found that like 5-^{hm}C, the distribution of oxidative-damaged DNA nucleotides are enriched in the promoter regions (**Figure 23 a**). Surprisingly, in the mitochondria, the levels of DNA oxidative damages in the promoter regions of mitochondrial genes are significantly reduced in *dTET*$^{EP/EP}$ *Drosophila* compared to control *Drosophila* (**Figure 23 b**). The relatively greater abundance of ConA in both control and dTET$^{EP/EP}$, in both nuclei and mitochondria, is different compared to other oxidative damage markers. We conclude that 5-^{hm}C oxidative modifications to DNA correspond to several other types of oxidative changes to DNA. This suggests that dTET, like the BER enzymes, is a DNA repair enzyme that is involved in removing 5-^{m}C from the genome.

4.4 dTET Mutations Enhance the Extra-Sex Combs Phenotype of PcG Mutations.

The Polycomb Group (PcG) is a protein family which regulates gene silencing through epigenetic chromatin remodeling and plays important roles in development (238). Conversely, the Trithorax Group (TrxG) proteins antagonize the effects of PcG proteins by maintaining an

activated status of target genes. An additional copy of the TRXG gene *kismet* (*kis*) was used in the genetic assay to screen for suppressor of *Polycomb* (*Pc*) activity because the insertion of an added copy of TrxG gene *kismet* sensitizes the genetic background and enhances the penetrance of the extra-sex-comb phenotype of PcG loss-of-function mutations.

In heterozygous TET mutant dTET^{EP}/TM6 male adult *Drosophila*, we observed an enhancement of the extra sex combs phenotype, which is the unique property of PcG mutations: the ectopic sex combs are on 2nd and 3rd pair of legs instead of only the first pair (Figure 24 a, E-

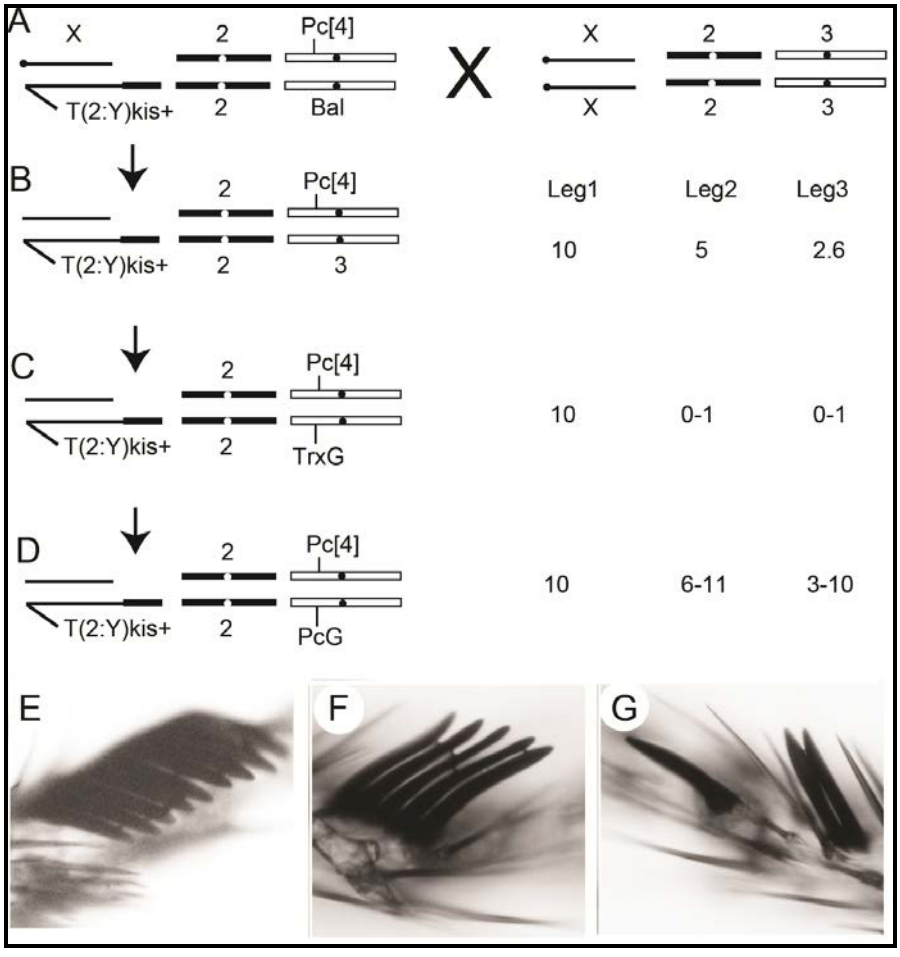

Figure 22: Extra sex combs in heterozygous TET mutant dTET EP/TM6 male adult *Drosophila*. (A) Cross scheme of extra sex comb assay. The duplication of *kismet* sensitizes the genetic background for the phenotype penetrance. (B) The cross scheme of introducing *PcG* mutation showed extra sex comb on the second and third legs. (C) The introducing of *TrxG* mutation showed limited extra sex comb on the second and third legs. (D) The introduction of an additional copy of *PcG* gene increased an extra sex comb number on second and third legs. (E-G) Microscope Images of sex combs on 1st. 2nd, and 3rd legs of *dTET*^{EP}/TM6 males.

G).This indicates that dTET belongs to the PcG family. To confirm this finding, we introduced series of mutant PcG alleles into dTET^{EP}/TM6 *Drosophila* (Table and Table 1). As we expected, the additional sex comb number was further increased due to the enhancement from the mutant PcG alleles. On the other hand, when a mutated *O-GlcNAcase* (*Oga*) allele was introduced, which is a TrxG member; the number of extra-sex combs on the 2nd and 3rd pairs of legs was suppressed. This suggests that Oga and dTET genetically interact. The TrxG property of Oga counteracted with dTET mutation and reduced the extra sex combs.

Genotype	Leg1	Leg2	Leg3	Comments
T124; *Pc*^{4} pp/TM3,Sb	1 0.19	5	2 .62	Reference
T124; *Scr*^{17}/ *Pc*^{4}	5 .75	0 .75	0	Scr is in TrxG
T124; *Oga*^{P}, *dTET*^{EP}/*Pc*^{4}	9 .85	1 .3	0 .5	Oga suppresses dTET
T124; *Oga*^{P} / *Pc*^{4}	1 0.33	4 .33	2 .18	Oga has no effect on Pc
T124; *dTET*^{EP} / *Pc*^{4}	1 1.05	8 .3	5 .7	dTET is in PcG
T124; *sxc*^{6}/ *Pc*^{4}	1 0.4	6 .125	4 .44	sxc is in PcG
T124; T-R/ *Pc*^{4}	1 0.75	7 .9	7 .3	Df(3L)(T-R) is in PcG
T124; *PCL*^{11}/ *Pc*^{4}	9 .8	9 .15	7 .95	Pcl is in PcG
T124; *Scm*^{01}/ *Pc*^{4}	1 0.88	1 0.5	9 .25	Scm is in PcG

Table 1: Mutations in dTET enhance the Pc4 ectopic sex comb phenotype.

4.5 The ELBO Assay Indicates that dTET is in the PcG

We further deployed another well-established model, the Ectopic Large Bristle Outgrowths (ELBO) phenotype, which was developed in the Ruden laboratory in 2003 (Sollars *et al.*), to assess whether dTET belongs to the PcG family (). The *Kruppel* (Kr) gene encodes a transcriptional factor that maintain the development of thoracic and abdominal sections(239). Its dominant allele $Kr^{\text{Irregular facet}}$, also called $Kr^{\text{lf-1}}$, showed a sensitized background responding to the mutation of *TrxG* or *PcG* genes. The inheritable epiallele could be induced by *TrxG* mutation and suppressed by PcG mutation, which exhibit the ectopic expression of Kr proteins in the ventral region of eye imaginal disc. This ectopic expression not only results in the crude appendage-like structure protruding from ventral regions but also reduced the size of eyes (240). As we expected, the presence of a $dTET^{\text{EP}}$ reduced the rate of ELBO formation from 60-70% to below 10% while the $Kr^{lf\text{-}1}$ heterozygous *Drosophila* only show less than 1% ELBO progeny in the presence of the dTET mutation. The introduction of ELBO enhancer and suppressor alleles increases or decreases the rates of ELBO phenotype, individually (Table 4, Figure 25 C and D). All of the results confirm that dTET belongs to PcG family.

Mother's Genotype	Father's Genotype	F1 Genotype	% ELBOs (total)	Comments
$Kr^{lf\text{-}1}$/ $Kr^{lf\text{-}1}$	w^{1118}	$Kr^{lf\text{-}1}$/ w^{1118}	0% (533)	Negative control
$Kr^{lf\text{-}1*}$/ $Kr^{lf\text{-}1*}$	w^{1118}	$Kr^{lf\text{-}1*}$/ w^{1118}	67% (551)	Positive control
Scr^{17} / Bal	$Kr^{lf\text{-}1*}$/ $Kr^{lf\text{-}1*}$	$Kr^{lf\text{-}1*}$/+; Scr^{17}/+	95% (508)	Scr is in the TrxG
Scr^{17} / Bal	$Kr^{lf\text{-}1*}$/ $Kr^{lf\text{-}1*}$	$Kr^{lf\text{-}1*}$/+; *Bal*/+	64% (555)	Scr has no ME
Oga^{P} / Bal	$Kr^{lf\text{-}1*}$/ $Kr^{lf\text{-}1*}$	$Kr^{lf\text{-}1*}$/+; Oga^{P}/+	94% (568)	Oga^{P} is in the TrxG
Oga^{P} / Bal	$Kr^{lf\text{-}1*}$/ $Kr^{lf\text{-}1*}$	$Kr^{lf\text{-}1*}$/+; *Bal*/+	62% (531)	Oga^{P} has no ME
$dTET^{EP}$/Bal	$Kr^{lf\text{-}1*}$/ $Kr^{lf\text{-}1*}$	$Kr^{lf\text{-}1*}$/+; $dTET^{EP}$/+	5% (539)	dTET is in the PcG
$dTET^{EP}$ /Bal	$Kr^{lf\text{-}1*}$/ $Kr^{lf\text{-}1*}$	$Kr^{lf\text{-}1*}$/+; *Bal*/+	69% (500)	dTET has no ME
Pc^{4} / Bal	$Kr^{lf\text{-}1*}$/ $Kr^{lf\text{-}1*}$	$Kr^{lf\text{-}1*}$/+; $dTET^{EP}$/+	7% (598)	Pc^{4} is in the PcG
Pc^{4} / Bal	$Kr^{lf\text{-}1*}$/ $Kr^{lf\text{-}1*}$	$Kr^{lf\text{-}1*}$/+; *Bal*/+	62% (583)	Pc^{4} has no ME
$dTET^{EP}$ Oga^{P} / Bal	$Kr^{lf\text{-}1*}$/ $Kr^{lf\text{-}1*}$	$Kr^{lf\text{-}1*}$/+; $dTET^{EP}$ Oga^{P}/+	9% (587)	Oga suppresses dTET
$dTET^{EP}$ Oga^{P} /Bal	$Kr^{lf\text{-}1*}$/ $Kr^{lf\text{-}1*}$	$Kr^{lf\text{-}1*}$/+; *Bal*/+	69% (542)	Oga and dTET have no ME

Table 4. Mutations in dTET suppress the Ectopic Large Bristle (ELBO) Phenotype.

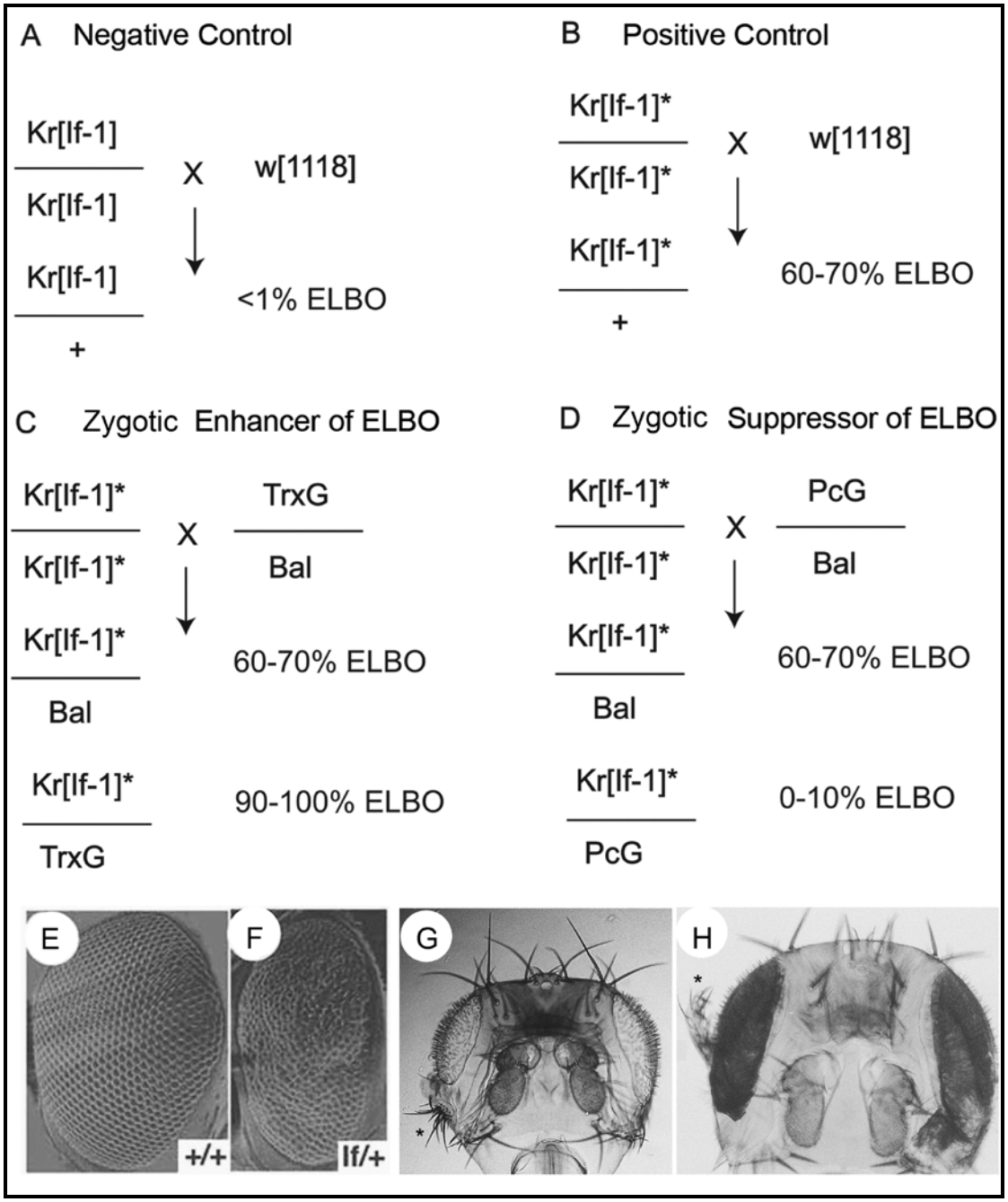

Figure 23: Ectopic Large Bristle Outgrowths (ELBO) phenotype, to assess whether dTET belongs to the PcG family. (A) The negative control cross plan showed maternal Kr [If-1] and WT had normal progeny. (B) The positive control cross plan showed Kr [If-1]* induces increased ELBO in progeny. (C) The introducing of *TrxG* gene showed more ELBO progeny. (D) The introduction of the extra copy of *PcG* gene showed reduced ELBO progeny. The electronic microscope results showed that compared with (E) WT, the Kr [If-1] mutant (F) showed irregularly formed and smaller eyes. (G-H) Microscope Images of bristle-like appendage structure (*).

4.6 The Genes Near the Chromosome 3L Telomere Require dTET for mRNA expression

Another interesting finding is that besides mitochondrial DNA, the telomere region near

NGS Technique	Method	Results
Pvu-seq	Digest DNA with PvuRts1I (Active Motif)	Maps **5hmC** sites (Ruden et al., 2013; in press)
AAG-seq	Digest DNA with mouse 3-methyladenine DNA glycosylase type II (Aag protein, Trevigen)	Maps 3-methyl adenine (**3mA**) (This grant)
ConA-seq	Purify sonicated DNA with concanavalin A lectin (ConA protein, Sigma)	Maps glycosylated sites in DNA (**glcDNA**) (This grant)
OGG1-seq	Digest DNA with human 8-oxoguanine DNA glycosylase (hOGG1 protein, Trevigen)	Maps 8-oxoguanine sites in DNA (8oxoG) (This grant)
TGDG-seq	Digest DNA with thymine glycol-DNA glycosylase (*E. coli* Endonuclease III, Trevigen)	Maps thymine glycol sites in DNA (This grant)
UNG-seq	Digest DNA with Uracil-N-glycosylase (*E. coli* UNGase, Trevigen)	Maps uracil sites in DNA (This grant)

Table 5. Next-generation sequencing (NGS) techniques developed by the Ruden laboratory to map oxidized DNA. To detect 5mC DNA in mtDNA, we will use the enzyme MbrBC, which cleaves 5mC DNA (1, 2)

chromosome 3L (from 0 kb to 140 kb) was also significantly hypo-hydroxyl methylated in *dTET*$^{EP/EP}$ pupae. Also, the mRNA transcription level of the genes in the 3L region was significantly reduced in *dTET*$^{EP/EP}$ pupae. As shown here, the Pvu-sequencing res7ults show that the 5-^{hm}C level near mth18 gene promoter region and within the gene body, which is within the first 140 kb of chromosome 3K, was diminished to an undetectable level (**Figure 26 A**). The RNA-Seq results showed that the mRNA level of mth18 is also brought down to less than 1% compared to control. We also examined the other genes within the 140k region of 3L telomere locus in *dTET*$^{EP/EP}$ pupae, including CG43149, Lsp1gamma, and Pdk1. All of the genes showed a reduction in the 5-^{hmc} level

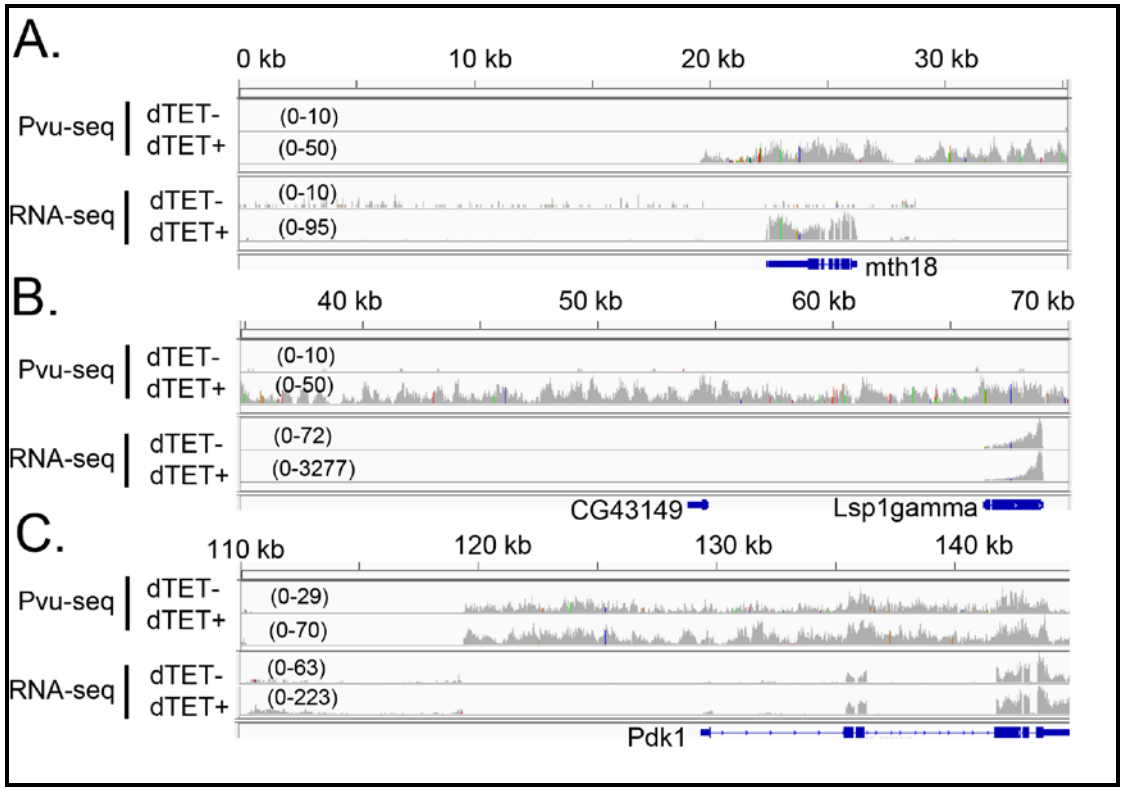

Figure 24: The Pvu-seq and RNA seq results compare dTET mutant (dTET-) and WT (dTET+) *Drosophila*. (A) Pvu-Seq and RNA-Seq showed dTET mutant had lower 5-^{hm}C level and mRNA transcription near 3L telomere region at mth18 gene promoter sites and within the gene. (B) CG43149 and Lsp1gamma showed both lower 5-^{hm}C and transcription level. (C), Pdk1 also showed lower 5-^{hm}C and transcription level, indicating reduced hydroxymethylation and transcription in 3L telomere regions.

and transcription levels (Figure 26 **B and C**). The Pdk1 gene, which was located furthest from the telomere region, shows a relatively moderate reduction in both 5-hmC and transcription. The difference between Pdk1 and other tested genes may be due to the distance from the 3L telomere. Since we do not observe the similar pattern in other telomere regions, it is possible that the 3L telomere region may contain certain chromatin structures with unique properties that affect hydroxymethylation and transcription activity. In summary, the genes within chromosome 3L telomere region show hypo-hydroxymethylation and limited transcription activity similar to mitochondrial genes. To our knowledge, this is a unique observation for which

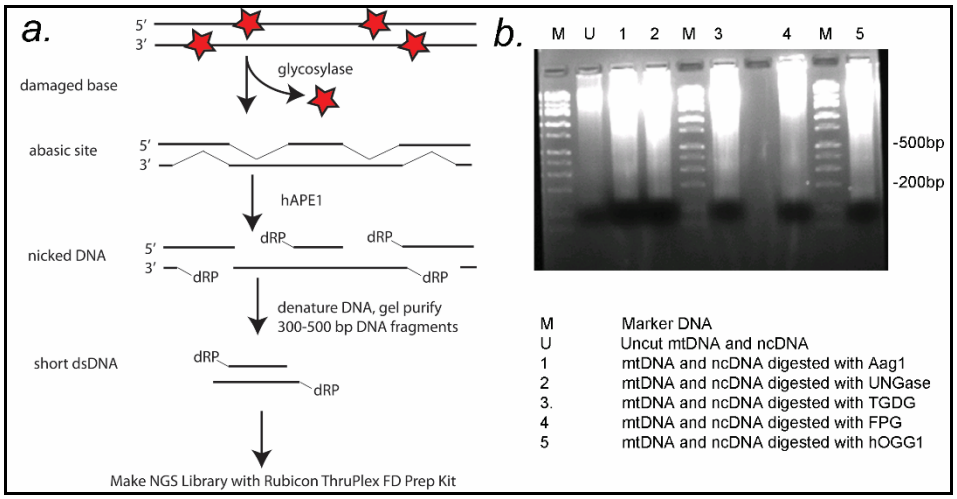

Figure 25: Protocol for glycosylase-seq experiments to analyze DNA damage in mtDNA and ncDNA. (a), Oxidized mtDNA and ncDNA is digested with a DNA repair glycosylase, which generates abasic sites in the DNA. hAPE1 (Sigma, Inc.) cleaves the DNA at the abasic sites, and the DNA is purified on an agarose gel. The next-generation sequencing (NGS) library is made with the short dsDNA with the Rubicon ThruPlex™ FD Prep Kit that requires only 5-10 ng of DNA. b, Agarose gene showing *Drosophila* pupae DNA digested with the indicated glycosylases and hAPE1 (this grant).

we have no explanation. Furthermore, we also looked at the distribution pattern of oxidative damage markers within the Chromosome 3L telomere regions. As we expected, control *Drosophila* show peaks of all six oxidative damage markers co-localized with 5-hmC peaks (**Figure 27 and Figure 28**), indicating possible oxidative damage sites coincide with hydroxymethylation locus. The dTET$^{EP/EP}$ *Drosophila*, however, have less oxidative damage in the 3L region. This phenomenon is much like the results in the mitochondrial genome. We also notice that when located further from the 3L telomere region, the CG13405 and CG12483 shows less reduction in hydroxymethylation level in dTET$^{EP/EP}$ *Drosophila* (**Figure 28 C**).

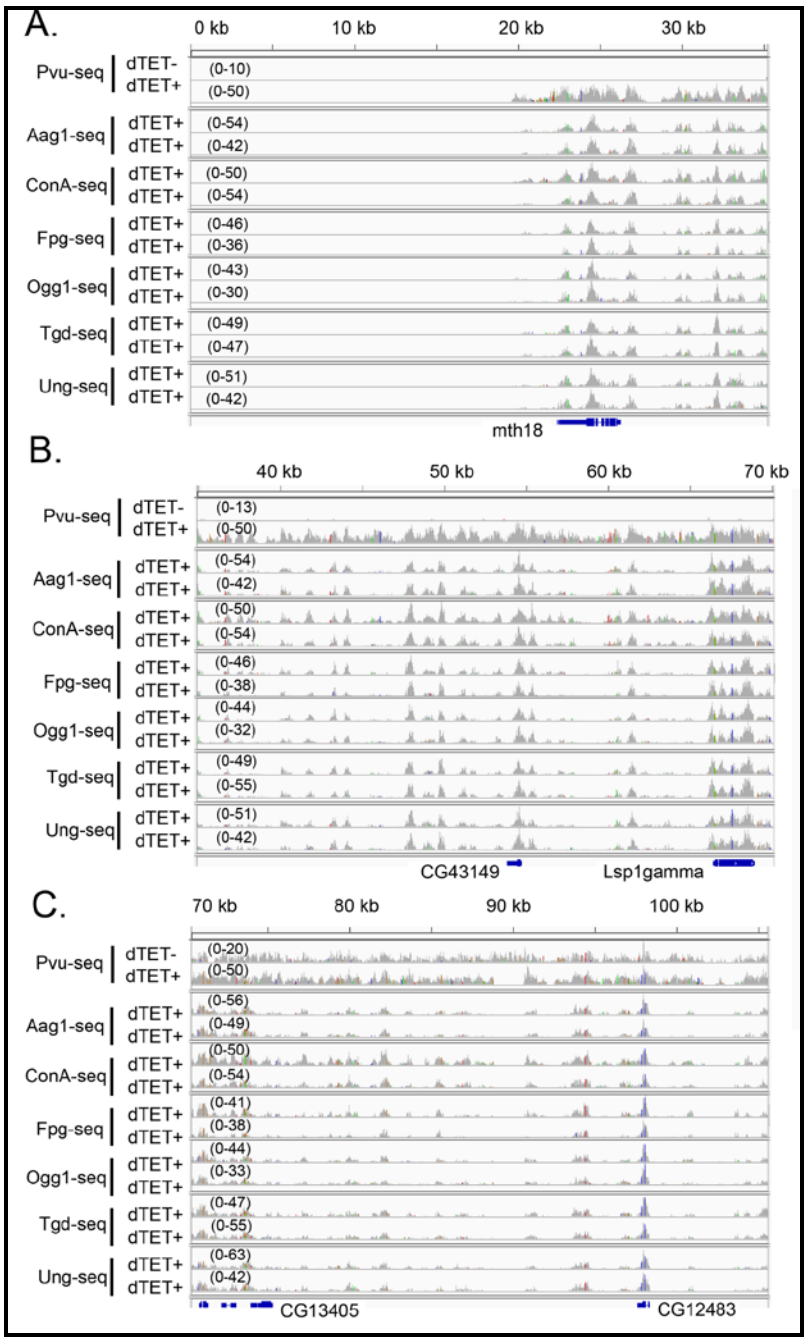

Figure 26: WT and dTET *Drosophila* show peaks of all six oxidative damage markers co-localized with 5-hmC peaks in 3L telomere region. WT and dTET *Drosophila* show peaks of all six oxidative damage markers co-localized with 5-^{hm}C peaks in 3L telomere region. (A) Pvu-seq and showed dTET mutant had lower 5-^{hm}C level, and the distribution pattern is similar to oxidative modification marker at *mth18* locus near 3L telomere region. (B) CG43149 and Lsp1gamma both showed lower 5-^{hm}C level in dTET mutant which co-localized with oxidative modification markers. (C) Pdk1 also showed lower 5-^{hm}C in *dTET* mutant and a similar pattern as oxidative modification markers

The *Drosophila* model has been deemed as one of the most powerful models in epigenetics research. However, the existence of DNA modification in *Drosophila* is still controversial despite the detection of a trace amount of 5-^{m}C in *Drosophila* by Achwal and colleagues in 1983 (241). The missing of 5-^{m}C from *Drosophila* genome raises the important question whether the DNA modification, including methylation and hydroxymethylation is essential for eukaryote cell development. It is well accepted that 5-^{m}C does not exist in the *Drosophila* genome until the identification of Dnmt2 homolog in *Drosophila* in 1999(242). The presence of 5-^{m}C was exploited and quantified by Gowher and colleagues at 2000 using methylation dependent restrictive enzyme McrBC analysis and HPLC. They quantified the percentage of 5-^{m}C to be 1 in 1000 to 2000 cytosines(243). Further research revealed more detailed information about the function and dynamic regulation of DNA methylation. The expanding investigation has advanced in recent years, especially after the significant progress towards the 5-^{hm}C function and the methylation dioxygenase TET family proteins (201, 204).

The role of TET in converting 5-^{m}C to 5-hmC, and to further products such as 5-fC and 5-caC, provides us with possible answers to a long-lasting question of how the 5-^{m}C is dynamically regulated and removed from the genome at certain development stages. But, when extensive studies had been conducted in mammalian models, ours is the first study of the 5-^{hmc} distribution and function in *Drosophila* models. Currently, there is no publication about the characterization of *Drosophila* TET homolog, dTET, nor the systematic analysis of its function. Our lab's previous study showed enriched non-CG hydroxymethylation in introns of honey bees (*Apis Mellifera*) using a highly sensitive whole-genome shotgun Pvu bisulfite sequencing method (244). To further characterize the properties and functions of TET, we extended the study to the field of

Drosophila.

The bioinformatics analysis shows that the *Drosophila* TET homolog CG2083 shares structural similarities with mammalian TET 1/3. The C-terminal conserved CXXC domain and Tet/ JBP family specific domain indicate that dTET is capable of binding chromatin independently without the assistance of partner proteins such as IDAX in mammalian cells. We obtained dTET mutant strain by inserting EP995 transposon into the dTET gene, resulting in a pupal lethal $dTET^{EP/EP}$ strain with more than 90% dTET mRNA reduction in the early pupal stage. Our findings from the Pvu-sequencing of $dTET^{EP/EP}$ confirm over 50% reduction of global 5-^{hm}C level. In previous study of mouse embryonic stem cell, the TET1 depletion causes about 40% loss of 5-^{hm}C level, which is similar to our results and confirms the essential role of dTET in hydroxymethylation process(207).

An unexpected finding is that we observed that the mitochondrial 5-^{hm}C level was nearly diminished compared to the control. At the same time, the mRNA levels of several mitochondrial genes like Co1, CoII, and ATPase 6 are significantly reduced in $dTET^{EP/EP}$ *Drosophila*, together with 3 fold reduction of hydroxymethylation level in the gene body. This is the first time that a significant impact of TET protein decrease in the mitochondrial gene transcription and hydroxymethylation levels were reported. The reduction of gene transcriptions matches the role of 5-^{hm}C in facilitating gene activation from previous research. Currently, there are very few studies on the mitochondrial DNA epigenetic modifications. In 1973, Nass showed that mtDNA in mouse, hamster, and hamster cells are hypomethylated compared to ncDNA(245). The existence of mtDNA methylation and hydroxymethylation were confirmed in mammalian cells again in 2011 by Shock et.al(246). They proposed that a special mtDNMT1 protein, which carries a

mitochondrial targeting sequence, translocated to mitochondria and processed the mtDNA methylation. Our finding suggests that dTET is essential for both the mitochondrial gene transcription and mtDNA hydroxymethylation. Currently, we have not identified how the dTET is associated with the reduction of mitochondrial DNA transcription, nor the causal relationship between the reduction of transcription and 5-^{hm}C level in mitochondrial. There may be possible interactions between dTET and the critical mitochondrial transcriptional factors such as POLRMT (mitochondrial RNA polymerase), TFAM (mitochondrial Transcription Factor A), or TFB2M (mitochondrial Transcription Factor B), which will be further tested (247, 248).

While some genes' transcription in dTET$^{EP/EP}$ show reduction compared to control, we observed a group of genes showing upregulation the mutant strains. Among the 200 most up-regulated genes are a group of 21 Cytochrome P450 (CPR) genes, including the top three: Cpr30B (up 13.39 folds), Cpr30F (up 12.13 folds), and Cpr76Bb (up 11.75 folds). CPR genes are required for the electron transfer and function of cytochrome P450 in the endoplasmic reticulum (ER)(249). It is not clear about the function of Cpr30B/30F/76Bb or the association with dTET reduction, but it may reflect a particular ER feedback to encounter the mitochondrial malfunction. The changes in dTET$^{EP/EP}$ strains were not only in the expression level of the gene but also the transcription pattern. We observed that the transcription direction of CG34199 gene was reversed in TET mutant *Drosophila* compared to control *Drosophila*. The Cpr56F gene in dTET$^{EP/EP}$, which is a skipped intron in the CG34199 transcription in control *Drosophila*, was transcribed instead. This phenomenon hasn't been reported before and may be associated with the different expression patterns in control and mutant *Drosophila*.

Another interesting finding is that although the *Drosophila* global genomic

hydroxymethylation is affected by the absence of dTET, most of the ncDNA regions still have measurable amounts of 5-^{hm}C left. The only exception is the chromosome 3L region, expanding about 140 kb from the 3L telomere, with almost undetectable 5-^{hm}C levels. Currently, it is not clear why the 3L telomere region has such significant reductions because the other telomere regions show average levels of 5-^{hm}C. A Study reported that 3L distal region has a lower-than-average gene density, which includes a dominant Polycomb group suppressor gene, lethal 1, and a lethal 3 gene which corresponds to a trithorax group gene verthandi (vtd)(250). The reduction of 5-^{hm}C may not be related to the formation of heterochromatin because previous studies show that the heterochromatin structure in chromosome 3L is genetically similar to chromosome 2L(251). The study from Zhang et.al shows Tet catalyzing active DNA demethylation mainly in distally located enhancers in mouse ESCs (252). They also observed Tet KD Escs have increased telomere-sister chromatid exchanging rates, indicating Tet may be related telomere homeostasis. The similarity of chromosome 3L and mtDNA in hydroxymethylcytosine distribution pattern and the aforementioned BER pathway enzymes will be further investigated.

Previously studies hypothesized that TDG activation and BER pathways may be downstream of the hydroxymethylation process to demethylate actively 5-^{m}C into cytosine. Muller et.al demonstrated that purified TET1 catalytic domain could reactivate the genes silenced by methylation. Interestingly, the reactivation requires the participation of a group of BER glycosylases such as TGD, PARP1, XRCC1, and LIG3(253). Sun and colleagues reported that when overexpressing TDG in Germinal Vesicle (GV) stage mouse oocyte, they observed decreased genomic 5-^{m}C, as well as decondensed chromatin (28). We tested five different types of DNA oxidation residues, such as AAG and ConA, using specific antibodies immunoprecipitation

followed by sequencing. We found their distribution patterns are similar to the 5-^{hm}C pattern, and all the oxidation nucleotides are enriched in promoter regions. The most similar pattern comes from ConA, which resembles most of the peaks from 5-^{hm}C in control Drosophila and dTET$^{EP/EP}$ Drosophila. We also observed the same similarity in *Drosophila* mitochondrial. This result supports the theory that dTET oxidizes DNA in the nuclear genes promoter region, and the product, such as 5-fC and 5-caC, might be recognized by Glycosylase members from BER pathways and restored to unmodified cytosine.

Since the OGT protein, which glycosylates histones, is encoded by a PcG gene Super Sex Comb (sxc) in *Drosophila*, we tested if dTET also belongs to the Polycomb Group. The testing of Sex Comb Model shows that when the T(2, Y) kismet allele sensitizing the multi-sex comb phenotype, the introducing of dTET allele increased extra sex combs on first pair of legs, and developed ectopic sex combs on the second and third pair of legs, which showed that dTET is a polycomb group protein. The ELBO model results also confirmed it. While the previous studies revealing that the connection between TET and PcG protein OGT in mouse ESCs, our findings provide evidence that these two PcG proteins could coordinate for a novel demethylation pathway by iteratively oxidizing 5-^{m}C(254). It is worth noticing that the OGA protein, which counteracts the OGT activity by catalyzing the reverse reaction of 5-^{hm}C oxidation, is a TrxG protein. The antagonism of OGA and OGT in oxidizing 5-^{hm}C could perfectly fit into the counteraction of PcG and TrxG members.

The model for How dTET Regulates Expression of the Mitochondrial Genome

Recently, Forneris *et al.* proposed that the lysine specific demethylase 1 (LSD1) could play a major role in *de novo* DNA methylation and formation of heterochromatin (255). It reported

that LSD1 not only act as a transcriptional co-repressor, but may also activate transcription by colocalize with RNA Pol II on many target gene's promoters(256). The crystallography results showed that LSD1 share 20% sequential similarity with flavin-dependent monoamine and polyamine oxidase (MAOs and PAOs) and are possible to act as amine oxidase under certain circumstances. It is very interesting that research shows the demethylation ability of LSD1 is not limited in Histone 3 lysine 4 tails. Reports revealed that LSD1 could also demethylate Histone 3 lysine 9 without change the methylation status of H3K4, which indicate the possibility of LSD1 to demethylate other Histone residues (257). More importantly, unlike the other jumonji family histone demethylases, LSD1 could produce H_2O_2 during the demethylation process, which acts as a signaling molecule for multiple pathways (258). And Perillo *et al.* reported that the DNA oxidation could also be promoted by the estrogen treatment induced H3K4/H3K9 demethylation process by LSD1, during which the produced H_2O_2 causes oxidative damages and recruited the 8-oxoguanine-DNA glycosylase 1 to modify DNA bases. (259). This observation could be further extended to explain the trigger for the demethylation process of 5-^{m}C to 5-^{hm}C in dTET nuclear and mitochondrial DNA. Based on the above results and previous studies, we propose a model that, under normal circumstances, the histones surrounding nuclear DNA were demethylated by Jumonji family proteins such as LSD1 or KDM2. The demethylation produced hydrogen peroxide, which may trigger hydroxymethylation by TET and/or recruits glycosylase to the nuclear DNA for oxidative damage modification, and turns on the gene transcription by Pol II. (**Figure 29 A**).In control mitochondria, although no histone and histone demethylase presents, dTET protein alone could still demethylate the 5-^{m}C and producing hydrogen peroxide to modify the bases and activate transcription. (**Figure 29B**). In contrast, the dTET mutant *Drosophila* lack the dTET protein,

but the nuclear histone and DNA can still be demethylated by LSD1. The $5^{-hm}C$ can be removed by oxidation modification caused by glycosylase for DNA modification while maintaining the transcription level (**Figure 29 C)**. So this could explain the relatively unchanged transcription activity in ncDNA between control and dTET mutants. But in dTET mutant mitochondria, because there are no histone demethylases available, the methylation level remains constant, and no hydrogen peroxide is produced to modify mtDNA. The transcription level remains low compared to control (**Figure 29 D**).

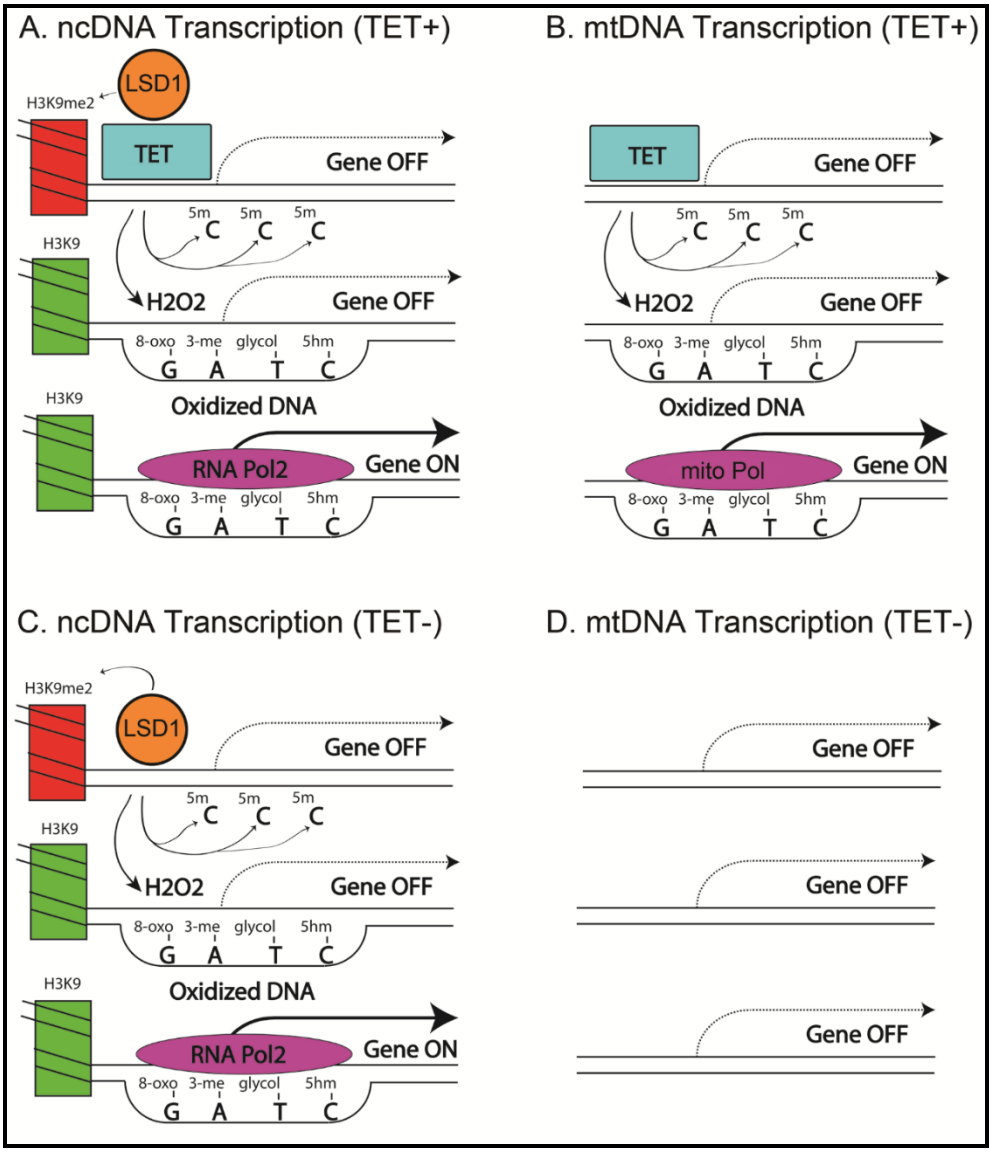

Figure 27: The Hypothetical model for dTET function. (A) Under normal conditions, the histones surrounding nuclear DNA are demethylated by Jumonji family proteins such as LSD1. The demethylation reaction by dTET produces formaldehyde which may modify the DNA and increase transcription by Pol II. (B) In WT mitochondria, where there are no histones on mtDNA, TET alone demethylates the 5-^{m}C and produces formaldehyde which modifies the bases and activate transcription. (C) In dTET mutant *Drosophila*, the nuclear histones and DNA can still be demethylated and by Jumonji proteins and oxidize the DNA. (D) In dTET mutant mitochondria, because there are no histone demethylases available, and no formaldehyde is produced to modify mtDNA. Therefore, the transcription levels of mitochondrial genes remain low.

According to the previous research showing that TET is interacting with OGT, we

constructed a series of *dTET* and *Oga* single and/or double-mutant to examine the outcome of mutation (Table 2). Here we found that *dTET* double mutant $dTET^{EP/EP}$ showed the severe developmental arrest and caused white pupal lethal, indicating the importance of dTET in development. While the $dTET^{EP/}$T-L with deleted *dTET* catalytic domain was black pupal lethal, $dTET^{EP/}$T-R, which has deleted 5' part of dTET gene but still contain the catalytic domain, shows only reduction of climbing ability, implying the dysfunction induced by limited *dTET* activity. In comparison, the homologous *Oga* mutant Oga^{P}/Oga^{P} showed relatively unchanged survival rates but a fraction of the male adults were sterile, indicating possible alternative pathways to substitute *Oga* functions. Interestingly, the *dTET* and *Oga* double knockout $dTET^{EP}$ Oga^{P} / $dTET^{EP}$ Oga^{P} showed black pupal lethal, which is less severe than dTET mutation.

Currently, it is not clear why the *Oga* mutant delays the developmental arrest in dTET mutation. The $dTET^{EP}$ Oga^{P} / T-R line contains one copy of *Oga* and one copy of dTET catalytic domain, showing declined locomotor ability but with normal viability. In contrast, the $dTET^{EP}$ Oga^{P} / T-L lost both copies of dTET catalytic domains, showing interrupted development during the black pupal stage. Taking together, the increasing survival rates of adults among $dTET^{EP}$ / $dTET^{EP}$, $dTET^{EP}$ / T-L, and $dTET^{EP}$ / T-R showed that one copy of 5' end dTET with no catalytic domain could delay the development stoppage a copy of 3' end dTET with catalytic domain could support partial adult survival but with reduced locomotor activity. But it is currently unknown why the $dTET^{EP}$ / T-R showed better survival than T-L / T-R. When the *Oga* mutant was introduced into dTET mutation background, we found that even with both copies of *Oga* deleted, the phenotype of progeny of $dTET^{EP}$ Oga^{P} / $dTET^{EP}$ Oga^{P} did not worsen compared to $dTET^{EP}$ / $dTET^{EP}$ single knockout. And the comparison between $dTET^{EP}$ / T-R *vs.* $dTET^{EP}$ Oga^{P} / T-R, and $dTET^{EP}$ / T-L

vs. dTET^{EP} *Oga*^{P} / T-L, showed that the absent of one copy of *Oga* on the background of TET heterozygous mutation background does not cause significant changes.

In conclusion, our work characterized and confirmed the vital role of TET function in DNA hydroxymethylation and demethylation, as those findings in other eukaryotes and mammalian organisms. By RNA-seq, we showed a reduction of dTET mRNA levels in dTET-mutant *Drosophila*. Pvu-seq demonstrates that the 5-hmc levels in nuclear and mitochondrial DNA were both significantly reduced, which confirms the role of dTET in the conversion of 5mc to 5hmc both nuclear and mitochondrial DNA. Finally, we propose a model that, under normal circumstances, dTET and Jumonji proteins bind to the promoter regions of target genes. In the nucleus, the dTET and the Jumonji histone demethylase families of dioxygenase proteins will produce formaldehyde and oxidize DNA in the promoters. This will lead to increased transcription by increasing the access to RNA polymerase. However, in mitochondria, Jumonji proteins are also absent because there are no histones, the oxidation is only produced by dTET. This helps explain why transcription is more dependent on dTET in the mitochondria than in the nucleus.

Ethics:

Since *Drosophila* is a member of the invertebrate and is used as an alternative subject in human research, it will not be considered bio-hazardous during the study.

REFERENCES

1. Sasnauskas G, Tamulaitis G, Sukackaite R, Siksnys V. DNA recognition by the methyl-specific endonuclease McrBC. Febs Journal. 2012;279:451-. PubMed PMID: WOS:000308128602471.

2. Sukackaite R, Grazulis S, Tamulaitis G, Siksnys V. The recognition domain of the methyl-specific endonuclease McrBC flips out 5-methylcytosine. Nucleic Acids Research. 2012;40(15):7552-62. doi: Doi 10.1093/Nar/Gks332. PubMed PMID: WOS:000308958600052.

3. Itoh K, Wakabayashi N, Katoh Y, Ishii T, Igarashi K, Engel JD, Yamamoto M. Keap1 represses nuclear activation of antioxidant responsive elements by Nrf2 through binding to the amino-terminal Neh2 domain. Genes & Development. 1999;13(1):76-86. doi: 10.1101/gad.13.1.76.

4. Lodi R Fau - Tonon C, Tonon C Fau - Calabrese V, Calabrese V Fau - Schapira AHV, Schapira AH. Friedreich's ataxia: from disease mechanisms to therapeutic interventions(1523-0864 (Print)).

5. Pandolfo M. Friedreich ataxia. Semin Pediatr Neurol. 2003;10(3):163-72. PubMed PMID: 14653404.

6. Gucev Z, Tasic V, Jancevska A, Popjordanova N, Koceva S, Kuturec M, Sabolic V. Friedreich ataxia (FA) associated with diabetes mellitus type 1 and hyperthrophic cardiomyopathy. Bosn J Basic Med Sci. 2009;9(2):107-10. PubMed PMID: 19485941.

7. Cavadini P, Gellera C, Patel PI, Isaya G. Human frataxin maintains mitochondrial iron homeostasis in Saccharomyces cerevisiae. Hum Mol Genet. 2000;9(17):2523-30. Epub 2000/10/13. PubMed PMID: 11030757.

8. Tan G, Chen LS, Lonnerdal B, Gellera C, Taroni FA, Cortopassi GA. Frataxin expression rescues mitochondrial dysfunctions in FRDA cells. Hum Mol Genet. 2001;10(19):2099-107. Epub 2001/10/09. PubMed PMID: 11590127.

9. Sarsero JP, Holloway TP, Li L, Finkelstein DI, Ioannou PA. Rescue of the Friedreich ataxia knockout mutation in transgenic mice containing an FXN-EGFP genomic reporter. PLoS One. 2014;9(3):e93307. Epub 2014/03/29. doi: 10.1371/journal.pone.0093307. PubMed PMID: 24667739; PMCID: Pmc3965543.

10. Navarro JA, Llorens JV, Soriano S, Botella JA, Schneuwly S, Martinez-Sebastian MJ, Molto MD. Overexpression of human and Drosophila frataxins in Drosophila provokes deleterious effects at biochemical, physiological and developmental levels. PLoS One. 2011;6(7):e21017. Epub 2011/07/23. doi: 10.1371/journal.pone.0021017. PubMed PMID: 21779322; PMCID: Pmc3136927.

11. Campuzano V, Montermini L, Molto MD, Pianese L, Cossee M, Cavalcanti F, Monros E, Rodius F, Duclos F, Monticelli A, Zara F, Canizares J, Koutnikova H, Bidichandani SI, Gellera C, Brice A, Trouillas P, De Michele G, Filla A, De Frutos R, Palau F, Patel PI, Di Donato S, Mandel J-L, Cocozza S, Koenig M, Pandolfo M. Friedreich's Ataxia: Autosomal Recessive Disease Caused by an Intronic GAA Triplet Repeat Expansion. Science. 1996;271(5254):1423-7.

12. Campuzano V, Montermini L, Lutz Y, Cova L, Hindelang C, Jiralerspong S, Trottier Y, Kish SJ, Faucheux B, Trouillas P, Authier FJ, Dürr A, Mandel J-L, Vescovi A, Pandolfo M, Koenig M. Frataxin is Reduced in Friedreich Ataxia Patients and is Associated with Mitochondrial Membranes. Human Molecular Genetics. 1997;6(11):1771-80. doi: 10.1093/hmg/6.11.1771.

13. Cho S-J, Lee MG, Yang JK, Lee JY, Song HK, Suh SW. Crystal structure of Escherichia coli CyaY protein reveals a previously unidentified fold for the evolutionarily conserved frataxin family. Proceedings of the National Academy of Sciences of the United States of America. 2000;97(16):8932-7.

14. Gibson TJ, Koonin EV, Musco G, Pastore A, Bork P. Friedreich's ataxia protein: phylogenetic evidence for mitochondrial dysfunction. Trends in neurosciences. 1996;19(11):465-8.

15. Koutnikova H, Campuzano V, Koenig M. Maturation of Wild-Type and Mutated Frataxin by the Mitochondrial Processing Peptidase. Human Molecular Genetics. 1998;7(9):1485-9. doi: 10.1093/hmg/7.9.1485.

16. Cavadini P, Adamec J, Taroni F, Gakh O, Isaya G. Two-step Processing of Human Frataxin by Mitochondrial Processing Peptidase: PRECURSOR AND INTERMEDIATE FORMS ARE CLEAVED AT DIFFERENT RATES. Journal of Biological Chemistry. 2000;275(52):41469-75. doi: 10.1074/jbc.M006539200.

17. Condò I, Ventura N, Malisan F, Rufini A, Tomassini B, Testi R. In vivo maturation of human frataxin. Human Molecular Genetics. 2007;16(13):1534-40. doi: 10.1093/hmg/ddm102.

18. Yoon T, Dizin E, Cowan JA. N-terminal iron-mediated self-cleavage of human frataxin: regulation of iron binding and complex formation with target proteins. J Biol Inorg Chem. 2007;12(4):535-42. doi: 10.1007/s00775-007-0205-2.

19. Gakh O, Bedekovics T, Duncan SF, Smith DY, Berkholz DS, Isaya G. Normal and Friedreich Ataxia Cells Express Different Isoforms of Frataxin with Complementary Roles in Iron-Sulfur Cluster Assembly. Journal of Biological Chemistry. 2010;285(49):38486-501. doi: 10.1074/jbc.M110.145144.

20. Lamont PJ, Davis MB, Wood NW. Identification and sizing of the GAA trinucleotide repeat expansion of

Friedreich's ataxia in 56 patients. Clinical and genetic correlates. Brain : a journal of neurology. 1997;120 (Pt 4):673-80.

21. Dürr A, Cossee M, Agid Y, Campuzano V, Mignard C, Penet C, Mandel JL, Brice A, Koenig M. Clinical and genetic abnormalities in patients with Friedreich's ataxia. The New England journal of medicine. 1996;335(16):1169-75.

22. Grabczyk E, Mancuso M, Sammarco MC. A persistent RNA.DNA hybrid formed by transcription of the Friedreich ataxia triplet repeat in live bacteria, and by T7 RNAP in vitro. Nucleic acids research. 2007;35(16):5351-9. Epub 2007/08/19. doi: 10.1093/nar/gkm589. PubMed PMID: 17693431; PMCID: Pmc2018641.

23. Wells RD. DNA triplexes and Friedreich ataxia. FASEB journal : official publication of the Federation of American Societies for Experimental Biology. 2008;22(6):1625-34. Epub 2008/01/24. doi: 10.1096/fj.07-097857. PubMed PMID: 18211957.

24. Baralle M, Pastor T, Bussani E, Pagani F. Influence of Friedreich Ataxia GAA Noncoding Repeat Expansions on Pre-mRNA Processing. The American Journal of Human Genetics. 2008;83(1):77-88.

25. Saveliev A, Everett C, Sharpe T, Webster Z, Festenstein R. DNA triplet repeats mediate heterochromatin-protein-1-sensitive variegated gene silencing. Nature. 2003;422(6934):909-13. doi: http://www.nature.com/nature/journal/v422/n6934/suppinfo/nature01596_S1.html.

26. Koutnikova H, Campuzano V, Foury F, Dolle P, Cazzalini O, Koenig M. Studies of human, mouse and yeast homologues indicate a mitochondrial function for frataxin. Nat Genet. 1997;16(4):345-51. Epub 1997/08/01. doi: 10.1038/ng0897-345. PubMed PMID: 9241270.

27. Cossee M, Puccio H, Gansmuller A, Koutnikova H, Dierich A, LeMeur M, Fischbeck K, Dolle P, Koenig M. Inactivation of the Friedreich ataxia mouse gene leads to early embryonic lethality without iron accumulation. Hum Mol Genet. 2000;9(8):1219-26. PubMed PMID: 10767347.

28. Solbach K, Kraff O, Minnerop M, Beck A, Schöls L, Gizewski ER, Ladd ME, Timmann D. Cerebellar pathology in Friedreich's ataxia: Atrophied dentate nuclei with normal iron content. NeuroImage: Clinical. 2014;6(0):93-9. doi: http://dx.doi.org/10.1016/j.nicl.2014.08.018.

29. Delatycki M, Williamson R, Forrest S. Friedreich ataxia: an overview. Journal of Medical Genetics. 2000;37(1):1-8. doi: 10.1136/jmg.37.1.1. PubMed PMID: PMC1734457.

30. Harding AE. Friedreich's ataxia: a clinical and genetic study of 90 families with an analysis of early diagnostic criteria and intrafamilial clustering of clinical features. Brain. 1981;104(3):589-620. PubMed PMID: 7272714.

31. Ormerod IE, Harding AE, Miller DH, Johnson G, MacManus D, du Boulay EP, Kendall BE, Moseley IF, McDonald WI. Magnetic resonance imaging in degenerative ataxic disorders. Journal of Neurology, Neurosurgery, and Psychiatry. 1994;57(1):51-7. PubMed PMID: PMC485039.

32. Koeppen AH. Friedreich's ataxia: Pathology, pathogenesis, and molecular genetics. Journal of the Neurological Sciences. 2011;303(1–2):1-12. doi: http://dx.doi.org/10.1016/j.jns.2011.01.010.

33. Akhlaghi H, Corben L, Georgiou-Karistianis N, Bradshaw J, Storey E, Delatycki MB, Egan GF. Superior cerebellar peduncle atrophy in Friedreich's ataxia correlates with disease symptoms. Cerebellum. 2011;10(1):81-7. Epub 2010/11/26. doi: 10.1007/s12311-010-0232-3. PubMed PMID: 21107777.

34. Koeppen AH. The history of iron in the brain. J Neurol Sci. 1995;134 Suppl:1-9. Epub 1995/12/01. PubMed PMID: 8847538.

35. Coppola G, Marmolino D, Lu D, Wang Q, Cnop M, Rai M, Acquaviva F, Cocozza S, Pandolfo M, Geschwind DH. Functional genomic analysis of frataxin deficiency reveals tissue-specific alterations and identifies the PPARgamma pathway as a therapeutic target in Friedreich's ataxia. Hum Mol Genet. 2009;18(13):2452-61. PubMed PMID: 19376812.

36. Lamarche JB, Cote M, Lemieux B. The cardiomyopathy of Friedreich's ataxia morphological observations in 3 cases. The Canadian journal of neurological sciences Le journal canadien des sciences neurologiques. 1980;7(4):389-96. Epub 1980/11/01. PubMed PMID: 6452194.

37. Stehling O, Elsasser HP, Bruckel B, Muhlenhoff U, Lill R. Iron-sulfur protein maturation in human cells: evidence for a function of frataxin. Hum Mol Genet. 2004;13(23):3007-15. PubMed PMID: 15509595.

38. Rotig A, de Lonlay P, Chretien D, Foury F, Koenig M, Sidi D, Munnich A, Rustin P. Aconitase and mitochondrial iron-sulphur protein deficiency in Friedreich ataxia. Nat Genet. 1997;17(2):215-7. PubMed PMID: 9326946.

39. Cadenas E, Davies KJ. Mitochondrial free radical generation, oxidative stress, and aging. Free radical biology & medicine. 2000;29(3-4):222-30. Epub 2000/10/18. PubMed PMID: 11035250.

40. Babcock M, de Silva D, Oaks R, Davis-Kaplan S, Jiralerspong S, Montermini L, Pandolfo M, Kaplan J. Regulation of Mitochondrial Iron Accumulation by Yfh1p, a Putative Homolog of Frataxin. Science. 1997;276(5319):1709-12. doi: 10.1126/science.276.5319.1709.

41. Foury F, Cazzalini O. Deletion of the yeast homologue of the human gene associated with Friedreich's ataxia elicits iron accumulation in mitochondria. FEBS Letters. 1997;411(2–3):373-7. doi: http://dx.doi.org/10.1016/S0014-5793(97)00734-5.

42. Yang J, Cavadini P, Gellera C, Lonnerdal B, Taroni F, Cortopassi G. The Friedreich's Ataxia Mutation Confers Cellular Sensitivity to Oxidant Stress Which Is Rescued by Chelators of Iron and Calcium and Inhibitors of Apoptosis. Human Molecular Genetics. 1999;8(3):425-30. doi: 10.1093/hmg/8.3.425.

43. Bolinches-Amorós A, Mollá B, Pla-Martín D, Palau F, Gonzalez-Cabo P. Mitochondrial dysfunction induced by frataxin deficiency is associated with cellular senescence and abnormal calcium metabolism. Frontiers in Cellular Neuroscience. 2014;8. doi: 10.3389/fncel.2014.00124.

44. Napoli E, Taroni F, Cortopassi GA. Forum Original Research Communication: Frataxin, Iron–Sulfur Clusters, Heme, ROS, and Aging. Antioxidants & redox signaling. 2006;8(3-4):506-16. doi: 10.1089/ars.2006.8.506. PubMed PMID: PMC1805116.

45. Armstrong JS, Khdour O, Hecht SM. Does oxidative stress contribute to the pathology of Friedreich's ataxia? A radical question. The FASEB Journal. 2010;24(7):2152-63. doi: 10.1096/fj.09-143222.

46. Calabrese V, Lodi R, Tonon C, D'Agata V, Sapienza M, Scapagnini G, Mangiameli A, Pennisi G, Stella AMG, Butterfield DA. Oxidative stress, mitochondrial dysfunction and cellular stress response in Friedreich's ataxia. Journal of the neurological sciences. 2005;233(1-2):145-62.

47. Seznec H, Simon D, Bouton C, Reutenauer L, Hertzog A, Golik P, Procaccio V, Patel M, Drapier JC, Koenig M, Puccio H. Friedreich ataxia: the oxidative stress paradox. Hum Mol Genet. 2005;14(4):463-74. Epub 2004/12/24. doi: 10.1093/hmg/ddi042. PubMed PMID: 15615771.

48. Yankovskaya V, Horsefield R, Tornroth S, Luna-Chavez C, Miyoshi H, Leger C, Byrne B, Cecchini G, Iwata S. Architecture of succinate dehydrogenase and reactive oxygen species generation. Science. 2003;299(5607):700-4. Epub 2003/02/01. doi: 10.1126/science.1079605. PubMed PMID: 12560550.

49. Anderson PR, Kirby K, Orr WC, Hilliker AJ, Phillips JP. Hydrogen peroxide scavenging rescues frataxin

deficiency in a Drosophila model of Friedreich's ataxia. Proceedings of the National Academy of Sciences. 2008;105(2):611-6. doi: 10.1073/pnas.0709691105.

50. Lefevre S, Sliwa D, Auchère F, Brossas C, Ruckenstuhl C, Boggetto N, Lesuisse E, Madeo F, Camadro J-M, Santos R. The yeast metacaspase is implicated in oxidative stress response in frataxin-deficient cells. FEBS Letters. 2012;586(2):143-8. doi: http://dx.doi.org/10.1016/j.febslet.2011.12.002.

51. Wilson RB, Roof DM. Respiratory deficiency due to loss of mitochondrial DNA in yeast lacking the frataxin homologue. Nat Genet. 1997;16(4):352-7.

52. Lewis PD, Corr JB, Arlett CF, Harcourt SA. INCREASED SENSITIVITY TO GAMMA IRRADIATION OF SKIN FIBROBLASTS IN FRIEDREICH'S ATAXIA. The Lancet. 1979;314(8140):474-5.

53. Karthikeyan G, Lewis LK, Resnick MA. The mitochondrial protein frataxin prevents nuclear damage. Human Molecular Genetics. 2002;11(11):1351-62.

54. Koehler CM, Beverly KN, Leverich EP. Redox pathways of the mitochondrion. Antioxid Redox Signal. 2006;8(5-6):813-22. Epub 2006/06/15. doi: 10.1089/ars.2006.8.813. PubMed PMID: 16771672.

55. Hirotsu Y, Katsuoka F, Funayama R, Nagashima T, Nishida Y, Nakayama K, Douglas Engel J, Yamamoto M. Nrf2–MafG heterodimers contribute globally to antioxidant and metabolic networks. Nucleic acids research. 2012. doi: 10.1093/nar/gks827.

56. Motohashi H, Katsuoka F, Engel JD, Yamamoto M. Small Maf proteins serve as transcriptional cofactors for keratinocyte differentiation in the Keap1-Nrf2 regulatory pathway. Proc Natl Acad Sci U S A. 2004;101(17):6379-84. Epub 2004/04/17. doi: 10.1073/pnas.0305902101. PubMed PMID: 15087497; PMCID: Pmc404053.

57. Huang H-C, Nguyen T, Pickett CB. Phosphorylation of Nrf2 at Ser-40 by Protein Kinase C Regulates Antioxidant Response Element-mediated Transcription. Journal of Biological Chemistry. 2002;277(45):42769-74. doi: 10.1074/jbc.M206911200.

58. Paupe V, Dassa EP, Goncalves S, Auchère F, Lönn M, Holmgren A, Rustin P. Impaired Nuclear Nrf2 Translocation Undermines the Oxidative Stress Response in Friedreich Ataxia. PLoS ONE. 2009;4(1):e4253. doi: 10.1371/journal.pone.0004253.

59. Auchère F, Santos R, Planamente S, Lesuisse E, Camadro J-M. Glutathione-dependent redox status of frataxin-deficient cells in a yeast model of Friedreich's ataxia. Human Molecular Genetics. 2008;17(18):2790-802.

doi: 10.1093/hmg/ddn178.

60. Tonon C, Lodi R. Idebenone in Friedreich's ataxia. Expert opinion on pharmacotherapy. 2008;9(13):2327-37. Epub 2008/08/20. doi: 10.1517/14656566.9.13.2327. PubMed PMID: 18710357.

61. Kearney M, Orrell RW, Fahey M, Pandolfo M. Antioxidants and other pharmacological treatments for Friedreich ataxia. Cochrane database of systematic reviews (Online). 2009(4).

62. Perlman SL. A review of Friedreich ataxia clinical trial results. Journal of child neurology. 2012;27(9):1217-22. Epub 2012/08/29. doi: 10.1177/0883073812453872. PubMed PMID: 22927692.

63. Meier T, Perlman SL, Rummey C, Coppard NJ, Lynch DR. Assessment of neurological efficacy of idebenone in pediatric patients with Friedreich's ataxia: data from a 6-month controlled study followed by a 12-month open-label extension study. Journal of neurology. 2012;259(2):284-91. Epub 2011/07/23. doi: 10.1007/s00415-011-6174-y. PubMed PMID: 21779958.

64. Soriano S, Llorens JV, Blanco-Sobero L, Gutiérrez L, Calap-Quintana P, Morales MP, Moltó MD, Martínez-Sebastián MJ. Deferiprone and idebenone rescue frataxin depletion phenotypes in a Drosophila model of Friedreich's ataxia. Gene. 2013;521(2):274-81. doi: http://dx.doi.org/10.1016/j.gene.2013.02.049.

65. Ebato C, Uchida T, Arakawa M, Komatsu M, Ueno T, Komiya K, Azuma K, Hirose T, Tanaka K, Kominami E, Kawamori R, Fujitani Y, Watada H. Autophagy is important in islet homeostasis and compensatory increase of beta cell mass in response to high-fat diet. Cell metabolism. 2008;8(4):325-32.

66. Nishino I, Fu J, Tanji K, Yamada T, Shimojo S, Koori T, Mora M, Riggs JE, Oh SJ, Koga Y, Sue CM, Yamamoto A, Murakami N, Shanske S, Byrne E, Bonilla E, Nonaka I, DiMauro S, Hirano M. Primary LAMP-2 deficiency causes X-linked vacuolar cardiomyopathy and myopathy (Danon disease). Nature. 2000;406(6798):906-10. Epub 2000/09/06. doi: 10.1038/35022604. PubMed PMID: 10972294.

67. Zhou X-j, Lu X-l, Lv J-c, Yang H-z, Qin L-x, Zhao M-h, Su Y, Li Z-g, Zhang H. Genetic association of PRDM1-ATG5 intergenic region and autophagy with systemic lupus erythematosus in a Chinese population. Annals of the Rheumatic Diseases. 2011;70(7):1330-7. doi: 10.1136/ard.2010.140111.

68. Wyttenbach A, Hands S, King MA, Lipkow K, Tolkovsky AM. Amelioration of protein misfolding disease by rapamycin: Translation or autophagy? Autophagy. 2008;4(4):542-5. doi: 10.4161/auto.6059.

69. Saito H, Inazawa J, Saito S, Kasumi F, Koi S, Sagae S, Kudo R, Saito J, Noda K, Nakamura Y. Detailed deletion

mapping of chromosome 17q in ovarian and breast cancers: 2-cM region on 17q21.3 often and commonly deleted in tumors. Cancer Res. 1993;53(14):3382-5. Epub 1993/07/15. PubMed PMID: 8100738.

70. Liang XH, Jackson S, Seaman M, Brown K, Kempkes B, Hibshoosh H, Levine B. Induction of autophagy and inhibition of tumorigenesis by beclin 1. Nature. 1999;402(6762):672-6.

71. Nakatogawa H, Suzuki K, Kamada Y, Ohsumi Y. Dynamics and diversity in autophagy mechanisms: lessons from yeast. Nat Rev Mol Cell Biol. 2009;10(7):458-67.

72. Chang Y-Y, Neufeld TP. An Atg1/Atg13 Complex with Multiple Roles in TOR-mediated Autophagy Regulation. Molecular Biology of the Cell. 2009;20(7):2004-14. doi: 10.1091/mbc.E08-12-1250.

73. Tooze SA, Yoshimori T. The origin of the autophagosomal membrane. Nat Cell Biol. 2010;12(9):831-5.

74. Chan EY, Longatti A, McKnight NC, Tooze SA. Kinase-inactivated ULK proteins inhibit autophagy via their conserved C-terminal domains using an Atg13-independent mechanism. Molecular and cellular biology. 2009;29(1):157-71. Epub 2008/10/22. doi: 10.1128/mcb.01082-08. PubMed PMID: 18936157; PMCID: Pmc2612494.

75. Jung CH, Jun CB, Ro S-H, Kim Y-M, Otto NM, Cao J, Kundu M, Kim D-H. ULK-Atg13-FIP200 Complexes Mediate mTOR Signaling to the Autophagy Machinery. Molecular Biology of the Cell. 2009;20(7):1992-2003. doi: 10.1091/mbc.E08-12-1249. PubMed PMID: PMC2663920.

76. Hara T, Takamura A, Kishi C, Iemura S, Natsume T, Guan JL, Mizushima N. FIP200, a ULK-interacting protein, is required for autophagosome formation in mammalian cells. J Cell Biol. 2008;181(3):497-510. Epub 2008/04/30. doi: 10.1083/jcb.200712064. PubMed PMID: 18443221; PMCID: Pmc2364687.

77. Suzuki K, Kirisako T, Kamada Y, Mizushima N, Noda T, Ohsumi Y. The pre-autophagosomal structure organized by concerted functions of APG genes is essential for autophagosome formation. The EMBO journal. 2001;20(21):5971-81.

78. Mari M, Griffith J, Rieter E, Krishnappa L, Klionsky DJ, Reggiori F. An Atg9-containing compartment that functions in the early steps of autophagosome biogenesis. The Journal of Cell Biology. 2010;190(6):1005-22. doi: 10.1083/jcb.200912089.

79. Geng J, Klionsky DJ. The Atg8 and Atg12 ubiquitin-like conjugation systems in macroautophagy. Protein Modifications: Beyond the Usual Suspects EMBO reports. 2008;9(9):859-64.

80. Satoo K, Suzuki NN, Fujioka Y, Mizushima N, Ohsumi Y, Inagaki F. Crystallization and preliminary

crystallographic analysis of human Atg4B-LC3 complex. Acta Crystallographica Section F: Structural Biology and Crystallization Communications. 2007.

81. Gabriely G, Kama R, Gelin-Licht R, Gerst JE. Different domains of the UBL-UBA ubiquitin receptor, Ddi1/Vsm1, are involved in its multiple cellular roles. Molecular biology of the cell. 2008;19(9):3625-37.

82. Kuma A, Mizushima N, Ishihara N, Ohsumi Y. Formation of the ~350-kDa Apg12-Apg5·Apg16 Multimeric Complex, Mediated by Apg16 Oligomerization, Is Essential for Autophagy in Yeast. Journal of Biological Chemistry. 2002;277(21):18619-25.

83. Romanov J, Walczak M, Ibiricu I, Schüchner S, Ogris E, Kraft C, Martens S. Mechanism and functions of membrane binding by the Atg5–Atg12/Atg16 complex during autophagosome formation2012 2012-11-14 00:00:00. 4304-17 p.

84. Orsi A, Polson HEJ, Tooze SA. Membrane trafficking events that partake in autophagy. Current Opinion in Cell Biology. 2010;22(2):150-6. doi: http://dx.doi.org/10.1016/j.ceb.2009.11.013.

85. Scott RC, Schuldiner O, Neufeld TP. Role and Regulation of Starvation-Induced Autophagy in the Drosophila Fat Body. Developmental Cell. 2004;7(2):167-78. doi: 10.1016/j.devcel.2004.07.009.

86. Sou Y-s, Waguri S, Iwata J-i, Ueno T, Fujimura T, Hara T, Sawada N, Yamada A, Mizushima N, Uchiyama Y, Kominami E, Tanaka K, Komatsu M. The Atg8 Conjugation System Is Indispensable for Proper Development of Autophagic Isolation Membranes in Mice. Molecular biology of the cell.

87. Sato K, Tsuchihara K, Fujii S, Sugiyama M, Goya T, Atomi Y, Ueno T, Ochiai A, Esumi H. Autophagy is activated in colorectal cancer cells and contributes to the tolerance to nutrient deprivation. Cancer research. 2007;67(20):9677-84.

88. Kuma A, Hatano M, Matsui M, Yamamoto A, Nakaya H, Yoshimori T, Ohsumi Y, Tokuhisa T, Mizushima N. The role of autophagy during the early neonatal starvation period. Nature. 2004;432(7020):1032-6.

89. Ishii T, Itoh K, Yamamoto M. Roles of Nrf2 in activation of antioxidant enzyme genes via antioxidant responsive elements. Methods in enzymology. 2002;348:182-90. Epub 2002/03/12. PubMed PMID: 11885271.

90. Tasdemir E, Maiuri MC, Galluzzi L, Vitale I, Djavaheri-Mergny M, D'Amelio M, Criollo A, Morselli E, Zhu C, Harper F, Nannmark U, Samara C, Pinton P, Vicencio JM, Carnuccio R, Moll UM, Madeo F, Paterlini-Brechot P, Rizzuto R, Szabadkai G, Pierron G, Blomgren K, Tavernarakis N, Codogno P, Cecconi F, Kroemer G. Regulation of

autophagy by cytoplasmic p53. Nat Cell Biol. 2008;10(6):676-87. doi: http://www.nature.com/ncb/journal/v10/n6/suppinfo/ncb1730_S1.html.

91. Morselli E, Shen S, Ruckenstuhl C, Bauer MA, Marino G, Galluzzi L, Criollo A, Michaud M, Maiuri MC, Chano T, Madeo F, Kroemer G. p53 inhibits autophagy by interacting with the human ortholog of yeast Atg17, RB1CC1/FIP200. Cell cycle (Georgetown, Tex). 2011;10(16):2763-9. Epub 2011/07/22. PubMed PMID: 21775823.

92. Scherz-Shouval R, Shvets E, Fass E, Shorer H, Gil L, Elazar Z. Reactive oxygen species are essential for autophagy and specifically regulate the activity of Atg4. The EMBO journal. 2007;26(7):1749-60. Epub 2007/03/10. doi: 10.1038/sj.emboj.7601623. PubMed PMID: 17347651; PMCID: Pmc1847657.

93. Crighton D, Wilkinson S, O'Prey J, Syed N, Smith P, Harrison PR, Gasco M, Garrone O, Crook T, Ryan KM. DRAM, a p53-induced modulator of autophagy, is critical for apoptosis. Cell. 2006;126(1):121-34. Epub 2006/07/15. doi: 10.1016/j.cell.2006.05.034. PubMed PMID: 16839881.

94. Gu ZT, Wang H, Li L, Liu YS, Deng XB, Huo SF, Yuan FF, Liu ZF, Tong HS, Su L. Heat stress induces apoptosis through transcription-independent p53-mediated mitochondrial pathways in human umbilical vein endothelial cell. Sci Rep. 2014;4. doi: 10.1038/srep04469.

95. Le Grand Jn Fau - Chakrama FZ, Chakrama Fz Fau - Seguin-Py S, Seguin-Py S Fau - Fraichard A, Fraichard A Fau - Delage-Mourroux R, Delage-Mourroux R Fau - Jouvenot M, Jouvenot M Fau - Boyer-Guittaut M, Boyer-Guittaut M. GABARAPL1 (GEC1): original or copycat?(1554-8635 (Electronic)).

96. Rouschop KM, Ramaekers CH, Schaaf MB, Keulers TG, Savelkouls KG, Lambin P, Koritzinsky M, Wouters BG. Autophagy is required during cycling hypoxia to lower production of reactive oxygen species. Radiotherapy and oncology : journal of the European Society for Therapeutic Radiology and Oncology. 2009;92(3):411-6. Epub 2009/07/21. doi: 10.1016/j.radonc.2009.06.029. PubMed PMID: 19616335.

97. Shimizu S, Kanaseki T, Mizushima N, Mizuta T, Arakawa-Kobayashi S, Thompson CB, Tsujimoto Y. Role of Bcl-2 family proteins in a non-apoptotic programmed cell death dependent on autophagy genes. Nature cell biology. 2004;6(12):1221-8.

98. Bursch W, Ellinger A, Kienzl H, Török L, Pandey S, Sikorska M, Walker R, Hermann RS. Active cell death induced by the anti-estrogens tamoxifen and ICI 164 384 in human mammary carcinoma cells (MCF-7) in culture: the role of autophagy. Carcinogenesis. 1996;17(8):1595-607.

99. Juhász G, Sass M. Hid can induce, but is not required for autophagy in polyploid larval Drosophila tissues. European journal of cell biology. 2005;84(4):491-502.

100. Young MM, Takahashi Y, Khan O, Park S, Hori T, Yun J, Sharma AK, Amin S, Hu CD, Zhang J, Kester M, Wang HG. Autophagosomal membrane serves as platform for intracellular death-inducing signaling complex (iDISC)-mediated caspase-8 activation and apoptosis. J Biol Chem. 2012;287(15):12455-68. Epub 2012/03/01. doi: 10.1074/jbc.M111.309104. PubMed PMID: 22362782; PMCID: Pmc3320995.

101. Igoillo-Esteve M, Gurgul-Convey E, Hu A, Romagueira Bichara Dos Santos L, Abdulkarim B, Chintawar S, Marselli L, Marchetti P, Jonas JC, Eizirik DL, Pandolfo M, Cnop M. Unveiling a common mechanism of apoptosis in beta-cells and neurons in Friedreich's ataxia. Hum Mol Genet. 2014. Epub 2015/01/02. doi: 10.1093/hmg/ddu745. PubMed PMID: 25552656.

102. Mincheva-Tasheva S, Obis E, Tamarit J, Ros J. Apoptotic cell death and altered calcium homeostasis caused by frataxin depletion in dorsal root ganglia neurons can be prevented by BH4 domain of Bcl-xL protein. Hum Mol Genet. 2014;23(7):1829-41. Epub 2013/11/19. doi: 10.1093/hmg/ddt576. PubMed PMID: 24242291.

103. Ballou LM, Lin RZ. Rapamycin and mTOR kinase inhibitors. Journal of Chemical Biology. 2008;1(1-4):27-36. doi: 10.1007/s12154-008-0003-5. PubMed PMID: PMC2698317.

104. Kim D-H, Sarbassov DD, Ali SM, King JE, Latek RR, Erdjument-Bromage H, Tempst P, Sabatini DM. mTOR Interacts with Raptor to Form a Nutrient-Sensitive Complex that Signals to the Cell Growth Machinery. Cell. 2002;110(2):163-75. doi: http://dx.doi.org/10.1016/S0092-8674(02)00808-5.

105. Xie L, Li W, Winters A, Yuan F, Jin K, Yang S. Methylene blue induces macroautophagy through 5′ adenosine monophosphate-activated protein kinase pathway to protect neurons from serum deprivation. Frontiers in Cellular Neuroscience. 2013;7:56. doi: 10.3389/fncel.2013.00056. PubMed PMID: PMC3642497.

106. Congdon EE, Wu JW, Myeku N, Figueroa YH, Herman M, Marinec PS, Gestwicki JE, Dickey CA, Yu WH, Duff KE. Methylthioninium chloride (methylene blue) induces autophagy and attenuates tauopathy in vitro and in vivo. Autophagy. 2012;8(4):609-22. doi: 10.4161/auto.19048.

107. Poole B, Ohkuma S. Effect of weak bases on the intralysosomal pH in mouse peritoneal macrophages. J Cell Biol. 1981;90(3):665-9. Epub 1981/09/01. PubMed PMID: 6169733; PMCID: Pmc2111912.

108. Yamamoto A, Tagawa Y, Yoshimori T, Moriyama Y, Masaki R, Tashiro Y. Bafilomycin A1 prevents maturation of autophagic vacuoles by inhibiting fusion between autophagosomes and lysosomes in rat hepatoma cell line, H-4-II-E cells. Cell structure and function. 1998;23(1):33-42. Epub 1998/06/25. PubMed PMID: 9639028.

109. Wu Y-T, Tan H-L, Shui G, Bauvy C, Huang Q, Wenk MR, Ong C-N, Codogno P, Shen H-M. Dual Role of 3-Methyladenine in Modulation of Autophagy via Different Temporal Patterns of Inhibition on Class I and III Phosphoinositide 3-Kinase. Journal of Biological Chemistry. 2010;285(14):10850-61. doi: 10.1074/jbc.M109.080796.

110. Martinet W, Agostinis P, Vanhoecke B, Dewaele M, De Meyer GRY. Autophagy in disease: a double-edged sword with therapeutic potential. Clinical science (London, England : 1979). 2009;116(9):697-712.

111. Day SM, Duquaine D, Mundada LV, Menon RG, Khan BV, Rajagopalan S, Fay WP. Chronic Iron Administration Increases Vascular Oxidative Stress and Accelerates Arterial Thrombosis. Circulation. 2003;107(20):2601-6. doi: 10.1161/01.cir.0000066910.02844.d0.

112. Chance B, Sies H, Boveris A. Hydroperoxide metabolism in mammalian organs. Physiological reviews. 1979;59(3):527-605.

113. Dawson TL, Gores GJ, Nieminen AL, Herman B, Lemasters JJ. Mitochondria as a source of reactive oxygen species during reductive stress in rat hepatocytes. The American journal of physiology. 1993;264(4 Pt 1):961-7.

114. Lemasters JJ, Nieminen AL, Qian T, Trost LC, Elmore SP, Nishimura Y, Crowe RA, Cascio WE, Bradham CA, Brenner DA, Herman B. The mitochondrial permeability transition in cell death: a common mechanism in necrosis, apoptosis and autophagy. Biochimica et biophysica acta. 1998;1366(1-2):177-96.

115. Whitnall M, Suryo Rahmanto Y, Huang ML, Saletta F, Lok HC, Gutierrez L, Lazaro FJ, Fleming AJ, St Pierre TG, Mikhael MR, Ponka P, Richardson DR. Identification of nonferritin mitochondrial iron deposits in a mouse model of Friedreich ataxia. Proc Natl Acad Sci U S A. 2012;109(50):20590-5. Epub 2012/11/22. doi: 10.1073/pnas.1215349109. PubMed PMID: 23169664; PMCID: Pmc3528580.

116. Gonzalez-Cabo P, Palau F. Mitochondrial pathophysiology in Friedreich's ataxia. Journal of neurochemistry. 2013;126 Suppl 1:53-64. Epub 2013/07/24. doi: 10.1111/jnc.12303. PubMed PMID: 23859341.

117. Cnop M, Igoillo-Esteve M, Rai M, Begu A, Serroukh Y, Depondt C, Musuaya AE, Marhfour I, Ladrière L, Moles Lopez X, Lefkaditis D, Moore F, Brion J-P, Cooper JM, Schapira AHV, Clark A, Koeppen AH, Marchetti P, Pandolfo M, Eizirik DL, Féry F. Central role and mechanisms of β-cell dysfunction and death in friedreich ataxia–

associated diabetes. Annals of Neurology. 2012;72(6):971-82. doi: 10.1002/ana.23698.

118. Cnop M, Mulder H, Igoillo-Esteve M. Diabetes in Friedreich Ataxia. Journal of neurochemistry. 2013;126:94-102. doi: 10.1111/jnc.12216.

119. Magrane J, Hervias I, Henning MS, Damiano M, Kawamata H, Manfredi G. Mutant SOD1 in neuronal mitochondria causes toxicity and mitochondrial dynamics abnormalities. Hum Mol Genet. 2009;18(23):4552-64. Epub 2009/09/26. doi: 10.1093/hmg/ddp421. PubMed PMID: 19779023; PMCID: Pmc2773270.

120. Frank S, Gaume B, Bergmann-Leitner ES, Leitner WW, Robert EG, Catez F, Smith CL, Youle RJ. The role of dynamin-related protein 1, a mediator of mitochondrial fission, in apoptosis. Dev Cell. 2001;1(4):515-25. Epub 2001/11/13. PubMed PMID: 11703942.

121. Olichon A, Baricault L, Gas N, Guillou E, Valette A, Belenguer P, Lenaers G. Loss of OPA1 perturbates the mitochondrial inner membrane structure and integrity, leading to cytochrome c release and apoptosis. J Biol Chem. 2003;278(10):7743-6. Epub 2003/01/02. doi: 10.1074/jbc.C200677200. PubMed PMID: 12509422.

122. Palomo GM, Manfredi G. Exploring new pathways of neurodegeneration in ALS: The role of mitochondria quality control. Brain Research. (0). doi: http://dx.doi.org/10.1016/j.brainres.2014.09.065.

123. Ashford TP, Porter KR. Cytoplasmic components in hepatic cell lysosomes. The Journal of cell biology. 1962;12:198-202.

124. Zhang Y, Qi H, Taylor R, Xu W, Liu LF, Jin S. The role of autophagy in mitochondria maintenance: characterization of mitochondrial functions in autophagy-deficient S. cerevisiae strains. Autophagy. 2007;3(4):337-46.

125. Anderson PR, Kirby K, Orr WC, Hilliker AJ, Phillips JP. Hydrogen peroxide scavenging rescues frataxin deficiency in a Drosophila model of Friedreich's ataxia. Proc Natl Acad Sci U S A. 2008;105(2):611-6. PubMed PMID: 18184803.

126. Scherz-Shouval R, Shvets E, Fass E, Shorer H, Gil L, Elazar Z. Reactive oxygen species are essential for autophagy and specifically regulate the activity of Atg4. The EMBO journal. 2007;26(7):1749-60.

127. Chang AL, Ulrich A, Suliman HB, Piantadosi CA. Redox regulation of mitophagy in the lung during murine Staphylococcus aureus sepsis. Free Radical Biology and Medicine. 2015;78(0):179-89. doi: http://dx.doi.org/10.1016/j.freeradbiomed.2014.10.582.

128. Elmore SP, Qian T, Grissom SF, Lemasters JJ. The mitochondrial permeability transition initiates autophagy in rat hepatocytes. The FASEB journal : official publication of the Federation of American Societies for Experimental Biology. 2001;15(12):2286-7.

129. Rodriguez-Enriquez S, Kim I, Currin RT, Lemasters JJ. Tracker dyes to probe mitochondrial autophagy (mitophagy) in rat hepatocytes. Autophagy. 2006;2(1):39-46.

130. Mizushima N, Yamamoto A, Matsui M, Yoshimori T, Ohsumi Y. In Vivo Analysis of Autophagy in Response to Nutrient Starvation Using Transgenic Mice Expressing a Fluorescent Autophagosome Marker. Molecular biology of the cell. 2004;15(3):1101-11.

131. Narendra D, Tanaka A, Suen D-F, Youle RJ. Parkin is recruited selectively to impaired mitochondria and promotes their autophagy. The Journal of cell biology. 2008;183(5):795-803.

132. Jin SM, Lazarou M, Wang C, Kane LA, Narendra DP, Youle RJ. Mitochondrial membrane potential regulates PINK1 import and proteolytic destabilization by PARL. J Cell Biol. 2010;191(5):933-42. Epub 2010/12/01. doi: 10.1083/jcb.201008084. PubMed PMID: 21115803; PMCID: Pmc2995166.

133. Zhou C, Huang Y, Shao Y, May J, Prou D, Perier C, Dauer W, Schon EA, Przedborski S. The kinase domain of mitochondrial PINK1 faces the cytoplasm. Proc Natl Acad Sci U S A. 2008;105(33):12022-7. Epub 2008/08/09. doi: 10.1073/pnas.0802814105. PubMed PMID: 18687899; PMCID: Pmc2575334.

134. Kim Y, Park J, Kim S, Song S, Kwon SK, Lee SH, Kitada T, Kim JM, Chung J. PINK1 controls mitochondrial localization of Parkin through direct phosphorylation. Biochem Biophys Res Commun. 2008;377(3):975-80. Epub 2008/10/30. doi: 10.1016/j.bbrc.2008.10.104. PubMed PMID: 18957282.

135. Geisler S, Holmstrom KM, Skujat D, Fiesel FC, Rothfuss OC, Kahle PJ, Springer W. PINK1/Parkin-mediated mitophagy is dependent on VDAC1 and p62/SQSTM1. Nat Cell Biol. 2010;12(2):119-31. Epub 2010/01/26. doi: 10.1038/ncb2012. PubMed PMID: 20098416.

136. Gegg ME, Cooper JM, Chau KY, Rojo M, Schapira AH, Taanman JW. Mitofusin 1 and mitofusin 2 are ubiquitinated in a PINK1/parkin-dependent manner upon induction of mitophagy. Hum Mol Genet. 2010;19(24):4861-70. Epub 2010/09/28. doi: 10.1093/hmg/ddq419. PubMed PMID: 20871098; PMCID: Pmc3583518.

137. Chan NC, Salazar AM, Pham AH, Sweredoski MJ, Kolawa NJ, Graham RL, Hess S, Chan DC. Broad activation

of the ubiquitin-proteasome system by Parkin is critical for mitophagy. Hum Mol Genet. 2011;20(9):1726-37. Epub 2011/02/08. doi: 10.1093/hmg/ddr048. PubMed PMID: 21296869; PMCID: Pmc3071670.

138. Tanaka A, Cleland MM, Xu S, Narendra DP, Suen DF, Karbowski M, Youle RJ. Proteasome and p97 mediate mitophagy and degradation of mitofusins induced by Parkin. J Cell Biol. 2010;191(7):1367-80. Epub 2010/12/22. doi: 10.1083/jcb.201007013. PubMed PMID: 21173115; PMCID: Pmc3010068.

139. Parone PA, Da Cruz S, Tondera D, Mattenberger Y, James DI, Maechler P, Barja F, Martinou J-C. Preventing mitochondrial fission impairs mitochondrial function and leads to loss of mitochondrial DNA. PloS one. 2008;3(9):e3257.

140. Arnoult D, Rismanchi N, Grodet A, Roberts RG, Seeburg DP, Estaquier J, Sheng M, Blackstone C. Bax/Bak-dependent release of DDP/TIMM8a promotes Drp1-mediated mitochondrial fission and mitoptosis during programmed cell death. Current biology : CB. 2005;15(23):2112-8.

141. Kageyama Y, Hoshijima M, Seo K, Bedja D, Sysa-Shah P, Andrabi SA, Chen W, Hoke A, Dawson VL, Dawson TM, Gabrielson K, Kass DA, Iijima M, Sesaki H. Parkin-independent mitophagy requires Drp1 and maintains the integrity of mammalian heart and brain. Embo j. 2014;33(23):2798-813. Epub 2014/10/29. doi: 10.15252/embj.201488658. PubMed PMID: 25349190; PMCID: Pmc4282557.

142. Twig G, Elorza A, Molina AJA, Mohamed H, Wikstrom JD, Walzer G, Stiles L, Haigh SE, Katz S, Las G, Alroy J, Wu M, Py BF, Yuan J, Deeney JT, Corkey BE, Shirihai OS. Fission and selective fusion govern mitochondrial segregation and elimination by autophagy. The EMBO journal. 2008;27(2):433-46.

143. Levine B, Yuan J. Autophagy in cell death: an innocent convict? J Clin Invest. 2005;115(10):2679-88. Epub 2005/10/04. doi: 10.1172/jci26390. PubMed PMID: 16200202; PMCID: Pmc1236698.

144. Twig G, Hyde B, Shirihai OS. Mitochondrial fusion, fission and autophagy as a quality control axis: the bioenergetic view. Biochimica et biophysica acta. 2008;1777(9):1092-7.

145. Chen H, Chomyn A, Chan DC. Disruption of fusion results in mitochondrial heterogeneity and dysfunction. Journal of Biological Chemistry. 2005;280(28).

146. Maiuri MC, Criollo A, Tasdemir E, Vicencio JM, Tajeddine N, Hickman JA, Geneste O, Kroemer G. BH3-only proteins and BH3 mimetics induce autophagy by competitively disrupting the interaction between Beclin 1 and Bcl-2/Bcl-X(L). Autophagy. 2007;3(4):374-6.

147. Tolkovsky AM. Mitophagy. Biochimica et biophysica acta. 2009;1793(9):1508-15.

148. Reiter LT, Potocki L, Chien S, Gribskov M, Bier E. A systematic analysis of human disease-associated gene sequences in Drosophila melanogaster. Genome research. 2001;11(6):1114-25.

149. Parks AL, Cook KR, Belvin M, Dompe NA, Fawcett R, Huppert K, Tan LR, Winter CG, Bogart KP, Deal JE, Deal-Herr ME, Grant D, Marcinko M, Miyazaki WY, Robertson S, Shaw KJ, Tabios M, Vysotskaia V, Zhao L, Andrade RS, Edgar KA, Howie E, Killpack K, Milash B, Norton A, Thao D, Whittaker K, Winner MA, Friedman L, Margolis J, Singer MA, Kopczynski C, Curtis D, Kaufman TC, Plowman GD, Duyk G, Francis-Lang HL. Systematic generation of high-resolution deletion coverage of the Drosophila melanogaster genome. Nature genetics. 2004;36(3):288-92.

150. Thibault ST, Singer MA, Miyazaki WY, Milash B, Dompe NA, Singh CM, Buchholz R, Demsky M, Fawcett R, Francis-Lang HL, Ryner L, Cheung LM, Chong A, Erickson C, Fisher WW, Greer K, Hartouni SR, Howie E, Jakkula L, Joo D, Killpack K, Laufer A, Mazzotta J, Smith RD, Stevens LM, Stuber C, Tan LR, Ventura R, Woo A, Zakrajsek I, Zhao L, Chen F, Swimmer C, Kopczynski C, Duyk G, Winberg ML, Margolis J. A complementary transposon tool kit for Drosophila melanogaster using P and piggyBac. Nature genetics. 2004;36(3):283-7.

151. Wolf MJ, Amrein H, Izatt JA, Choma MA, Reedy MC, Rockman HA. Drosophila as a model for the identification of genes causing adult human heart disease. Proceedings of the National Academy of Sciences of the United States of America. 2006;103(5):1394-9.

152. Bodmer R. Heart development in Drosophila and its relationship to vertebrates. Trends in Cardiovascular Medicine. 1995;5(1):21-8. doi: http://dx.doi.org/10.1016/1050-1738(94)00032-Q.

153. Molina MR, Cripps RM. Ostia, the inflow tracts of the Drosophila heart, develop from a genetically distinct subset of cardial cells. Mechanisms of Development. 2001;109(1):51-9.

154. Rugendorff A, Younossi-Hartenstein A, Hartenstein V. Embryonic origin and differentiation of the Drosophila heart. Roux's Archives of Developmental Biology. 1994;203(5):266-80.

155. Dulcis D, Levine RB. Glutamatergic Innervation of the Heart Initiates Retrograde Contractions in Adult Drosophila melanogaster. Journal of Neuroscience. 2005;25(2):271-80.

156. Wessells RJ, Bodmer R. Screening assays for heart function mutants in Drosophila. BioTechniques. 2004;37(1):58-60.

157. Nishida Y, Arakawa S, Fujitani K, Yamaguchi H, Mizuta T, Kanaseki T, Komatsu M, Otsu K, Tsujimoto Y,

Shimizu S. Discovery of Atg5/Atg7-independent alternative macroautophagy. Nature. 2009;461(7264):654-8. doi: http://www.nature.com/nature/journal/v461/n7264/suppinfo/nature08455_S1.html.

158. Ocorr K, Reeves NL, Wessells RJ, Fink M, Chen H-SV, Akasaka T, Yasuda S, Metzger JM, Giles W, Posakony JW, Bodmer R. KCNQ potassium channel mutations cause cardiac arrhythmias in Drosophila that mimic the effects of aging. Proceedings of the National Academy of Sciences. 2007;104(10):3943-8. doi: 10.1073/pnas.0609278104.

159. Wessells RJ, Fitzgerald E, Cypser JR, Tatar M, Bodmer R. Insulin regulation of heart function in aging fruit flies. Nat Genet. 2004;36(12):1275-81. doi: http://www.nature.com/ng/journal/v36/n12/suppinfo/ng1476_S1.html.

160. Li GH, Shi Y, Chen Y, Sun M, de Couto G, Fukuoka M, Wang X, Dawood F, Chen M, Li M, Liu Y, Khaper N, Liu P. The Role of Autophagy in Iron-Overload Cardiomyopathy: A Model of Diastolic Heart Failure Due to Oxidative Stress. Journal of Cardiac Failure. 2009;15(6, Supplement 1):S42-S3.

161. Shan Y, Napoli E, Cortopassi G. Mitochondrial frataxin interacts with ISD11 of the NFS1/ISCU complex and multiple mitochondrial chaperones. Hum Mol Genet. 2007;16(8):929-41. PubMed PMID: 17331979.

162. Filla A, De Michele G, Cavalcanti F, Perretti A, Santoro L, Barbieri F, D'Arienzo G, Campanella G. Clinical and genetic heterogeneity in early onset cerebellar ataxia with retained tendon reflexes. J Neurol Neurosurg Psychiatry. 1990;53(8):667-70. PubMed PMID: 2213043.

163. Tanaka H, Hashimoto N. A multiple ion channel blocker, NIP-142, for the treatment of atrial fibrillation. Cardiovasc Drug Rev. 2007;25(4):342-56. PubMed PMID: 18078434.

164. Gottdiener JS, Hawley RJ, Maron BJ, Bertorini TF, Engle WK. Characteristics of the cardiac hypertrophy in Friedreich's ataxia. Am Heart J. 1982;103(4 Pt 1):525-31. PubMed PMID: 6461236.

165. Harding AE, Hewer RL. The heart disease of Friedreich's ataxia: a clinical and electrocardiographic study of 115 patients, with an analysis of serial electrocardiographic changes in 30 cases. The Quarterly journal of medicine. 1983;52(208):489-502.

166. Giunta A, Maione S, Biagini R, Filla A, De Michele G, Campanella G. Noninvasive assessment of systolic and diastolic function in 50 patients with Friedreich's ataxia. Cardiology. 1988;75(5):321-7. PubMed PMID: 3233613.

167. Tsou AY, Paulsen EK, Lagedrost SJ, Perlman SL, Mathews KD, Wilmot GR, Ravina B, Koeppen AH, Lynch DR. Mortality in Friedreich ataxia. J Neurol Sci. 2011;307(1-2):46-9. Epub 2011/06/10. doi: 10.1016/j.jns.2011.05.023. PubMed PMID: 21652007.

168. Michael S, Petrocine SV, Qian J, Lamarche JB, Knutson MD, Garrick MD, Koeppen AH. Iron and iron-responsive proteins in the cardiomyopathy of Friedreich's ataxia. Cerebellum. 2006;5(4):257-67. doi: 10.1080/14734220600913246. PubMed PMID: WOS:000242911700002.

169. Mottram PM, Delatycki MB, Donelan L, Gelman JS, Corben L, Peverill RE. Early Changes in Left Ventricular Long-Axis Function in Friedreich Ataxia: Relation with the FXN Gene Mutation and Cardiac Structural Change. Journal of the American Society of Echocardiography. 2011;24(7):782-9. doi: http://dx.doi.org/10.1016/j.echo.2011.04.004.

170. Vyas PM, Tomamichel WJ, Pride PM, Babbey CM, Wang Q, Mercier J, Martin EM, Payne RM. A TAT–Frataxin fusion protein increases lifespan and cardiac function in a conditional Friedreich's ataxia mouse model. Human Molecular Genetics. 2012;21(6):1230-47. doi: 10.1093/hmg/ddr554.

171. Puccio H, Simon D, Cossee M, Criqui-Filipe P, Tiziano F, Melki J, Hindelang C, Matyas R, Rustin P, Koenig M. Mouse models for Friedreich ataxia exhibit cardiomyopathy, sensory nerve defect and Fe-S enzyme deficiency followed by intramitochondrial iron deposits. Nat Genet. 2001;27(2):181-6. Epub 2001/02/15. doi: 10.1038/84818. PubMed PMID: 11175786.

172. Ristow M, Pfister MF, Yee AJ, Schubert M, Michael L, Zhang C-Y, Ueki K, Michael MD, Lowell BB, Kahn CR. Frataxin activates mitochondrial energy conversion and oxidative phosphorylation. Proceedings of the National Academy of Sciences. 2000;97(22):12239-43.

173. Shoichet SA, Bäumer AT, Stamenkovic D, Sauer H, Pfeiffer AFH, Kahn CR, Müller-Wieland D, Richter C, Ristow M. Frataxin promotes antioxidant defense in a thiol-dependent manner resulting in diminished malignant transformation in vitro. Human Molecular Genetics. 2002;11(7):815-21.

174. Navarro Ja Fau - Llorens JV, Llorens Jv Fau - Soriano S, Soriano S Fau - Botella JA, Botella Ja Fau - Schneuwly S, Schneuwly S Fau - Martinez-Sebastian MJ, Martinez-Sebastian Mj Fau - Molto MD, Molto MD. Overexpression of human and Drosophila frataxins in Drosophila provokes deleterious effects at biochemical, physiological and developmental levels(1932-6203 (Electronic)). doi: D - NLM: PMC3136927 EDAT- 2011/07/23 06:00 MHDA- 2011/11/16 06:00 CRDT- 2011/07/23 06:00 PHST- 2011/02/28 [received] PHST- 2011/05/16 [accepted] PHST- 2011/07/11 [epublish] AID - 10.1371/journal.pone.0021017 [doi] AID - PONE-D-11-04053 [pii] PST - ppublish.

175. Gwinn DM, Shackelford DB, Egan DF, Mihaylova MM, Mery A, Vasquez DS, Turk BE, Shaw RJ. AMPK

phosphorylation of raptor mediates a metabolic checkpoint. Molecular cell. 2008;30(2):214-26. Epub 2008/04/29. doi: 10.1016/j.molcel.2008.03.003. PubMed PMID: 18439900; PMCID: Pmc2674027.

176. Zhu X, Castellani RJ, Takeda A, Nunomura A, Atwood CS, Perry G, Smith MA. Differential activation of neuronal ERK, JNK/SAPK and p38 in Alzheimer disease: the 'two hit' hypothesis. Mechanisms of ageing and development. 2001;123(1):39-46. Epub 2001/10/20. PubMed PMID: 11640950.

177. Zhou Y, Wang Q, Evers BM, Chung DH. Signal transduction pathways involved in oxidative stress-induced intestinal epithelial cell apoptosis. Pediatric research. 2005;58(6):1192-7. Epub 2005/11/25. doi: 10.1203/01.pdr.0000185133.65966.4e. PubMed PMID: 16306192; PMCID: Pmc2653865.

178. Wu H, Wang MC, Bohmann D. JNK protects Drosophila from oxidative stress by trancriptionally activating autophagy. Mechanisms of development. 2009;126(8-9):624-37. doi: 10.1016/j.mod.2009.06.1082. PubMed PMID: PMC2750887.

179. Wessells RJ, Bodmer R. Cardiac aging. Seminars in Cell & Developmental Biology. 2007;18(1):111-6.

180. Brand AH, Perrimon N. Targeted gene expression as a means of altering cell fates and generating dominant phenotypes. Development. 1993;118(2):401-15. Epub 1993/06/01. PubMed PMID: 8223268.

181. Anderson PR, Kirby K, Hilliker AJ, Phillips JP. RNAi-mediated suppression of the mitochondrial iron chaperone, frataxin, in Drosophila. Hum Mol Genet. 2005;14(22):3397-405. Epub 2005/10/06. doi: 10.1093/hmg/ddi367. PubMed PMID: 16203742.

182. Shpilka T, Weidberg H, Pietrokovski S, Elazar Z. Atg8: an autophagy-related ubiquitin-like protein family. Genome Biology. 2011;12(7):226. PubMed PMID: doi:10.1186/gb-2011-12-7-226.

183. Pandolfo M. Molecular genetics and pathogenesis of Friedreich ataxia. Neuromuscular Disorders. 1998;8(6):409-15. doi: http://dx.doi.org/10.1016/S0960-8966(98)00039-X.

184. Guccini I, Serio D, Condo I, Rufini A, Tomassini B, Mangiola A, Maira G, Anile C, Fina D, Pallone F, Mongiardi MP, Levi A, Ventura N, Testi R, Malisan F. Frataxin participates to the hypoxia-induced response in tumors. Cell Death and Dis. 2011;2:e123. doi: http://www.nature.com/cddis/journal/v2/n2/suppinfo/cddis20115s1.html.

185. Nicholson DW. Caspase structure, proteolytic substrates, and function during apoptotic cell death. Cell death and differentiation. 1999;6(11):1028-42. Epub 1999/12/01. doi: 10.1038/sj.cdd.4400598. PubMed PMID: 10578171.

186. Kim J, Kundu M, Viollet B, Guan K-L. AMPK and mTOR regulate autophagy through direct phosphorylation of Ulk1. Nat Cell Biol. 2011;13(2):132-41. doi: http://www.nature.com/ncb/journal/v13/n2/abs/ncb2152.html#supplementary-information.

187. Zhu X, Ogawa O, Wang Y, Perry G, Smith MA. JKK1, an upstream activator of JNK/SAPK, is activated in Alzheimer's disease. Journal of neurochemistry. 2003;85(1):87-93. Epub 2003/03/19. PubMed PMID: 12641730.

188. Martelli A, Wattenhofer-Donze M, Schmucker S, Bouvet S, Reutenauer L, Puccio H. Frataxin is essential for extramitochondrial Fe-S cluster proteins in mammalian tissues. Hum Mol Genet. 2007;16(22):2651-8. Epub 2007/06/29. doi: 10.1093/hmg/ddm163. PubMed PMID: 17597094.

189. Casati B, Terova G, Cattaneo AG, Rimoldi S, Franzetti E, de Eguileor M, Tettamanti G. Molecular cloning, characterization and expression analysis of ATG1 in the silkworm, Bombyx mori. Gene. 2012;511(2):326-37. Epub 2012/10/09. doi: 10.1016/j.gene.2012.09.086. PubMed PMID: 23041082.

190. Schaaf MBE, Cojocari D, Keulers TG, Jutten B, Starmans MH, de Jong MC, Begg AC, Savelkouls KGM, Bussink J, Vooijs M, Wouters BG, Rouschop KMA. The autophagy associated gene, ULK1, promotes tolerance to chronic and acute hypoxia. Radiotherapy and Oncology. 2013;108(3):529-34. doi: http://dx.doi.org/10.1016/j.radonc.2013.06.015.

191. Yang Y, Zheng X, Li B, Jiang S, Jiang L. Increased activity of osteocyte autophagy in ovariectomized rats and its correlation with oxidative stress status and bone loss. Biochemical and Biophysical Research Communications. 2014;451(1):86-92. doi: http://dx.doi.org/10.1016/j.bbrc.2014.07.069.

192. Honda S, Arakawa S, Nishida Y, Yamaguchi H, Ishii E, Shimizu S. Ulk1-mediated Atg5-independent macroautophagy mediates elimination of mitochondria from embryonic reticulocytes. Nat Commun. 2014;5. doi: 10.1038/ncomms5004.

193. Morishita H, Eguchi S, Kimura H, Sasaki J, Sakamaki Y, Robinson ML, Sasaki T, Mizushima N. Deletion of autophagy-related 5 (Atg5) and Pik3c3 in the lens causes cataract independent of programmed organelle degradation. Journal of Biological Chemistry. 2013. doi: 10.1074/jbc.M112.437103.

194. Runko AP, Griswold AJ, Min K-T. Overexpression of frataxin in the mitochondria increases resistance to oxidative stress and extends lifespan in Drosophila. FEBS Letters. 2008;582(5):715-9. doi: http://dx.doi.org/10.1016/j.febslet.2008.01.046.

195. Miranda CJ, Santos MM, Ohshima K, Tessaro M, Sequeiros J, Pandolfo M. Frataxin overexpressing mice. FEBS Letters. 2004;572(1–3):281-8. doi: http://dx.doi.org/10.1016/j.febslet.2004.07.022.

196. Tricoire H, Palandri A, Bourdais A, Camadro JM, Monnier V. Methylene blue rescues heart defects in a Drosophila model of Friedreich's ataxia. Hum Mol Genet. 2014;23(4):968-79. Epub 2013/10/10. doi: 10.1093/hmg/ddt493. PubMed PMID: 24105471.

197. Klose RJ, Bird AP. Genomic DNA methylation: The mark and its mediators. Trends in Biochemical Sciences. 2006;31(2):89-97.

198. Riggs AD. X inactivation, differentiation, and DNA methylation. Cytogenetic and Genome Research. 1975;14(1):9-25.

199. Holliday R, Pugh J. DNA modification mechanisms and gene activity during development. Science. 1975;187(4173):226-32. doi: 10.1126/science.187.4173.226.

200. Ito S, Dalessio AC, Taranova OV, Hong K, Sowers LC, Zhang Y. Role of tet proteins in 5mC to 5hmC conversion, ES-cell self-renewal and inner cell mass specification. Nature. 2010;466(7310):1129-33.

201. Tahiliani M, Koh KP, Shen Y, Pastor WA, Bandukwala H, Brudno Y, Agarwal S, Iyer LM, Liu DR, Aravind L, Rao A. Conversion of 5-methylcytosine to 5-hydroxymethylcytosine in mammalian DNA by MLL partner TET1. Science. 2009;324(5929):930-5. Epub 2009/04/18. doi: 10.1126/science.1170116. PubMed PMID: 19372391; PMCID: Pmc2715015.

202. Ito S, Shen L, Dai Q, Wu SC, Collins LB, Swenberg JA, He C, Zhang Y. Tet proteins can convert 5-methylcytosine to 5-formylcytosine and 5-carboxylcytosine. Science. 2011;333(6047):1300-3. Epub 2011/07/23. doi: 10.1126/science.1210597. PubMed PMID: 21778364; PMCID: Pmc3495246.

203. G. R W, S. S C. A New Pyrimidine Base from Bacteriophage Nucleic Acids. Nature. 1952;170(4338):1072-3. doi: 10.1038/1701072a0.

204. Kriaucionis S, Heintz N. The nuclear DNA base 5-hydroxymethylcytosine is present in purkinje neurons and the brain. Science. 2009;324(5929):929-30.

205. Ficz G, Branco MR, Seisenberger S, Santos F, Krueger F, Hore TA, Marques CJ, Andrews S, Reik W. Dynamic regulation of 5-hydroxymethylcytosine in mouse ES cells and during differentiation. Nature. 2011;473(7347):398-402. doi: http://www.nature.com/nature/journal/v473/n7347/abs/10.1038-nature10008-

unlocked.html#supplementary-information.

206. Ito S, D'Alessio AC, Taranova OV, Hong K, Sowers LC, Zhang Y. Role of Tet proteins in 5mC to 5hmC conversion, ES-cell self-renewal and inner cell mass specification. Nature. 2010;466(7310):1129-33. Epub 2010/07/20. doi: 10.1038/nature09303. PubMed PMID: 20639862; PMCID: Pmc3491567.

207. Koh KP, Yabuuchi A, Rao S, Huang Y, Cunniff K, Nardone J, Laiho A, Tahiliani M, Sommer CA, Mostoslavsky G, Lahesmaa R, Orkin SH, Rodig SJ, Daley GQ, Rao A. Tet1 and Tet2 Regulate 5-Hydroxymethylcytosine Production and Cell Lineage Specification in Mouse Embryonic Stem Cells. Cell Stem Cell. 2011;8(2):200-13. doi: http://dx.doi.org/10.1016/j.stem.2011.01.008.

208. Dang L, White DW, Gross S, Bennett BD, Bittinger MA, Driggers EM, Fantin VR, Jang HG, Jin S, Keenan MC, Marks KM, Prins RM, Ward PS, Yen KE, Liau LM, Rabinowitz JD, Cantley LC, Thompson CB, Vander Heiden MG, Su SM. Erratum: Cancer-associated IDH1 mutations produce 2-hydroxyglutarate (Nature (2010) 462 (739-744)). Nature. 2010;465(7300):966. doi: 10.1038/nature09132.

209. Ito S, Shen L, Dai Q, Wu SC, Collins LB, Swenberg JA, He C, Zhang Y. Tet Proteins Can Convert 5-Methylcytosine to 5-Formylcytosine and 5-Carboxylcytosine. Science. 2011;333(6047):1300-3. doi: 10.1126/science.1210597.

210. Shen L, Wu H, Diep D, Yamaguchi S, D'Alessio Ana C, Fung H-L, Zhang K, Zhang Y. Genome-wide Analysis Reveals TET- and TDG-Dependent 5-Methylcytosine Oxidation Dynamics. Cell. 2013;153(3):692-706. doi: http://dx.doi.org/10.1016/j.cell.2013.04.002.

211. Lian Christine G, Xu Y, Ceol C, Wu F, Larson A, Dresser K, Xu W, Tan L, Hu Y, Zhan Q, Lee C-w, Hu D, Lian Bill Q, Kleffel S, Yang Y, Neiswender J, Khorasani Abraham J, Fang R, Lezcano C, Duncan Lyn M, Scolyer Richard A, Thompson John F, Kakavand H, Houvras Y, Zon Leonard I, Mihm Jr Martin C, Kaiser Ursula B, Schatton T, Woda Bruce A, Murphy George F, Shi Yujiang G. Loss of 5-Hydroxymethylcytosine Is an Epigenetic Hallmark of Melanoma. Cell. 2012;150(6):1135-46. doi: http://dx.doi.org/10.1016/j.cell.2012.07.033.

212. Kroeze LI, van der Reijden BA, Jansen JH. 5-Hydroxymethylcytosine: An epigenetic mark frequently deregulated in cancer. Biochimica et Biophysica Acta (BBA) - Reviews on Cancer. 2015;1855(2):144-54. doi: http://dx.doi.org/10.1016/j.bbcan.2015.01.001.

213. Yang H, Liu Y, Bai F, Zhang JY, Ma SH, Liu J, Xu ZD, Zhu HG, Ling ZQ, Ye D, Guan KL, Xiong Y. Tumor

development is associated with decrease of TET gene expression and 5-methylcytosine hydroxylation. Oncogene. 2013;32(5):663-9. doi: 10.1038/onc.2012.67.

214. Du C, Kurabe N, Matsushima Y, Suzuki M, Kahyo T, Ohnishi I, Tanioka F, Tajima S, Goto M, Yamada H, Tao H, Shinmura K, Konno H, Sugimura H. Robust quantitative assessments of cytosine modifications and changes in the expressions of related enzymes in gastric cancer. Gastric cancer : official journal of the International Gastric Cancer Association and the Japanese Gastric Cancer Association. 2014. Epub 2014/08/08. doi: 10.1007/s10120-014-0409-4. PubMed PMID: 25098926.

215. Kudo Y, Tateishi K, Yamamoto K, Yamamoto S, Asaoka Y, Ijichi H, Nagae G, Yoshida H, Aburatani H, Koike K. Loss of 5-hydroxymethylcytosine is accompanied with malignant cellular transformation. Cancer Science. 2012;103(4):670-6. doi: 10.1111/j.1349-7006.2012.02213.x.

216. Orr BA, Haffner MC, Nelson WG, Yegnasubramanian S, Eberhart CG. Decreased 5-hydroxymethylcytosine is associated with neural progenitor phenotype in normal brain and shorter survival in malignant glioma. PLoS One. 2012;7(7):e41036. Epub 2012/07/26. doi: 10.1371/journal.pone.0041036. PubMed PMID: 22829908; PMCID: Pmc3400598.

217. Vosseller K, Sakabe K, Wells L, Hart GW. Diverse regulation of protein function by O-GlcNAc: a nuclear and cytoplasmic carbohydrate post-translational modification. Current opinion in chemical biology. 2002;6(6):851-7. Epub 2002/12/10. PubMed PMID: 12470741.

218. Ingham PW. A gene that regulates the bithorax complex differentially in larval and adult cells of Drosophila. Cell. 1984;37(3):815-23. Epub 1984/07/01. PubMed PMID: 6430566.

219. Sinclair DAR, Syrzycka M, Macauley MS, Rastgardani T, Komljenovic I, Vocadlo DJ, Brock HW, Honda BM. Drosophila O-GlcNAc transferase (OGT) is encoded by the Polycomb group (PcG) gene, super sex combs (sxc). Proceedings of the National Academy of Sciences. 2009;106(32):13427-32. doi: 10.1073/pnas.0904638106.

220. Chen Q, Chen Y, Bian C, Fujiki R, Yu X. TET2 promotes histone O-GlcNAcylation during gene transcription. Nature. 2013;493(7433):561-4. doi: http://www.nature.com/nature/journal/v493/n7433/abs/nature11742.html#supplementary-information.

221. Tanaka Y, Umata T, Okamoto K, Obuse C, Tsuneoka M. CxxC-ZF domain is needed for KDM2A to demethylate histone in rDNA promoter in response to starvation. Cell structure and function. 2014;39(1):79-92.

Epub 2014/02/21. PubMed PMID: 24553073.

222. Khoury-Haddad H, Nadar-Ponniah PT, Awwad S, Ayoub N. The Emerging Role of Lysine Demethylases in DNA Damage Response: Dissecting the recruitment mode of KDM4D/JMJD2D to DNA damage sites. Cell cycle (Georgetown, Tex). 2015:0. Epub 2015/02/26. doi: 10.1080/15384101.2015.1014147. PubMed PMID: 25714495.

223. Anderson S, Bankier AT, Barrell BG, de Bruijn MH, Coulson AR, Drouin J, Eperon IC, Nierlich DP, Roe BA, Sanger F, Schreier PH, Smith AJ, Staden R, Young IG. Sequence and organization of the human mitochondrial genome. Nature. 1981;290(5806):457-65. Epub 1981/04/09. PubMed PMID: 7219534.

224. Andrews RM, Kubacka I, Chinnery PF, Lightowlers RN, Turnbull DM, Howell N. Reanalysis and revision of the Cambridge reference sequence for human mitochondrial DNA. Nat Genet. 1999;23(2):147. Epub 1999/10/03. doi: 10.1038/13779. PubMed PMID: 10508508.

225. Zhang J, Li X, Mueller M, Wang Y, Zong C, Deng N, Vondriska TM, Liem DA, Yang JI, Korge P, Honda H, Weiss JN, Apweiler R, Ping P. Systematic characterization of the murine mitochondrial proteome using functionally validated cardiac mitochondria. Proteomics. 2008;8(8):1564-75. Epub 2008/03/19. doi: 10.1002/pmic.200700851. PubMed PMID: 18348319; PMCID: Pmc2799225.

226. Lee W, Johnson J, Gough DJ, Donoghue J, Cagnone GL, Vaghjiani V, Brown KA, Johns TG, St John JC. Mitochondrial DNA copy number is regulated by DNA methylation and demethylation of POLGA in stem and cancer cells and their differentiated progeny. Cell death & disease. 2015;6:e1664. Epub 2015/02/27. doi: 10.1038/cddis.2015.34. PubMed PMID: 25719248.

227. Sollars V, Lu X, Xiao L, Wang X, Garfinkel MD, Ruden DM. Evidence for an epigenetic mechanism by which Hsp90 acts as a capacitor for morphological evolution. Nature Genetics. 2003;33(1):70-4. Epub 2002/12/17. doi: 10.1038/ng1067. PubMed PMID: 12483213.

228. Love MI, Huber W, Anders S. Moderated estimation of fold change and dispersion for RNA-seq data with DESeq2. Genome biology. 2014;15(12):550. doi: 10.1186/s13059-014-0550-8. PubMed PMID: 25516281; PMCID: 4302049.

229. Szwagierczak A, Brachmann A, Schmidt CS, Bultmann S, Leonhardt H, Spada F. Characterization of PvuRts1I endonuclease as a tool to investigate genomic 5-hydroxymethylcytosine. Nucleic acids research. 2011;39(12):5149-56. doi: 10.1093/nar/gkr118. PubMed PMID: 21378122; PMCID: 3130283.

230. Cingolani P, Cao X, Khetani RS, Chen CC, Coon M, Sammak A, Bollig-Fischer A, Land S, Huang Y, Hudson ME, Garfinkel MD, Zhong S, Robinson GE, Ruden DM. Intronic non-CG DNA hydroxymethylation and alternative mRNA splicing in honey bees. BMC genomics. 2013;14:666. doi: 10.1186/1471-2164-14-666. PubMed PMID: 24079845; PMCID: 3850688.

231. Robinson MD, McCarthy DJ, Smyth GK. edgeR: a Bioconductor package for differential expression analysis of digital gene expression data. Bioinformatics. 2010;26(1):139-40. doi: 10.1093/bioinformatics/btp616. PubMed PMID: 19910308; PMCID: 2796818.

232. Yao Z, Macquarrie KL, Fong AP, Tapscott SJ, Ruzzo WL, Gentleman RC. Discriminative motif analysis of high-throughput dataset. Bioinformatics. 2014;30(6):775-83. doi: 10.1093/bioinformatics/btt615. PubMed PMID: 24162561; PMCID: 3957073.

233. Biemar F, Nix DA, Piel J, Peterson B, Ronshaugen M, Sementchenko V, Bell I, Manak JR, Levine MS. Comprehensive identification of Drosophila dorsal-ventral patterning genes using a whole-genome tiling array. Proceedings of the National Academy of Sciences of the United States of America. 2006;103(34):12763-8. Epub 2006/08/16. doi: 10.1073/pnas.0604484103. PubMed PMID: 16908844; PMCID: Pmc1636694.

234. Loenarz C, Schofield CJ. Physiological and biochemical aspects of hydroxylations and demethylations catalyzed by human 2-oxoglutarate oxygenases. Trends Biochem Sci. 2011;36(1):7-18. Epub 2010/08/24. doi: 10.1016/j.tibs.2010.07.002. PubMed PMID: 20728359.

235. Ko M, An J, Bandukwala HS, Chavez L, Aijo T, Pastor WA, Segal MF, Li H, Koh KP, Lahdesmaki H, Hogan PG, Aravind L, Rao A. Modulation of TET2 expression and 5-methylcytosine oxidation by the CXXC domain protein IDAX. Nature. 2013;497(7447):122-6. Epub 2013/04/09. doi: 10.1038/nature12052. PubMed PMID: 23563267; PMCID: Pmc3643997.

236. !!! INVALID CITATION !!!

237. Szwagierczak A, Brachmann A, Schmidt CS, Bultmann S, Leonhardt H, Spada F. Characterization of PvuRts1I endonuclease as a tool to investigate genomic 5–hydroxymethylcytosine. Nucleic Acids Research. 2011;39(12):5149-56. doi: 10.1093/nar/gkr118.

238. Zhu P, Zhou W, Wang J, Puc J, Ohgi KA, Erdjument-Bromage H, Tempst P, Glass CK, Rosenfeld MG. A histone H2A deubiquitinase complex coordinating histone acetylation and H1 dissociation in transcriptional regulation.

Molecular cell. 2007;27(4):609-21. Epub 2007/08/21. doi: 10.1016/j.molcel.2007.07.024. PubMed PMID: 17707232; PMCID: Pmc2709280.

239. Jackle H, Rosenberg UB, Preiss A, Seifert E, Knipple DC, Kienlin A, Lehmann R. Molecular analysis of Kruppel, a segmentation gene of Drosophila melanogaster. Cold Spring Harbor symposia on quantitative biology. 1985;50:465-73. Epub 1985/01/01. PubMed PMID: 3007002.

240. Sollars V, Lu X, Xiao L, Wang X, Garfinkel MD, Ruden DM. Evidence for an epigenetic mechanism by which Hsp90 acts as a capacitor for morphological evolution. Nat Genet. 2003;33(1):70-4. Epub 2002/12/17. doi: 10.1038/ng1067. PubMed PMID: 12483213.

241. Achwal CW, Iyer CA, Chandra HS. Immunochemical evidence for the presence of 5mC, 6mA and 7mG in human, Drosophila and mealybug DNA. FEBS letters. 1983;158(2):353-8. Epub 1983/07/25. PubMed PMID: 6409666.

242. Hung MS, Karthikeyan N, Huang B, Koo HC, Kiger J, Shen CJ. Drosophila proteins related to vertebrate DNA (5-cytosine) methyltransferases. Proceedings of the National Academy of Sciences of the United States of America. 1999;96(21):11940-5. Epub 1999/10/16. PubMed PMID: 10518555; PMCID: Pmc18391.

243. Gowher H, Leismann O, Jeltsch A. DNA of Drosophila melanogaster contains 5-methylcytosine. The EMBO journal. 2000;19(24):6918-23. Epub 2000/12/16. doi: 10.1093/emboj/19.24.6918. PubMed PMID: 11118227; PMCID: Pmc305887.

244. Cingolani P, Cao X, Khetani R, Chen C-C, Coon M, Sammak Aa, Bollig-Fischer A, Land S, Huang Y, Hudson M, Garfinkel M, Zhong S, Robinson G, Ruden D. Intronic Non-CG DNA hydroxymethylation and alternative mRNA splicing in honey bees. BMC Genomics. 2013;14(1):666. PubMed PMID: doi:10.1186/1471-2164-14-666.

245. Nass MM. Differential methylation of mitochondrial and nuclear DNA in cultured mouse, hamster and virus-transformed hamster cells. In vivo and in vitro methylation. J Mol Biol. 1973;80(1):155-75. Epub 1973/10/15. PubMed PMID: 4361747.

246. Shock LS, Thakkar PV, Peterson EJ, Moran RG, Taylor SM. DNA methyltransferase 1, cytosine methylation, and cytosine hydroxymethylation in mammalian mitochondria. Proceedings of the National Academy of Sciences. 2011;108(9):3630-5. doi: 10.1073/pnas.1012311108.

247. Shutt TE, Shadel GS. A compendium of human mitochondrial gene expression machinery with links to disease. Environmental and molecular mutagenesis. 2010;51(5):360-79. Epub 2010/06/15. doi: 10.1002/em.20571.

PubMed PMID: 20544879; PMCID: Pmc2886302.

248. Manev H, Dzitoyeva S, Chen H. Mitochondrial DNA: A Blind Spot in Neuroepigenetics. Biomolecular concepts. 2012;3(2):107-15. Epub 2012/05/29. doi: 10.1515/bmc-2011-0058. PubMed PMID: 22639700; PMCID: Pmc3359012.

249. Lu AY, Junk KW, Coon MJ. Resolution of the cytochrome P-450-containing omega-hydroxylation system of liver microsomes into three components. J Biol Chem. 1969;244(13):3714-21. Epub 1969/07/10. PubMed PMID: 4389465.

250. Schulze S, Sinclair DA, Silva E, Fitzpatrick KA, Singh M, Lloyd VK, Morin KA, Kim J, Holm DG, Kennison JA, Honda BM. Essential genes in proximal 3L heterochromatin of Drosophila melanogaster. Molecular & general genetics : MGG. 2001;264(6):782-9. Epub 2001/03/20. PubMed PMID: 11254125.

251. Marchant GE, Holm DG. Genetic Analysis of the Heterochromatin of Chromosome 3 in Drosophila Melanogaster. II. Vital Loci Identified through Ems Mutagenesis. Genetics. 1988;120(2):519-32. Epub 1988/10/01. PubMed PMID: 17246481; PMCID: Pmc1203529.

252. Lu F, Liu Y, Jiang L, Yamaguchi S, Zhang Y. Role of Tet proteins in enhancer activity and telomere elongation. Genes Dev. 2014;28(19):2103-19. Epub 2014/09/17. doi: 10.1101/gad.248005.114. PubMed PMID: 25223896; PMCID: Pmc4180973.

253. Müller U, Bauer C, Siegl M, Rottach A, Leonhardt H. TET-mediated oxidation of methylcytosine causes TDG or NEIL glycosylase dependent gene reactivation. Nucleic Acids Research. 2014. doi: 10.1093/nar/gku552.

254. Vella P, Scelfo A, Jammula S, Chiacchiera F, Williams K, Cuomo A, Roberto A, Christensen J, Bonaldi T, Helin K, Pasini D. Tet Proteins Connect the O-Linked N-acetylglucosamine Transferase Ogt to Chromatin in Embryonic Stem Cells. Molecular cell.49(4):645-56. doi: 10.1016/j.molcel.2012.12.019.

255. Forneris F, Binda C, Battaglioli E, Mattevi A. LSD1: oxidative chemistry for multifaceted functions in chromatin regulation. Trends in biochemical sciences. 2008;33(4):181-9. Epub 2008/03/18. doi: 10.1016/j.tibs.2008.01.003. PubMed PMID: 18343668.

256. Garcia-Bassets I, Kwon Y-S, Telese F, Prefontaine GG, Hutt KR, Cheng CS, Ju B-G, Ohgi KA, Wang J, Escoubet-Lozach L, Rose David W, Glass CK, Fu X-D, Rosenfeld MG. Histone Methylation-Dependent Mechanisms Impose Ligand Dependency for Gene Activation by Nuclear Receptors. Cell. 2007;128(3):505-18. doi:

http://dx.doi.org/10.1016/j.cell.2006.12.038.

257. Binda C, Mattevi A, Edmondson DE. Structure-Function Relationships in Flavoenzyme-dependent Amine Oxidations: A COMPARISON OF POLYAMINE OXIDASE AND MONOAMINE OXIDASE. Journal of Biological Chemistry. 2002;277(27):23973-6. doi: 10.1074/jbc.R200005200.

258. Giorgio M, Trinei M, Migliaccio E, Pelicci PG. Hydrogen peroxide: A metabolic by-product or a common mediator of ageing signals? Nature Reviews Molecular Cell Biology. 2007;8(9):722-8. doi: 10.1038/nrm2240.

259. Perillo B, Ombra MN, Bertoni A, Cuozzo C, Sacchetti S, Sasso A, Chiariotti L, Malorni A, Abbondanza C, Avvedimento EV. DNA oxidation as triggered by H3K9me2 demethylation drives estrogen-induced gene expression. Science. 2008;319(5860):202-6. Epub 2008/01/12. doi: 10.1126/science.1147674. PubMed PMID: 18187655.

ABSTRACT

A PROTECTIVE ROLE OF AUTOPHAGY IN A *DROSOPHILA* MODEL OF FRIEDREICH'S ATAXIA (FRDA)

by

LUAN WANG

December 2015

Advisor: Dr. Douglas Ruden

Major: Molecular and Cellular Toxicology

Degree: Doctor of Philosophy

Friedreich's ataxia (FRDA) is an inherited autosomal recessive neurodegenerative disease. It affects 1 in every 50,000 people in central Europe and North America. FRDA is caused by deficiency of *Frataxin*, an essential mitochondrial iron chaperone protein, and the associated oxidative stress damages. Autophagy, a housekeeping process responsible for the bulk degradation and turnover of long half-life proteins and organelles, is featured by the formation of double-membrane vacuoles and lysosomal degradation. Previous researches indicate that Danon's disease, the inherited neural disorder disease that shares similar symptoms with FRDA, is due to the malfunction of autophagy. Based on this, we raise the question whether the autophagy activity is modified and what is its role in FRDA. Study has shown that oxidative stress may play a major role in the progression of neurodegenerative diseases by attacking the cytoplasmic molecules and organelles, and autophagy is the major pathway in reducing oxidative stress and removal of malfunctioned organelles. Additionally, autophagy has been closely related

to cell apoptosis and organism remodeling. Mitochondrial Autophagy (mitophagy) is also the major turnover pathway for damaged mitochondria. Therefore, the dysfunctional autophagy in removing the malfunctioned mitochondria in FRDA may responsible for its pathogenesis. Since the mechanism of autophagy in the development of FRDA is still largely unknown, a systematic analysis of the status and function of autophagy pathway is needed.

My thesis is targeting at four goals: (1) to construct FRDA *Drosophila* model and characterize autophagy expression pattern in each stage; (2) to determine the effect of autophagy modification on the symptoms of the FRDA *Drosophila*; (3) to identify the potential downstream events of autophagy; (4) to explore the possible upstream activities by examine whether the AMPK or SAPK stress response pathway is involved in FRDA *Drosophila*. Our hypothesis is the up-regulation of autophagy occurs in the early stage of FRDA and may induce apoptosis or mitophagy. We identified that autophagy level is up-regulated in FRDA *Drosophila* at both transcriptional and translational levels. Moreover, the overexpression of *Frataxin* also increases autophagy activity. The comparable Atg5 mRNA level in both *Frataxin* deficiency and overexpression *Drosophila* indicates this induction of autophagy in FRDA *Drosophila* is Atg5 independent. Autophagy inducer Methylene blue and rapamycin could partially prolong the longevity and restore the fertility of FRDA *Drosophila*, but could not rescue the pupal lethal phenotype. When treated with the autophagy inhibitor chloroquine, FRDA KD *Drosophila* showed reduced longevity and locomotor activity, implying the beneficial effect of autophagy in certain development stages. The FRDA KD *Drosophila* also showed up-regulated caspases-3 and cytochrome C level, indicating enhanced apoptosis in cells with reduced *Frataxin*. We also attempt to apply the heart pacing assay to evaluate the FRDA *Drosophila* cardiac function.

Although the results are inconclusive, the heart pacing assay appears to be a valuable tool for future research.

AUTOBIOGRAPHICAL STATEMENT

Luan Wang

EDUCATION: Master of Science in Beijing Normal University (August, 2004)

AWARDS:

Mott Center Scientific Retreat Poster Award, Wayne State University 2012

University Dissertation Fellowship, Wayne State University, winter 2011

PUBLICATIONS:

Wang, L., Lu, X. & Ruden, D. Transgenerational Epigenetic Inheritance in Drosophila. in *Environmental Epigenomics in Health and Disease* (eds. Jirtle, R.L. & Tyson, F.L.) 227-244 (Springer Berlin Heidelberg, 2013).

Luan Wang, Pablo Cingolani, Wen Qu, Alya'a Sammak, Susan J. Land, and Douglas M. Ruden. The Drosophila TET 0rtholog, dTET, is required for hydroxymethylation of nuclear and mitochondrial DNA and Enhances the Polycomb-mutant phenotype in adults. 2015 (submitted to Genome Biology)

Luan Wang, Douglas M. Ruden. The role of autophagy in a FRDA Drosophila Model. 2014 (in preparation for Frontiers in Genetics).

Lu, X., **Wang, L.** & Ruden, D.M. Hsp90 inhibitors and the reduction of anti-cancer drug resistance by non-genetic and genetic mechanisms. Pharmaceuticals (Basel) 5, 890-8 (2012). Published online 2012 Aug 30. doi: 10.3390/ph5090890

Lu X, Xiao L, **Wang L,** Ruden DM. Hsp90 inhibitors and drug resistance in cancer: the potential benefits of combination therapies of Hsp90 inhibitors and other anti-cancer drugs. Biochem Pharmacol. 2012 Apr 15; 83(8):995-1004. doi: 10.1016/j.bcp.2011.11.011. Epub 2011 Nov 22. Review. PubMed PMID: 22120678.

Chia N, **Wang L,** Lu X, Senut MC, Brenner C, Ruden DM. Hypothesis: environmental regulation of 5-hydroxymethylcytosine by oxidative stress. Epigenetics. 2011 Jul; 6(7):853-6. Epub 2011 Jul 1. Review. PubMed PMID: 2161769.